

EXECUTIVE SUMMARY

TO

THE ROLE OF NITROGENOUS POLLUTANTS  
IN THE FORMATION OF ATMOSPHERIC MUTAGENS  
AND ACID DEPOSITION

Final Report

Contract No. A4-081-32

California Air Resources Board

March 1987

Principal Investigator

Dr. Arthur M. Winer

Co-Investigator

Dr. Roger Atkinson

Program Research Staff

Dr. Janet Arey  
Dr. Heinz W. Biermann  
Mr. William P. Harger  
Dr. Ernesto C. Tuazon  
Dr. Barbara Zielinska

STATEWIDE AIR POLLUTION RESEARCH CENTER  
UNIVERSITY OF CALIFORNIA  
RIVERSIDE, CALIFORNIA 92521



Emissions of oxides of nitrogen not only contribute to increased concentrations of three of the four pollutants for which ambient air quality standards are exceeded in California (i.e., O<sub>3</sub>, NO<sub>2</sub> and total suspended particulate) but they also play a critical role in the formation of atmospheric mutagens and acidic deposition. Our previous research provided evidence for a nighttime pathway for formation of nitric acid (via NO<sub>2</sub>, NO<sub>3</sub> and N<sub>2</sub>O<sub>5</sub> reactions) and for atmospheric transformations of polycyclic aromatic hydrocarbons (PAH) via reaction with nitrogenous pollutants to form mutagenic nitroarenes. This latter finding has important regulatory implications. First, with respect to the need for risk assessments to include not only the mutagenicity/carcinogenicity of directly emitted particulate organic matter (POM), but also the impacts of chemically-modified POM on populations downwind from primary sources. Second, the possibility of artifact formation/destruction of mutagens during the collection of ambient POM, leading to overestimates/underestimates of the actual mutagenic burden impacting human populations must be investigated.

In this program we conducted three separate field studies in the California South Coast Air Basin to (a) provide information concerning the relative importance of atmospheric transformations and sampling artifacts in determining the mutagenic burden in California's atmospheres and (b) generate in-situ, quantitative, and interference-free measurements of the ambient concentrations of the nitrogenous species HONO, NO<sub>2</sub>, HNO<sub>3</sub>, NH<sub>3</sub> and NO<sub>3</sub> radicals (as well as HCHO) which could serve as benchmark data for comparison with other, less specific, analytical methods participating in the CARB-sponsored Nitrogen Species Measurement Methods and Carbonaceous Species Methods Intercomparison Studies. Specifically, intensive monitoring programs were conducted between September 11 and 19, 1985 at Pomona College in Claremont, during January and February 1986 at El Camino Community College in Torrance, and between August 12 and 21, 1986 at Citrus College in Glendora. To avoid problems in comparing spectroscopic data obtained over kilometer distances with data from point monitors, two entirely new 25 m basepath multiple reflection optical systems were designed, constructed and interfaced to our FT-IR and differential optical absorption spectrometer (DOAS) systems.

For the Claremont study, the SAPRC ultra-high volume "mega-sampler" was moved to the study site along with two high-volume (Hi-vol) samplers, and particulate sample collections were conducted in 6-hr intervals. The study at Torrance was conducted on the roof of a two-story building and involved a total of sixteen Hi-vol samplers (as well as the DOAS and FT-IR systems), utilizing Teflon-impregnated glass fiber (TIGF) and glass fiber (GF) filters for particulate collection. Five of these Hi-vols were equipped with three polyurethane foam (PUF) plugs for the collection of gaseous and "blown-off" PAH. In addition, Tenax-GC sampling cartridges were operated. A comparable array of samplers were employed in the Glendora study operating on 12-hr sample collection periods.

Our major findings and conclusions include the following:

- As we have observed previously, the most abundant nitroarene in the ambient POM analyzed was 2-nitrofluoranthene (observed at levels as high as  $1.7 \text{ ng m}^{-3}$ ), which is not emitted from known emission sources in the South Coast Air Basin.

- Several other m/z 247 nitroarene isomers were also observed, most of these less abundant isomers being reported in ambient POM for the first time. Their typical order of abundance was: 2-nitrofluoranthene > 1-nitropyrene ~ 2-nitropyrene > 8-nitrofluoranthene > 3-nitrofluoranthene ~ 4-nitropyrene ~ 7-nitrofluoranthene ~ nitroacephenanthrylene.

- The most abundant gas-phase PAH at Torrance were naphthalene, the 1- and 2-methylnaphthalenes and biphenyl, together with lesser amounts of C<sub>2</sub>-naphthalenes, fluorene and phenanthrene.

- An important observation made at Torrance was that the most abundant nitroarenes were the more volatile species. In particular, levels of 1- and 2-nitronaphthalene and 3-nitrobiphenyl as high as 3.0, 2.9, and  $6.0 \text{ ng m}^{-3}$ , respectively, were measured, and several methylnitronaphthalenes were also observed. These volatile nitroarene species appear to be atmospheric transformation products of the parent aromatic species. Clearly, the health implications of these abundant, largely gas-phase, nitroarene species must be evaluated.

- Utilizing results from this research program concerning the formation of nitroarenes in the adsorbed phase during atmospheric transport and sampling, we suggest that the m/z 247 nitroarene species we observed in ambient samples can be explained by the following major formation routes:

1-nitropyrene is a direct emission from combustion sources, with a small amount being formed in the atmosphere from adsorbed phase reactions of pyrene; 2-nitropyrene is formed in the atmosphere, predominantly via the gas-phase OH radical-initiated reaction with pyrene; 4-nitropyrene is formed in the atmosphere, both from the gas-phase reaction of pyrene with  $N_2O_5$  (when present) during nighttime hours and from the adsorbed-phase reaction of pyrene during atmospheric transport from source to receptor; 2-nitrofluoranthene is formed in the atmosphere both from the gas-phase reactions of fluoranthene with OH radicals, in the presence of  $NO_x$ , during daytime hours and with  $N_2O_5$  (when present) during nighttime hours; 3-nitrofluoranthene is a minor direct emission from combustion sources, and can also be formed from adsorbed-phase reactions during atmospheric transport; the 7- and 8-nitrofluoranthenes can be formed from both the gas-phase reactions of the OH radical with fluoranthene and from adsorbed-phase reactions of fluoranthene during atmospheric transport conditions, although it appears likely that 7-nitrofluoranthene is formed mainly via OH radical-initiated reaction.

- We obtained no evidence for mutagenicity artifacts occurring on TIGF filters, but the results for the GF filters indicated that the uncoated glass fiber surface was more reactive. For this reason, we will continue to use TIGF filters for the Hi-vol collection of ambient POM for mutagenicity determinations.

- Of particular importance was our observation that the method of POM extraction has a considerable effect on its mutagenicity. Specifically, we have established that the Soxhlet extraction of POM with acetonitrile produces artifactual mutagenicity, and we recommend that acetonitrile not be used to extract POM for mutagenicity testing.

- The contributions of the m/z 247 nitroarenes to the overall direct mutagenicity of the dichloromethane extracts of several ambient POM samples from Claremont and Torrance were calculated to range from ~1 to ~10%. In one Claremont sample, 2-nitrofluoranthene alone contributed as much as 5% to the observed mutagenicity. In the Torrance sample in which 10% of the mutagenicity could be attributed to these nitroarene species, 8-nitrofluoranthene, 3-nitrofluoranthene and 2-nitrofluoranthene each contributed comparable amounts. 1-Nitropyrene, the only m/z 247 isomer

well documented to be present in several direct particulate emissions, contributed a maximum of only 0.2% to the observed mutagenicity.

From intercomparisons between data obtained with the long pathlength FT-IR and DOAS systems with data obtained with other methods employed at the Nitrogen Species Measurement Methods Intercomparison Study and the Carbonaceous Species Methods Comparison Study, the following conclusions can be drawn.

- Measurements of  $\text{HNO}_3$  by the FT-IR spectrometer and two tunable-diode laser systems (TDLS) agreed to within ~15-25% depending upon the concentration of  $\text{HNO}_3$ , with the TDLS generally yielding systematically lower values.

- Results from two non-continuous sampling methods, the annular denuder and the denuder difference methods, agreed well with the FT-IR data, while the filter pack yielded values approximately 30% high. For ammonia, on the other hand, the citric-acid impregnated filter pack yielded values which agreed with the FT-IR measurements to within better than 15%.

- Excellent agreement was obtained between the FT-IR and DOAS systems for ambient formaldehyde concentrations.

- An interesting feature of the DOAS data from the Claremont study was the observation of peak HONO concentrations before midnight which declined rather than increased (as observed previously) until sunrise.

- At the Torrance site we failed to see any significant levels of  $\text{NO}_3$  radicals and conclude that  $\text{NO}_3$ , and thus  $\text{N}_2\text{O}_5$ , play only a minor role in nighttime chemistry in the source areas in the western part of the South Coast basin impacted by elevated NO concentrations.

- A notable aspect of the Torrance study was our observation of ~11 ppb of HONO during the evening of January 27-28, the highest value we have measured to date in the South Coast Air Basin.

In summary, in the South Coast Air Basin, a significant portion of ambient particulate mutagenicity can be accounted for by a relatively few highly mutagenic nitroarenes. We now know that these species are indeed formed from their parent PAH as particle emissions travel from source to receptor and that nitrogenous species such as  $\text{N}_2\text{O}_5$  can play a major role in their formation. We have elucidated both the formation pathways for these nitroarenes and their contributions to the observed direct mutagenic

activity of ambient POM. Thus, our data allow the relative importance of the formation of mutagenic nitroarenes during transport and during Hi-vol collection of ambient POM and the role of nitrogenous pollutants in these processes to be assessed.

The statements and conclusions in this report are those of the contractor and not necessarily those of the California Air Resources Board. The mention of commercial products, their source or their use in connection with material reported herein is not to be construed as either an actual or implied endorsement of such products.



**THE ROLE OF NITROGENOUS POLLUTANTS  
IN THE FORMATION OF ATMOSPHERIC MUTAGENS  
AND ACID DEPOSITION**

Final Report

Contract No. A4-081-32

California Air Resources Board

March 1987

Principal Investigator

Dr. Arthur M. Winer

Co-Investigator

Dr. Roger Atkinson

Program Research Staff

Dr. Janet Arey  
Dr. Heinz W. Biermann  
Mr. William P. Harger  
Dr. Ernesto C. Tuazon  
Dr. Barbara Zielinska

STATEWIDE AIR POLLUTION RESEARCH CENTER  
UNIVERSITY OF CALIFORNIA  
RIVERSIDE, CALIFORNIA 92521



## ABSTRACT

Previous research from this laboratory provided evidence for a nighttime pathway for formation of nitric acid (via  $\text{NO}_2$ ,  $\text{NO}_3$  and  $\text{N}_2\text{O}_5$  reactions) and for atmospheric transformations of polycyclic aromatic hydrocarbons (PAH) via reaction with nitrogenous species to form mutagenic nitroarenes. In this program we conducted three separate field studies in the California South Coast Air Basin to (a) provide information concerning the relative importance of atmospheric transformations and sampling artifacts in determining the mutagenic burden in California's atmospheres and (b) generate in-situ, quantitative, and interference-free measurements of the ambient concentrations of  $\text{HONO}$ ,  $\text{NO}_2$ ,  $\text{HNO}_3$ ,  $\text{NH}_3$  and  $\text{NO}_3$  radicals (as well as  $\text{HCHO}$ ) which could serve as benchmark data for comparison with other less specific analytical methods participating in the CARB-sponsored Nitrogen Species Measurement Methods and Carbonaceous Species Methods Intercomparison Studies. Specifically, intensive monitoring programs were conducted between September 11 and 19, 1985 at Pomona College in Claremont, during January and February 1986 at El Camino Community College in Torrance, and between August 12 and 21, 1986 at Citrus College in Glendora.

Our major findings and conclusions include the following:

- As we have observed previously, the most abundant nitroarene in the ambient POM was 2-nitrofluoranthene (observed at levels as high as  $1.7 \text{ ng m}^{-3}$ ) which is not emitted from known emission sources in the South Coast Air Basin.

- Several other  $m/z$  247 nitroarene isomers were also observed, most of these less abundant isomers being reported in ambient POM for the first time. Their typical order of abundance was: 2-nitrofluoranthene > 1-nitropyrene ~ 2-nitropyrene > 8-nitrofluoranthene > 3-nitrofluoranthene ~ 4-nitropyrene ~ 7-nitrofluoranthene ~ nitroacephenanthrylene.

- The most abundant gas-phase PAH at Torrance were naphthalene, the 1- and 2-methylnaphthalenes and biphenyl, together with lesser amounts of  $\text{C}_2$ -naphthalenes, fluorene and phenanthrene.

- An important observation made at Torrance was that the most abundant nitroarenes were the more volatile species (e.g., 1- and 2-nitro-naphthalene and 3-nitrobiphenyl) and these hydrocarbons volatile nitroarenes appear to be atmospheric transformation products of the parent aromatic. Clearly, the health implications of these abundant, largely gas-phase, nitroarene species must be evaluated.

- Utilizing the findings from this research program concerning the formation of nitroarenes in the adsorbed phase during atmospheric transport and sampling, together with results from our laboratory research, we have elucidated the major atmospheric formation routes for these nitroarenes.

- We found no evidence for mutagenicity artifacts occurring on TIGF filters, but the results for the GF filters indicated that the uncoated glass fiber surface was more reactive. For this reason, we will continue to use TIGF filters for the Hi-vol collection of ambient POM for mutagenicity determinations.

- Of particular importance was our observation that the method of POM extraction has a considerable effect on its mutagenicity. Specifically, we have established that the Soxhlet extraction of POM with acetonitrile produces artifactual mutagenicity, and we recommend that acetonitrile not be used to extract POM for mutagenicity testing.

- The contributions of the m/z 247 nitroarenes to the overall direct mutagenicity of the dichloromethane extracts of several ambient POM samples from Claremont and Torrance were calculated to range from 1 to 10%. In one Claremont sample, 2-nitrofluoranthene alone contributed as much as 5% to the observed mutagenicity.

From intercomparisons between data obtained with the long pathlength FT-IR and DOAS systems with data obtained with other methods employed at the Nitrogen Species Measurement Methods Intercomparison Study and the Carbonaceous Species Methods Comparison Study, the following conclusions can be drawn.

- Measurements of HNO<sub>3</sub> by the FT-IR spectrometer and two tunable-diode laser systems (TDLs) agreed within ~15-25% depending upon the concentration of HNO<sub>3</sub>, with the TDLs generally yielding systematically lower values.

- Results from two non-continuous sampling methods, the annular denuder and the denuder difference methods, agreed well with the FT-IR data, while the filter pack yielded values ~30% high. For ammonia, on the other hand, the citric-acid impregnated filter pack yielded values which agreed with the FT-IR measurement to within better than 15%.

- Excellent agreement was obtained between the FT-IR and DOAS systems for ambient formaldehyde concentrations.

- An interesting feature of the DOAS data from the Claremont study was the observation of peak HONO concentrations before midnight which declined rather than increased (as observed previously) until sunrise.

- At the Torrance site we failed to see any significant levels of NO<sub>3</sub> radicals and we conclude that NO<sub>3</sub>, and thus N<sub>2</sub>O<sub>5</sub>, plays only a minor role in nighttime chemistry in source areas in the western part of the South Coast basin impacted by elevated levels of NO.

- A notable aspect of the Torrance study was our observation of ~11 ppb of HONO during the evening of January 27-28, the highest value we have measured to date in the South Coast Air Basin.

In summary, in the South Coast Air Basin a significant portion of ambient particulate mutagenicity can be accounted for by a relatively few highly mutagenic nitroarenes which are largely atmospheric reaction products, rather than directly-emitted species. We have elucidated both the formation pathways for these nitroarenes and their contribution to the observed direct mutagenic activity of ambient POM. Thus, our data allow the relative importance of the formation of mutagenic nitroarenes during transport and during Hi-vol collection of ambient POM, and the role of nitrogenous pollutants in these processes, to be assessed.

## TABLE OF CONTENTS

	<u>Page</u>
Abstract	ii
Acknowledgment	viii
Disclaimer	ix
List of Figures	x
List of Tables	xviii
Glossary of Terms, Abbreviations and Symbols	xxiii
I. PROJECT SUMMARY	
A. Introduction and Statement of the Problem	I-1
B. Objectives	I-2
C. Methods of Approach	I-3
D. Summary of Results and Conclusions	I-4
E. Recommendations for Future Research	I-8
II. INTRODUCTION	II-1
A. Background to Present Study	II-1
B. Major Objectives	II-1
C. Changes in Program Emphasis to Meet CARB Objectives	II-7
D. Organization of this Final Report	II-8
III. MEASUREMENT SITES AND PROTOCOLS	III-1
A. Introduction	III-1
1. Pomona College Study (Claremont)	III-2
2. El Camino Community College (Torrance)	III-6
3. Citrus Community College (Glendora)	III-9
IV. MEASUREMENTS OF HONO, NO <sub>2</sub> , NO <sub>3</sub> RADICALS AND HCHO BY DIFFERENTIAL OPTICAL ABSORPTION SPECTROSCOPY	IV-1
A. Introduction	IV-1
B. Experimental Methods	IV-1
1. Design and Construction of 25 m Basepath DOAS System	IV-1
C. Results and Discussion	IV-8
1. Pomona College Study (Claremont), September 1985	IV-8
2. El Camino Community College Study (Torrance)	IV-21
3. Citrus College Study (Glendora)	IV-33

TABLE OF CONTENTS  
(continued)

	<u>Page</u>
V. LONG PATHLENGTH FT-IR MEASUREMENTS OF HNO <sub>3</sub> , NH <sub>3</sub> AND HCHO	V-1
A. Introduction	V-1
B. Experimental	V-3
1. Kilometer Pathlength FT-IR System	V-3
2. Acquisition of Spectra	V-6
3. Calibration	V-6
4. Treatment of Data	V-11
C. Results and Discussion	V-14
1. The 1985 Summer Field Study at Pomona College (Claremont, CA)	V-14
2. The 1985/1986 Winter Field Study at El Camino Community College (Torrance, CA)	V-27
3. The 1986 Summer Field Study at Citrus College (Glendora, CA)	V-31
VI. AMBIENT MEASUREMENTS OF GASEOUS AND PARTICLE-ASSOCIATED POLYCYCLIC AROMATIC HYDROCARBONS AND MUTAGENIC NITROARENES	VI-1
A. Introduction	VI-1
B. Experimental	VI-1
1. Pomona College (Claremont) Summer Field Study: Sample Collection and Extraction	VI-1
2. El Camino Community College (Torrance) Winter Field Study: Sample Collection, Extraction and Fractionation	VI-3
3. Analysis	VI-6
C. Results and Discussion	VI-7
1. Claremont Summertime Samples	VI-7
2. Torrance Wintertime Samples	VI-11
3. Claremont Summertime and Torrance Wintertime Samples	VI-17
VII. CONTRIBUTION OF NITROARENES TO THE MUTAGENICITY OF AMBIENT POM DURING WINTER AND SUMMER AIR POLLUTION EPISODES	VII-1
A. Introduction	VII-1
B. Experimental	VII-2
1. Pomona College (Claremont) Sample Collection, Extraction and Mutagenicity Testing	VII-2
2. El Camino Community College (Torrance) Sample Collection, Extraction and Mutagenicity Testing	VII-5

TABLE OF CONTENTS  
(continued)

	<u>Page</u>
C. Results and Discussion	VII-6
1. Nitroarene Mutagenicity in Ambient POM	VII-6
2. Ambient Mutagenicity of Dichloromethane Extracts on Strains TA98NR and TA98/1,8-DNP <sub>6</sub>	VII-9
3. General Observations on Ambient Particulate Mutagenicity	VII-12
VIII. INVESTIGATION OF NITROARENE FORMATION IN THE ADSORBED PHASE DURING TRANSPORT AND SAMPLING	VIII-1
A. Introduction	VIII-1
B. Experimental	VIII-3
1. Active Exposures of Deuterated PAH at El Camino Community College (Torrance)	VIII-3
2. Passive Exposures at Torrance and Riverside	VIII-6
C. Results	VIII-7
1. Active Exposures of Deuterated PAH at Torrance	VIII-7
2. Passive Exposures	VIII-16
IX. STUDIES OF POTENTIAL MUTAGENICITY ARTIFACTS	IX-1
A. Introduction	IX-1
B. Experimental	IX-2
1. Mutagen Densities of Ambient POM Collected on Two Filter Types at Claremont, CA (1985)	IX-2
2. Effect of Extraction Method on the Mutagenicity of POM	IX-4
3. Investigation of Mutagenicity Artifacts During Hi-vol Collection	IX-4
C. Results and Discussion	IX-6
1. Mutagen Densities of Ambient POM at Claremont	IX-6
2. Effect of Extraction Method on the Mutagenicity of POM	IX-8
3. Investigation of Mutagenicity Artifacts During Hi-vol Collection	IX-11
X. THE MUTAGENICITY OF 2-NITROFLUORANTHENE AND ITS <u>IN VITRO</u> HEPATIC METABOLITES	X-1
A. Introduction	X-1
B. Experimental	X-1
C. Results and Discussion	X-3
XI. CONCLUSIONS AND RECOMMENDATIONS	XI-1
A. Introduction	XI-1

TABLE OF CONTENTS  
(continued)

	<u>Page</u>
B. <u>In-Situ</u> Spectroscopic Measurements of Gas-Phase Atmospheric Species	XI-2
C. Nitroarene Formation During Atmospheric Transport and Sampling: Implications for Health Effects and Ambient Mutagenicity	XI-10
D. Recommendations for Future Research	XI-27
XII. REFERENCES	XII-1
APPENDIX A: Research Papers, and Publications Resulting from Technical Presentations, Arising Wholly or in Part from this Research Program	A-1
APPENDIX B: DOAS Data for HONO, HCHO and NO <sub>2</sub> from the Pomona College, Claremont (September 1985) and Citrus College, Glendora (August 1986) Studies	B-1
APPENDIX C: Supplementary Ambient Air Data from the El Camino Community College Study at Torrance, January/February 1986	C-1
APPENDIX D: FT-IR Spectroscopic Data for HNO <sub>3</sub> , NH <sub>3</sub> and HCHO Concentrations During the Citrus College Study (Glendora), August 12-21, 1986	D-1
APPENDIX E: GS/MS-MID Traces for Ambient POM Collected at Pomona College (Claremont) and El Camino Community College (Torrance) Studies	E-1

## ACKNOWLEDGMENTS

Stimulating discussion and valuable exchanges of technical information, for which we express our appreciation, took place at various times during this program with Drs. Douglas R. Lawson, John R. Holmes and Jack K. Suder, members of the California Air Resources Board research staff.

We gratefully acknowledge Mr. Chris Berglund, Mr. Travis Dinoff, Mr. Frank Finazzo, Mr. Michael Kienitz, Mr. William Long, Mr. Ervin Mateer, Ms. Patricia McElroy, Ms. Li Li Parker, and Mr. Phillip Pelzel for assistance in carrying out this research. We thank Ms. Christy LaClaire and Ms. Barbara Cooper for typing and assembling this report and Ms. Diane Skaggs, Ms. Anne Greene and Ms. Cheryl Starr for their assistance in the fiscal administration of this project.

Numerous individuals and organizations made valuable contributions to this work and we wish to express our appreciation to the following: Dr. James N. Pitts, Jr., Director of SAPRC, encouraged us to undertake this research and generously made available to the program substantial equipment and instrument resources. The administrators and staff of El Camino Community College, especially Mr. John Stimac and Mr. Hernani Ledesma, were exceptionally cooperative in allowing us to conduct the winter field study on their campus. Mr. Jerry Arnold and Mr. Arthur Davidson of the South Coast Air Quality Management District graciously provided air quality forecasts which were used to choose monitoring days during the winter field study. Drs. Robert Haas and Carl Hanson collaborated with us on the identification of the in vitro hepatic metabolites of 2-nitrofluoranthene. Ms. Susanne Hering provided valuable logistical support during the Pomona College and Citrus College studies.

This report was submitted in fulfillment of Contract No. A4-081-32 by the Statewide Air Pollution Research Center, University of California, Riverside, under the partial sponsorship of the California Air Resources Board. Work on this program was completed as of March 14, 1987.

The statements and conclusions in this report are those of the contractor and not necessarily those of the California Air Resources Board. The mention of commercial products, their source or their use in connection with material reported herein is not to be construed as either an actual or implied endorsement of such products.

LIST OF FIGURES

<u>Figure Number</u>	<u>Title</u>	<u>Page</u>
III-1	Locations of the three study sites used in this program	III-3
III-2	Location of September 1985 field study on Pomona College campus. ★ - Field study site	III-4
III-3	Layout of the Claremont study site illustrating the positions of the longpath FT-IR and DOAS systems and other SAPRC instruments relative to the instruments of the other participants on the Pomona College campus, September 1985	III-5
III-4	El Camino Community College campus showing location of winter field study on the roof of the Technical Arts building. ★ - Field study site	III-8
III-5	Citrus College campus showing location of August 1986 field study adjacent to football stadium. ★ - Field study site	III-10
III-6	Positions of the longpath FT-IR and DOAS systems and UCR Hi-vols relative to the instruments of the other participants in the Carbonaceous Aerosol Study on the Citrus College campus, August 1986	III-11
IV-1	Schematic diagram of the longpath DOAS system	IV-2
IV-2	Reflectance properties of 37-layer dielectric coating employed in DOAS multiple reflection optical system	IV-7
IV-3	DOAS reference spectra generated for nitrogen dioxide, nitrous acid and formaldehyde, indicating principal absorption bands used for quantitative atmospheric measurements	IV-9
IV-4	DOAS spectrum of ambient air covering the wavelength region ~340-375 nm from the night of September 15-16, 1985: (a) full scale air spectrum [the zero intensity line overlaps trace (b)]; (b) after removal of background curvature; (c) same as (b), magnified by a factor of 16; (d) NO <sub>2</sub> reference; (e) after NO <sub>2</sub> subtraction, magnified by a factor of 4; (f) HONO reference spectrum.	IV-11
IV-5	Nitrous acid and NO <sub>2</sub> time-concentration profiles for September 11-13, 1985, measured by DOAS system at Claremont, CA	IV-17
IV-6	Nitrous acid and NO <sub>2</sub> time-concentration profiles for September 13-15, 1985, measured by DOAS system at Claremont, CA	IV-18

LIST OF FIGURES  
(continued)

<u>Figure Number</u>	<u>Title</u>	<u>Page</u>
IV-7	Nitrous acid and NO <sub>2</sub> time-concentration profiles for September 15-17, 1985, measured by DOAS system at Claremont, CA	IV-19
IV-8	Nitrous acid and NO <sub>2</sub> time-concentration profiles for September 17-19, 1985, measured by DOAS system at Claremont, CA	IV-20
IV-9	NO <sub>2</sub> (○) and HONO (●) profiles on January 27-28, 1986, at El Camino Community College, Torrance, CA. Measured by longpath (600 m) DOAS	IV-23
IV-10	Nitrous acid time-concentration profile measured with long pathlength DOAS system during the evening of January 21-22, 1986, at El Camino Community College, Torrance, CA	IV-24
IV-11	Nitrous acid time-concentration profile measured with long pathlength DOAS system during the evening of January 23-24, 1986, at El Camino Community College, Torrance, CA	IV-25
IV-12	Nitrous acid time-concentration profile measured with long pathlength DOAS system during the evening of January 24-25, 1986, at El Camino Community College, Torrance, CA	IV-26
IV-13	Nitrous acid time-concentration profile measured with long pathlength DOAS system during the evening of January 28-29, 1986, at El Camino Community College, Torrance, CA	IV-27
IV-14	Nitrous acid time-concentration profile measured with long pathlength DOAS system during the evening of February 5-6, 1986, at El Camino Community College, Torrance, CA	IV-28
IV-15	Time concentration profiles for nitrogen dioxide measured by DOAS and chemiluminescence (NO <sub>x</sub> -NO) at Citrus College (Glendora) in August 1986	IV-35
IV-16	Time concentration profiles for formaldehyde measured by long pathlength DOAS and FT-IR spectrometers at Citrus College (Glendora) in August 1986	IV-36

LIST OF FIGURES  
(continued)

<u>Figure Number</u>	<u>Title</u>	<u>Page</u>
IV-17	Nitrous acid time-concentration profiles measured by long pathlength DOAS system at Citrus College (Glendora) in August 1986	IV-37
V-1	Relative arrangement of the longpath FT-IR and DOAS systems	V-4
V-2	Schematic optical diagram of the longpath FT-IR spectrometer	V-5
V-3	Reference spectra of gaseous HNO <sub>3</sub> (0.61 torr) and NH <sub>3</sub> (0.23 torr) at spectral resolution of 0.125 cm <sup>-1</sup> , path length of 25 cm, total pressure with N <sub>2</sub> of 740 torr. The HNO <sub>3</sub> plot is offset by 0.30 absorbance (base 10) unit for clarity. Asterisks mark the absorption peaks used for analysis	V-7
V-4	Infrared absorption peaks of HNO <sub>3</sub> (lower trace) relative to atmospheric H <sub>2</sub> O absorptions (upper trace) in the 870-910 cm <sup>-1</sup> region	V-8
V-5	Infrared absorption peaks of NH <sub>3</sub> (lower trace) relative to atmospheric H <sub>2</sub> O and CO <sub>2</sub> absorptions (upper trace) in the 1080-1120 cm <sup>-1</sup> region	V-10
V-6	FT-IR spectroscopic detection of HNO <sub>3</sub> during the pollution episode of September 14, 1985 in Claremont, CA	V-18
V-7	Comparison of 5-minute average concentrations from the TDLS and FT-IR methods. The 1:1 line is shown (adapted from Hering et al. 1987)	V-22
V-8	Period averages measured by FT-IR compared to those of the other methods (adapted from Hering et al. 1987)	V-22
V-9	Instantaneous NH <sub>3</sub> concentrations in Claremont, CA, during the period September 12-18, 1985, as measured by FT-IR spectroscopy	V-25
V-10	FT-IR spectroscopic detection of NH <sub>3</sub> in Claremont, CA, on September 16, 1985. The arrow indicated the measurement peak of NH <sub>3</sub> at 1103.4 cm <sup>-1</sup>	V-26
V-11	Time-concentration profiles for formaldehyde, nitric acid and ammonia measured by long pathlength FT-IR spectroscopy during the 1986 Citrus College study	V-33

LIST OF FIGURES  
(continued)

<u>Figure Number</u>	<u>Title</u>	<u>Page</u>
V-12	Time-concentration plots of average HNO <sub>3</sub> (FT-IR), NO <sub>2</sub> (DOAS), and O <sub>3</sub> (Dasibi monitor) at Citrus College for August 15-16, 1986	V-38
V-13	Time concentration plots of average HNO <sub>3</sub> (FT-IR), NO <sub>2</sub> (DOAS), and O <sub>3</sub> (Dasibi monitor) at Citrus College for August 18-19, 1986	V-39
VI-1	Schematic of modified Hi-vol sampler with PUF plugs underneath the filter to collect gas phase species and compounds "blown-off" the filter	VI-4
VI-2	GS/MS-MID traces showing nitroarene molecular ion peaks for: A: Nitroarene-containing HPLC fraction of extract from first PUF plug, nighttime sample (1800-0600 hr). B: Nitroarene-containing HPLC fraction of extract from first PUF plug, daytime sample (0600-1800 hr). m/z = 180, Molecular ion of deuterated 1-nitronaphthalene (1-NN-d <sub>7</sub> ) added to both extracts in equal amounts as in internal standard; m/z = 173, molecular ion of nitronaphthalenes (NN); m/z = 187, molecular ion of methylnitronaphthalenes; m/z = 199, molecular ion of nitrobiphenyls(NBPh). GC separation on a 30 m DB-5 fused silica capillary column. Injection at 50°C, then programmed at 8°C min <sup>-1</sup> to 250°C. (Additional retention times: 2-nitrobiphenyl, 12.2-12.3 min; 4-nitrobiphenyl 14.4-14.5 min.) [From Arey et al. 1987]	VI-16
VI-3	GS/MS-MID traces from the analysis of an HPLC fraction of an extract of an ambient POM sample collected at Torrance, CA from 0500-1700 hr on January 28, 1986. Shown are the m/z 247 molecular ion of the nitrofluoranthene (NF) and nitropyrene (NP) isomers and the m/z 256 molecular ion of the deuterated internal standards, 2-nitrofluoranthene-d <sub>9</sub> (2-NF-d <sub>9</sub> ) and 1-nitropyrene-d <sub>9</sub> (1-NP-d <sub>9</sub> ). Chromatography was done on a 30 m DB-5 fused silica capillary column with injection at 50°C, then programming at 8°C min <sup>-1</sup> (from Arey et al. 1986)	VI-18
VI-4	GS/MS-MID traces of the m/z 247 molecular ion of the nitrofluoranthenes (NF) and nitropyrenes (NP) using a 60-m DB-5 narrow bore fused-silica capillary column directly interfaced to the MS. A: Analysis of a standard mixture of all eight NF and NP isomers. B: Analysis of Claremont 1800-2400 hr 9/14/85 ambient POM sample. C: Analysis of Torrance 1700-0500 hr	VI-19

LIST OF FIGURES  
(continued)

<u>Figure Number</u>	<u>Title</u>	<u>Page</u>
VI-4 (contd)	1/27-28/86 ambient POM sample. The peak labeled "a" is a nitroacephenanthrylene isomer (see Section XI.C for detailed discussion). See text for details of POM extraction and HPLC fractionations. Column conditions: injection at 50°C, programmed at 20°C min <sup>-1</sup> to 200°C, then at 4°C min <sup>-1</sup> to ~340°C. Complete ion traces showing fragment ion and deuterated internal standards are given in Appendix E	
VII-1	The SAPRC four-by-four high-volume mega-sampler	VII-3
VII-2	Diurnal variations of the collected particulate matter (µg m <sup>-3</sup> ), nitrogen dioxide concentration (ppb), nitro-PAH (N-PAH) concentration (sum of 2-NF, 1-NP and 2-NP, µg g <sup>-1</sup> particulate matter) for September 14-15, 1985, at Claremont, CA	VII-13
VII-3	Mutagen density, mutagen loading, and specific activity, January and February 1986, Torrance, CA. A: 1/21, 0000-0700 hr; B: 1/21, 0700-1700 hr; C: 1/27-28, 1700-0500 hr; D: 1/28, 0500-1700 hr; E: 2/23, 1800-2400 hr; F: 2/24, 0000-0600 hr; G: 2/24, 0600-1800 hr; H: 2/24, 1800-2400 hr; I: 2/25, 0000-0600 hr; J: 2/25 0600-1800 hr	VII-15
VIII-1	GS/MS-MID analysis of the nitroarene fraction (from an HPLC separation) of the extract of a POM-laden TIGF filter doped with 1 mg PY-d <sub>10</sub> and placed in a Hi-vol sampler operating from 1700-2400 hr on January 27, 1986 at Torrance, CA. On the left are the characteristic fragment ions of the nitrofluoranthenes (NF) and nitropyrenes (NP): [M] <sup>+</sup> = m/z 247, [M-NO] <sup>+</sup> = m/z 217, [M-HNO <sub>2</sub> ] <sup>+</sup> = m/z 200. On the right are the corresponding fragment ions for the deuterated species: [M] <sup>+</sup> = m/z 256, [M-NO] <sup>+</sup> = m/z 226, [M-DNO <sub>2</sub> ] <sup>+</sup> = m/z 208. GC separation on a 29 m DB-5 column. Injection at 50°C, then programmed at 8°C min <sup>-1</sup> . The scaling factor for each ion is given	VIII-12
VIII-2	GS/MS-MID analysis of the nitroarene fraction of the extract of a POM-laden GF filter doped with 1 mg BaP-d <sub>12</sub> and placed in a Hi-vol sampler operating from 0700-1700 hr on January 28, 1986. Co-injected with this extract was a standard solution of 6-nitrobenzo(a)pyrene (6-NBaP). On the left are the characteristic fragment ions of the 6-NBaP: [M] <sup>+</sup> = m/z 297, [M-NO] <sup>+</sup> = m/z 267, [M-NO <sub>2</sub> ] <sup>+</sup>	VIII-13

LIST OF FIGURES  
(continued)

<u>Figure Number</u>	<u>Title</u>	<u>Page</u>
VIII-2 (contd)	= m/z 251. On the right are the corresponding fragment ions for the artifactually formed 6-nitrobenzo(a)pyrene-d <sub>11</sub> (6-NBaP-d <sub>11</sub> ): [M] <sup>+</sup> = m/z 308, [M-NO] <sup>+</sup> = m/z 278, [M-NO <sub>2</sub> ] <sup>+</sup> = m/z 262. GC conditions as given in Figure VIII-1; scaling for each ion is given.	
VIII-3	GS/MS-MID analysis of the nitroarene fraction of the extract of a POM-laden GF filter doped with 1 mg PER-d <sub>12</sub> (exposure interval as given in Figure VIII-2) and co-injected with a standard solution of 3-nitroperylene (3-NPER). On the left are the characteristic fragment ions of th 3-NPER and on the right are the corresponding fragment ions for the artifactually formed 3-nitroperylene-d <sub>11</sub> (3-NPER-d <sub>11</sub> ). Identification of the fragment ions is as given in Figure VIII-2 for the isomeric nitrobenzo(a)pyrene. GC conditions as given in Figure VIII-1; scaling factor for each ion is given	VIII-14
X-1	HPLC traces (semi-preparative Ultrasphere ODS column: CH <sub>3</sub> OH/H <sub>2</sub> O, 80%/20%, 3 ml min <sup>-1</sup> ) of extracts of four incubation mixtures of 2-nitrofluoranthene with varying amounts of S9. S9/2-nitrofluoranthene ratios (ml mg <sup>-1</sup> ) were as follows: <u>A</u> , 10; <u>B</u> , 5; <u>C</u> , 2; <u>D</u> , 1	X-5
X-2	Mass spectra of the three metabolites of 2-nitrofluoranthene labelled 1, 2, and 3 according to their HPLC retention times (RT) as shown in Figure X-1. The spectra were recorded by GC/MS using a 29 m DB-5 capillary column with injection at 50°C followed by temperature programming at 8°C min <sup>-1</sup> . The GC RT of the isomers were as follows: 1, 25.7 min; 2, 25.6 min; 3, 25.3 min	X-7
X-3	300 MHz <sup>1</sup> H NMR spectra of the metabolites 1 and 2 (in CD <sub>3</sub> OD), identified as 8-hydroxy-2-nitrofluoranthene (1) and 9-hydroxy-2-nitrofluoranthene (2) and the spectrum of 2-nitrofluoranthene (3) in CD <sub>3</sub> OD.	X-8
XI-1	Comparison of 5-minute average concentrations from the TDLS and FT-IR methods. The 1:1 line is shown (adapted from Hering et al 1987)	XI-4
XI-2	Period averages measured by FT-IR compared to those of the other methods (adapted from Hering et al. 1987)	XI-4

LIST OF FIGURES  
(continued)

<u>Figure Number</u>	<u>Title</u>	<u>Page</u>
XI-3	Time-concentration profiles for formaldehyde, nitric acid and ammonia measured by long pathlength FT-IR spectroscopy during the Citrus College study	XI-6
XI-4	Time concentration profiles for nitrogen dioxide measured by DOAS and chemiluminescence (NO <sub>x</sub> -NO) at Citrus College (Glendora) in August 1986	XI-7
XI-5	Time concentration profiles for formaldehyde measured by long pathlength DOAS and FT-IR spectrometers at Citrus College (Glendora) in August 1986	XI-9
XI-6	GS/MS-MID traces of the molecular ions of the NF and NP isomers present in ambient POM. The sample extraction and clean-up procedures have been described above (Section IV). The ambient particulate samples were collected as follows: (A) At Torrance, CA on January 28, 1986 from 0500-1700 hr., (B) At Torrance, CA on January 27-28, 1986 from 1700-1500 hr., (C) At Claremont, CA on September 18, 1985 from 1200-1800 hr., (D) At Claremont, CA on September 18, 1985 from 1800-2400 hr.	XI-19
XI-7	GS/MS-MID traces of the molecular ions of the NF and NP isomers present: (A) as products from the gas-phase reactions of fluoranthene and pyrene with the OH radical in the presence of NO <sub>x</sub> ; (B) in the extract of the ambient POM sample collected at Torrance, CA on January 28, 1986 from 0500-1700 hr. Two different (~30 m) GC columns were used for these analyses and thus the retention times are slightly different. The ambient sample is that shown in Figure XI-6(A) with the 2-nitrofluoranthene peak plotted off-scale to allow the minor isomers to be readily identified	XI-20
XI-8	GS/MS-MID traces of the m/z 247 molecular ions of: (A) A standard mixture containing all eight NF and NP isomers. (B) the NF and NP isomers present in the ambient POM sampler collected at Torrance, CA on January 27-28, 1986 from 1700-0500 hr [(the peak labeled "a" can be seen to elute at the retention time of the most abundant nitroacephenanthrylene isomer shown in (C)]. (C) The nitroarene products of the gas-phase reaction of acephenanthrylene with the OH radical in the presence of NO <sub>x</sub> . GC column and conditions: 60 m DB-5N column, injection at 50°C, then programmed at 20°C min <sup>-1</sup> to 200°C, then at 4°C min <sup>-1</sup> . 2-Nitrofluoranthene-d <sub>9</sub> was used as an internal standard to give the precise relative retention times. See Appendix E for additional ion traces	XI-21

LIST OF FIGURES  
(continued)

<u>Figure Number</u>	<u>Title</u>	<u>Page</u>
XI-9	GS/MS-MID traces of the m/z 247 molecular ion of the NF, NP and nitroacephenanthrylene (labeled "a") isomers present in ambient POM samples collected at: (A) Claremont, CA on September 14, 1985 from 1800-2400 hr. (B) Torrance, CA on January 28, 1986 from 0500-1700 hr. GC column and conditions as given in Figure XI-8	XI-22

LIST OF TABLES

<u>Table Number</u>	<u>Title</u>	<u>Page</u>
IV-1	Calculated Detection Limits for 25-m Basepath Multiple-Reflection Cell DOAS System Operated at 1km Pathlength	IV-5
IV-2	Hourly Average NO <sub>2</sub> Concentrations (ppb) <sup>a</sup> Measured During the 1985 Claremont Study by the Long Pathlength DOAS System	IV-13
IV-3	Hourly Average HONO Concentrations (ppb) <sup>a,b</sup> Measured During the 1985 Claremont Study by the Long Pathlength DOAS System	IV-14
IV-4	Average NO <sub>2</sub> Concentrations (ppb) Measured by the Long Pathlength DOAS System for the Designated Sampling Periods at Claremont (1985)	IV-15
IV-5	Average HONO Concentrations (ppb) Measured by the Long Pathlength DOAS System for the Designated Sampling Periods at Claremont (1985) <sup>a</sup>	IV-15
IV-6	Half-Hour Average NO <sub>2</sub> and HONO Concentrations (ppb) <sup>a</sup> at El Camino Community College, Torrance, CA	IV-29
IV-7	Maximum O <sub>3</sub> Levles and Observations of NO <sub>3</sub> Radicals at Citrus College, Glendora, CA, During August 13-20, 1986	IV-34
IV-8	Hourly Average HONO Concetrations (ppb) <sup>a,b</sup> Measured by the Long Pathlength DOAS system During the 1986 Citrus College Study	IV-38
IV-9	Hourly Average NO <sub>2</sub> Concentrations (ppb) <sup>a</sup> Measured by the Long Pathlength DOAS System During the 1986 Citrus College Study	IV-39
IV-10	Hourly Average HCHO Concentrations (ppb) <sup>a</sup> Measured by the Long Pathlength DOAS System During the 1986 Citrus College Study	IV-40
V-1	Infrared Absorptivities and Calculated Detection Limits for Long Pathlength FT-IR Spectroscopic Measurements of Ambient Pollutants	V-12
V-2	HNO <sub>3</sub> and NH <sub>3</sub> Concentrations (ppb) <sup>a,b,c</sup> vs. Time in Claremont, CAA, on September 14, 1985, by Long Pathlength FT-IR Spectroscopy	V-15
V-3	HNO <sub>3</sub> and NH <sub>3</sub> Concentrations (ppb) <sup>a,b</sup> vs. Time in Claremont, CA, on September 17, 1985, by Long Pathlength FT-IR Spectroscopy	V-16

LIST OF TABLES  
(continued)

<u>Table Number</u>	<u>Title</u>	<u>Page</u>
V-4	Hourly Average HNO <sub>3</sub> Concentrations (ppb) <sup>a,b,c</sup> at Claremont, CA, During September 1986, Measured by Long Pathlength FT-IR Spectroscopy	V-19
V-5	Average HNO <sub>3</sub> Concentrations (ppb) <sup>a,b,c</sup> Measured by Long Pathlength FT-IR Spectroscopy for the Designated Sampling Periods During the Claremont Study in 1985	V-20
V-6	Hourly Average NH <sub>3</sub> Concentrations (ppb) <sup>a,b,c</sup> Measured by Long Pathlength FT-IR Spectroscopy at Claremont, 1985	V-24
V-7	Average NH <sub>3</sub> Concentrations (ppb) <sup>a</sup> Measured by Long Pathlength FT-IR Spectroscopy for the Designated Sampling Periods	V-27
V-8	HNO <sub>3</sub> and HN <sub>3</sub> Concentrations (ppb) vs. Time in Torrance, CA on February 24, 1986, Measured by Long Pathlength FT-IR Spectroscopy	V-29
V-9	HNO <sub>3</sub> and HN <sub>3</sub> Concentrations (ppb) vs Time in Torrance, CA, on February 25, 1986, Measured by Long Pathlength FT-IR Spectroscopy	V-30
V-10	HNO <sub>3</sub> and HN <sub>3</sub> Concentrations (ppb) vs. Time in Torrance, CA, on February 26, 1986, Measured by Long Pathlength FT-IR Spectroscopy	V-31
V-11	Hourly Average HNO <sub>3</sub> Concentrations (ppb) at Glendora, CA, August 12-20, 1986, Measured by Long Pathlength FT-IR Spectroscopy	V-34
V-12	Hourly Average NH <sub>3</sub> Concentrations (ppb) at Glendora, CA, August 12-21, 1986, Measured by Long Pathlength FT-IR Spectroscopy <sup>a</sup>	V-35
V-13	Hourly Average HCHO Concentrations (ppb) at Glendora, CA, August 12-21, 1986, Measured by Long Pathlength FT-IR Spectroscopy <sup>a</sup>	V-36
VI-1	Molecular Ions, Characteristic Fragment Ions and Relative Abundances Used for Identification of Nitroarenes by GS/MS-MID	VI-8
VI-2	Particle Concentrations, Percent Extractable, Average Temperature and Concentrations of Selected PAH in Ambient POM Samples Collected on September 14-15, 1985, at Claremont, CA	VI-9

LIST OF TABLES  
(continued)

<u>Table Number</u>	<u>Title</u>	<u>Page</u>
VI-3	The Concentrations of 2-Nitrofluoranthene (2-NF), 1-Nitropyrene (1-NP) and 2-Nitropyrene (2-NP) in Ambient POM Samples Collected on TIGF Filters in September 1985 at Claremont, CA	VI-10
VI-4	Ambient Concentrations ( $\text{ng m}^{-3}$ ) of PAH and Nitroarenes. Nighttime Sample Collected at El Camino Community College, Torrance, CA February 24 - 25, 1986, 1800 - 0600 hr	VI-12
VI-5	Ambient Concentrations ( $\text{ng m}^{-3}$ ) of PAH and Nitroarenes. Daytime Sample Collected at El Camino Community College, Torrance, CA February 25, 1986, 0600 - 1800 hr	VI-13
VI-6	The Concentrations of 2-Nitrofluoranthene (2-NF), 1-Nitropyrene (1-NP) and 2-Nitropyrene (2-NP) in Ambient POM Samples Collected on TIGF Filters During January and February 1986 at Torrance, CA	VI-15
VII-1	Direct Mutagenicity of Standard Nitroarenes (-S9)	VII-4
VII-2	Contribution of Nitrofluoranthene (NF) and Nitropyrene (NP) Isomers to the Direct Mutagenicity of Ambient POM	VII-7
VII-3	The Mutagenicity of Other Nitroarenes Detected in Ambient Air in Torrance, CA	VII-9
VII-4	Mutagenicities of Dichloromethane Extracts of Ambient Particulate Matter Collected at Claremont and Torrance, CA	VII-10
VII-5	Contributions of Measured Nitrofluoranthenes and Nitropyrenes to the Reduced Response on Strains TA98NR and TA98/1,8-DNP <sub>6</sub> at Claremont and Torrance, CA	VII-11
VIII-1	Sampling Protocol for "Active" Exposure of Deuterated PAH January 27-28, 1986, at El Camino Community College, Torrance, CA	VIII-4
VIII-2	Recovery of FL-d <sub>10</sub> in "Active" Exposures on Filters with Pre-Collected POM During the Torrance Winter Field Study	VIII-8
VIII-3	Recovery of PY-d <sub>10</sub> in "Active" Exposures on Filters with Pre-Collected POM During the Torrance Winter Field Study	VIII-8

LIST OF TABLES  
(continued)

<u>Table Number</u>	<u>Title</u>	<u>Page</u>
VIII-4	Recovery of Bap-d <sub>12</sub> in "Active" Exposures on Filters with Pre-Collected POM in the Torrance Winter Field Study	VIII-9
VIII-5	Deuterated Nitroarenes Formed Artifactually During Hi-vol Sampling	VIII-10
VIII-6	Recover of FL-d <sub>10</sub> , BaP-d <sub>12</sub> and PER-d <sub>12</sub> in "Passive" Exposures on Filters with Pre-Collected POM; Torrance Winter Field Study	VIII-17
VIII-7	Recovery of Flouranthene and Pyrene in "Passive" Exposures on Clean TIGF and GF Filters; Torrance Winter Field Study	VIII-17
VIII-8	Results of Passive Exposures of Fluoranthene (FL) and Pyrene (PY) on GF and TIGF Filters and FL-d <sub>10</sub> and PY-d <sub>10</sub> on Filters Coated with POM at El Camino Community College, Torrance, CA, in January 1986. Relative Abundances of Observed Nitroarenes	VIII-19
VIII-9	Results of Passive Exposures of Flouranthene-d <sub>10</sub> and Pyrene-d <sub>10</sub> (PY-d <sub>10</sub> ) at Riverside in August, 1986. Relative Abundance of Observed Nitroarenes	VIII-20
IX-1	Net Particulate Weights for Hi-Vol POM Collections at Claremont, CA, on TIGF and GF Filters	IX-3
IX-2	Total Activity (Net Revertants) of 16 Filter Pieces from a Single Mega-Sampler POM Collection, Compared to Single Concurrent Hi-vol Filter Sample. Carried out at Riverside, CA, 1200-1800 hr, April 16, 1986	IX-5
IX-3	Mutagen Densities TA98,-S9 (Revertants m <sup>-3</sup> ) of POM Simultaneously Collected on TiGF and GF Filters at Claremont, CA, and the Ratio of the Mutagen Densities of the Two Filter Types	IX-7
IX-4	Comparison of Total Mutagenic Activities (TA98,-S9) of Ambient POM Acetonitrile Extracts, Using Soxhlet Extraction and Ultrasonication	IX-9
IX-5	Comparison of the Total Mutagenic Activities (-S9) and the Weight of Extracts (mg) of Ambient POM Extracted by Soxhlet Extraction with Dichloromethane (CH <sub>2</sub> Cl <sub>2</sub> ) Followed by Acetonitrile (ACN) or Methanol (MeOH) -	IX-10

LIST OF TABLES  
(continued)

<u>Table Number</u>	<u>Title</u>	<u>Page</u>
IX-6	Mutagen Densities of POM Collected in Torrance, CA - Winter 1986	IX-12
IX-7	Total Activities and Mutagenicity Filter Artifacts Torrance, CA - Winter 1986	IX-13
X-1	Mutagenicity ( $\text{rev nmol}^{-1}$ ) of 2-Nitrofluoranthene and its Hydroxylated Metbolites Towards <u>Salmonella</u> <u>Typhimurium</u>	X-4
XI-1	Vapor Pressures at 298 K for Series of PAH <sup>a</sup>	XI-11
XI-2	Room Temperature Rate Constants for the Gas-Phase Reaction of OH Radicals, O <sub>3</sub> and N <sub>2</sub> O <sub>5</sub> with PAH	XI-11
XI-3	Calculated Atmospheric Lifetimes for Gas-Phase PAH Due to Reaction with OH Radicals, O <sub>3</sub> and N <sub>2</sub> O <sub>5</sub>	XI-12
XI-4	Nitroarene Products Formed from the Gas Phase Reactions of PAH, Known to be Present in Ambient Air, with OH Radicals (in the Presence of NO <sub>x</sub> ) and N <sub>2</sub> O <sub>5</sub> , Together with their Yields	XI-14
XI-5	The Possible Formation Routes to the m/z 247 Nitroarenes Under Atomspheric Conditions	XI-15
XI-6	Comparison of 2-Nitrofluoranthen (2-NF), 1-Nitropyrene (1-NP) and 2-Nitropyrene (2-NP) Concentrations in Winter and Summertime Ambient POM Samples	XI-18



## GLOSSARY OF TERMS, ABBREVIATIONS AND SYMBOLS

<u>AES</u>	Atmospheric Environment Service, Ontario, Canada
<u>AIHL</u>	Air Industrial Hygiene Laboratory, Berkely
<u>atm</u>	Atmosphere (pressure)
<u>BaP</u>	Benzo(a)pyrene
<u>BaP-d<sub>12</sub></u>	Deuterated benzo(a)pyrene
<u>°C</u>	Degrees Centigrade
<u>CARB</u>	California Air Resources Board
<u>CH<sub>2</sub>Cl<sub>2</sub></u>	Dichloromethane
<u>CH<sub>2</sub>O</u>	Formaldehyde
<u>CH<sub>3</sub>CN</u>	Acetonitrile
<u>CH<sub>3</sub>OH</u>	Methanol
<u>cm</u>	Centimeter
<u>CO</u>	Carbon monoxide
<u>Δppm</u>	Difference in parts-per-million between measured and calculated exact mass
<u>DMSO</u>	Dimethyl sulfoxide
<u>DOAS</u>	Differential optical absorption spectroscopy
<u>DOE</u>	U.S. Department of Energy
<u>EPA</u>	U.S. Environmental Protection Agency
<u>eV</u>	Electron volt
<u>°F</u>	Degrees Fahrenheit
<u>FL-d<sub>10</sub></u>	Deuterated fluoranthene
<u>ft</u>	Feet
<u>FT-IR</u>	Fourier-transform infrared absorption spectroscopy
<u>g</u>	Gram
<u>x g</u>	Force of gravity

GLOSSARY OF TERMS  
(continued)

<u>GC</u>	Gas chromatograph, gas chromatography, or gas chromatographic
<u>GC-MS</u>	Gas chromatography-mass spectrometry
<u>GF filters</u>	Glass fiber filters
<u><math>^1\text{H}</math> NMR</u>	Proton nuclear magnetic resonance
<u>HCHO</u>	Formaldehyde
<u>HCOOH</u>	Formic acid
<u>Hi-vol</u>	High volume sampler
<u>HNO<sub>3</sub></u>	Nitric acid
<u>H<sub>2</sub>O</u>	Water
<u>HONO</u>	Nitrous acid
<u>HPLC</u>	High performance liquid chromatography
<u>hr</u>	Hour
<u>Hz</u>	Hertz (cycle s <sup>-1</sup> )
<u>I</u>	Light intensity
<u>I<sub>0</sub></u>	Initial light intensity
<u>i.d.</u>	Internal diameter
<u>K</u>	Thousand
<u>K</u>	Degrees Kelvin
<u>KCl</u>	Potassium chloride
<u>km</u>	Kilometer
<u>L-broth or LB-broth</u>	Growth medium for overnight culture of <u>Salmonella</u> strains
<u>m</u>	Meter
<u>m<sup>3</sup></u>	Cubic meter
<u>M</u>	A third body, in all cases in this report M refers to air

GLOSSARY OF TERMS  
(continued)

<u>M</u>	Molar
<u>mega-sampler</u>	Ultra-high volume sampler (equivalent to 16 standard Hi-vols)
<u>mg</u>	Milligram
<u>MgCl<sub>2</sub></u>	Magnesium chloride
<u>MgF<sub>2</sub></u>	Magnesium fluoride
<u>MHz</u>	Megahertz (10 <sup>6</sup> Hz)
<u>MID</u>	Multiple ion detection technique, used together with GC-MS
<u>min</u>	Minute
<u>min<sup>-1</sup></u>	Per minute
<u>mℓ</u>	Milliliter
<u>mm</u>	Millimeter
<u>mol</u>	mole (6.022 x 10 <sup>23</sup> molecules)
<u>MS</u>	Mass spectrometer
<u>m/z</u>	Mass to charge ratio
<u>Mutagen density</u>	Atmospheric mutagenicity "concentration"; total activity divided by sampling volume (rev m <sup>-3</sup> )
<u>Mutagen loading</u>	Specific mutagenicity of the particulate matter; total activity divided by particulate weight (rev mg <sup>-1</sup> )
<u>m.w.</u>	Molecular weight
<u>NADP<sup>+</sup></u>	Nicotinamide adenine dinucleotide phosphate; cofactor for S9 activation
<u>NBS SRM 1648</u>	National Bureau of Standards, Standard Reference Material 1648, urban dust collected in St. Louis, MO
<u>NBS SRM 1649</u>	National Bureau of Standards, Standard Reference Material 1649, urban dust collected in Washington, D.C.
<u>NF</u>	Nitrofluoranthene
<u>ng</u>	Nanogram (10 <sup>-9</sup> gram)

GLOSSARY OF TERMS (continued)

<u>NH<sub>3</sub></u>	Ammonia
<u>NH<sub>4</sub>NO<sub>3</sub></u>	Ammonium nitrate
<u>Nitroarenes</u>	Nitrated polycyclic aromatic hydrocarbons (PAH)
<u>nm</u>	Nanometer (10 <sup>-9</sup> meter)
<u>NO</u>	Nitric oxide
<u>NO<sub>2</sub></u>	Nitrogen dioxide
<u>NO<sub>3</sub></u>	Gaseous nitrate radical
<u>NO<sub>x</sub></u>	Oxides of nitrogen (NO + NO <sub>2</sub> )
<u>N<sub>2</sub>O<sub>4</sub></u>	Dinitrogen tetraoxide
<u>N<sub>2</sub>O<sub>5</sub></u>	Dinitrogen pentoxide
<u>NP</u>	Nitropyrene
<u>O.D.</u>	Optical density
<u>OH</u>	Hydroxyl radical
<u>O<sub>3</sub></u>	Ozone
<u>Open column chromatography</u>	Liquid chromatography technique, used for compound separation or purification
<u>PAH</u>	Polycyclic aromatic hydrocarbons
<u>PAN</u>	Peroxyacetyl nitrate
<u>PDT</u>	Pacific daylight time
<u>PER-d<sub>12</sub></u>	Deuterated perylene
<u>pg</u>	Picogram (10 <sup>-12</sup> gram)
<u>pH</u>	-log <sub>10</sub> [H] <sup>+</sup> ; [H] <sup>+</sup> = hydrogen ion concentration in mol l <sup>-1</sup>
<u>PST</u>	Pacific standard time
<u>PER</u>	Perylene
<u>POM</u>	Particulate organic matter
<u>ppb</u>	Part per billion

GLOSSARY OF TERMS  
(continued)

<u>ppt</u>	Part per trillion
<u>PUF</u>	Polyurethane foam
<u>PY-d<sub>10</sub></u>	Deuterated pyrene
<u>rev</u>	Revertants; net response above background in the <u>Salmonella</u> mutagenicity test
<u>S9</u>	Supernatant from a 9000 x g centrifugation of rat liver homogenate
<u>SAPRC</u>	Statewide Air Pollution Research Center
<u>SCE</u>	Southern California Edison
<u>SCFM</u>	Standard cubic feet per minute
<u>Semi-prep column</u>	Semi-preparative scale column used for compound separation or purification by HPLC
<u>SO<sub>2</sub></u>	Sulfur dioxide
<u>Specific activity</u>	Specific mutagenicity of the particulate extract; slope of the <u>Salmonella</u> dose-response curve (rev $\mu\text{g}^{-1}$ )
<u>TA98</u>	Ames <u>Salmonella typhimurium</u> strain, detects frameshift mutations. Most sensitive strain for detecting ambient particulate mutagens
<u>TA98NR</u>	Nitroreductase-deficient isolate of strain TA98; less sensitive than TA98 to many mononitroarenes
<u>TA98/1,8-DNP<sub>6</sub></u>	Transacetylase-deficient isolate of strain TA98; less sensitive than TA98 to dinitropyrenes
<u>TDLS</u>	Tunable diode laser spectrometer
<u>Tenax-GC</u>	Solid adsorbent used for the collection of volatile organics
<u>TIGF filters</u>	Teflon impregnated glass fiber filters
<u>Total activity</u>	The product of specific activity and total extract weight for a given collection period (rev)
<u>UCR</u>	University of California, Riverside
<u><math>\mu\text{g}</math></u>	Microgram ( $10^{-6}$ gram)
<u><math>\mu\text{l}</math></u>	Microliter ( $10^{-6}$ liter)

GLOSSARY OF TERMS  
(continued)

<u>μm</u>	Micrometer ( $10^{-6}$ meter)
<u>μmol</u>	Micromole ( $10^{-6}$ mole)
<u>uv/vis</u>	Ultraviolet/visible
<u>W</u>	Watt

## I. PROJECT SUMMARY

### A. Introduction and Statement of the Problem

Despite enormous progress over the past fifteen years in elucidating the complex atmospheric processes which produce such phenomena as photochemical air pollution, acid deposition, visibility reduction and airborne mutagens, the specific role of nitrogenous pollutants in many aspects of air quality has remained uncertain and, in some cases, the subject of controversy. In part, these uncertainties have arisen from difficulties in quantitatively measuring the atmospheric concentrations of nitrogenous species such as nitric ( $\text{HNO}_3$ ) and nitrous ( $\text{HONO}$ ) acid, the nitrate ( $\text{NO}_3$ ) radical, dinitrogen pentoxide ( $\text{N}_2\text{O}_5$ ) and ammonia ( $\text{NH}_3$ ). Similarly, there has been a need to better characterize ambient burdens of atmospheric mutagens in highly populated airsheds, such as the South Coast Air Basin, and to determine those species responsible for such observed mutagenicity. More specifically, it is important to assess the potential role of gaseous nitrogenous pollutants in producing mutagenic compounds, in particular through reactions with the polycyclic aromatic hydrocarbons (PAH) which are emitted into ambient air.

In contrast to the Federal regulatory approach, the California Air Resources Board has historically supported development of emission control strategies for sources of oxides of nitrogen, as well as reactive organic gases. However, this dual approach, designed to address the full spectrum of adverse air quality problems and not just the ozone problem, has been challenged, particularly concerning the need for additional control of oxides of nitrogen.

To provide the necessary scientific and technical underpinnings for its emission control policies, the CARB has supported a series of field studies over the past decade designed to generate essential information concerning the reactions and ambient concentrations of key atmospheric species. The present program represents an extension of such investigations through three separate field studies focusing on the role of nitrogenous species, including an intensive application of long pathlength spectroscopy (and concurrent ambient particulate collection), at an emission "source" site at the western end of the CSCAB during characteristic high- $\text{NO}_x$  wintertime episode conditions.

## B. Objectives

As originally proposed, this program was to have involved two coordinated ambient air monitoring studies employing our in situ long path-length spectroscopic techniques, our expertise in polycyclic aromatic hydrocarbon (PAH) chemistry, and our experience in utilizing mutagenic assays as a tool for elucidating chemical transformations of PAH. However, subsequent to initiation of the present program, the CARB expressed a strong interest in obtaining in situ absolute, interference-free measurements of key species accessible to the SAPRC long pathlength optical spectrometers. Specifically, we were asked to provide quantitative and time-resolved ambient concentration data for the nitrogenous species HONO, NO<sub>2</sub>, HNO<sub>3</sub>, NH<sub>3</sub> and NO<sub>3</sub> radicals (as well as HCHO) which could serve as benchmark data for comparison with other, less specific, analytical methods for those species during the Nitrogen Species Measurement Methods Intercomparison and the Carbonaceous Species Methods Comparison Studies. As a result of these measurement protocol changes, mutually agreed to by SAPRC and CARB, a change in emphasis to provide a reliable and expanded data base for the above species is reflected in the final results and in the treatment of data in this report. Indeed, to meet this objective a total of three rather than two field studies were conducted.

The second major objective of this program involved elucidation of the role which nitrogenous species play in the atmospheric transformations of particulate organic matter (POM), including the potential for artifact formation of direct mutagens (not requiring S9 activation) from PAH during the collection of ambient POM. These issues are of direct relevance to obtaining reliable data concerning the mutagenic constituents of ambient POM which are in turn necessary for risk assessments of the mutagenic burden in California's atmospheres. Our specific objectives in this regard were to determine:

- The potential for the mutagenicity of direct POM emissions to be enhanced due to chemical transformations resulting from reactions of PAH with gaseous nitrogenous species during the residence time for POM in the atmosphere. Specifically, to determine whether mutagenic nitroarenes are formed from the reactions of adsorbed PAH with ambient levels of nitrogenous species under "passive" conditions simulating atmospheric transport.

- The extent to which the observed direct-acting mutagenicity of ambient POM could be enhanced due to artifactual formation of strongly mutagenic products during filter collections, and which nitrogenous and/or oxidative species might cause such artifacts.

- The levels of the PAH and nitroarenes present in ambient POM during a winter high-NO<sub>x</sub> pollution episode and during a summer high-oxidant episode, and the contributions these nitroarenes make to the observed ambient mutagenicity in each case.

### C. Methods of Approach

To achieve the objectives of this program intensive monitoring programs were conducted between September 11 and 19, 1985 at Pomona College in Claremont (in conjunction with the Nitrogen Species Measurement Methods Intercomparison Study), during January and February 1986 at El Camino Community College in Torrance, and between August 12 and 21, 1986 at Citrus College in Glendora (in conjunction with the Carbonaceous Species Methods Comparison Study). To avoid problems in comparing spectroscopic data obtained over kilometer distances with data from point monitors, two entirely new 25 m basepath multiple reflection optical systems were designed, constructed and interfaced to our FT-IR and differential optical absorption spectrometer (DOAS) systems. Also, for the first time, both long pathlength spectrometers were elevated on massive cement blocks (for the Claremont and Glendora studies), raising the optical beam to a height of 8 feet, and thereby minimizing any complications due to dry deposition of species such as HNO<sub>3</sub>.

For the Claremont study, the SAPRC ultra-high volume "mega-sampler" was moved to Pomona College along with two high-volume (Hi-vol) samplers, and particulate sample collections were conducted in 6-hr intervals. The study at Torrance was conducted on the roof of a two-story building and involved a total of sixteen Hi-vol samplers (as well as the DOAS and FT-IR systems). These included six standard Hi-vol samplers with 10 μm cut-off inlets run at 40 SCFM and utilizing Teflon-impregnated glass fiber (TIGF) and glass fiber (GF) filters for particulate collection; five Hi-vol samplers without inlets run at 40 SCFM; five Hi-vol samplers equipped with three polyurethane foam (PUF) plugs downstream of TIGF and GF filters, run

at flow rates of ~30 SCFM; and two Tenax-GC sampling cartridges in series, each packed with 0.1 g of the solid adsorbent and run at 1 liter min<sup>-1</sup>.

A comparable array of samplers was employed in the Glendora study operating on 12-hr sample collection periods.

#### D. Summary of Results and Conclusions

Spectroscopic Measurements. From intercomparisons between data obtained with the long pathlength FT-IR and DOAS systems vs. data obtained with other methods employed at the Nitrogen Species Measurement Methods Intercomparison Study and the Carbonaceous Aerosol Study, the following conclusions can be drawn.

- Measurements of HNO<sub>3</sub> by the FT-IR spectrometer and two tunable-diode laser systems (TDLS) agreed within ~15-25% depending upon the concentration of HNO<sub>3</sub>, with the TDLS generally yielding systematically lower values, with a greater divergence at the higher HNO<sub>3</sub> concentrations.

- Results from two non-continuous sampling methods for HNO<sub>3</sub>, the annular denuder and the denuder difference methods, agreed well with the FT-IR data, while the filter pack yielded values approximately 30% high. For ammonia, on the other hand, the citric-acid impregnated filter pack yielded values which agreed with the FT-IR measurement to within better than 15%.

- Excellent agreement was obtained between the FT-IR and DOAS systems for ambient formaldehyde concentrations.

An interesting feature of the DOAS data from the Claremont study was the observation of peak HONO concentrations before midnight which declined rather than increased (as observed previously) until sunrise. This observation was consistent with more elevated levels of NO<sub>2</sub> early in the evening which yielded calculated HONO formation rates of ~0.5 ppb hr<sup>-1</sup>, consistent with the observed increases in HONO early in the evening.

Our observations for the NO<sub>3</sub> radical were consistent with the fact that NO<sub>3</sub> radicals formed after sunset will react quickly with any NO present in the atmosphere. Thus, at the Torrance site we failed to see any significant levels of NO<sub>3</sub> radicals and we conclude that NO<sub>3</sub>, and thus N<sub>2</sub>O<sub>5</sub>, plays only a minor role in nighttime chemistry in source areas in the western part of the South Coast basin. Only in polluted areas downwind from large NO emission sources, where NO has been converted to NO<sub>2</sub>,

can higher concentrations of  $\text{NO}_3$  radicals be observed (as, for example, the 430 ppt measured in our earlier CARB-funded study in Riverside).

A notable aspect of the Torrance study was our observation of ~11 ppb of HONO during the evening of January 27-28, the highest value we have measured to date in the South Coast Air Basin. The consistently elevated levels of nitrous acid observed during this winter measurement period, in the range from 6 to 10 ppb, confirms our postulate that the highest levels of HONO in the South Coast Air Basin occur in the western end of the basin under high- $\text{NO}_x$  episode conditions. Since HONO was observed consistently in all three studies, it is clearly an ubiquitous pollutant in nighttime atmospheres. Based on the results from the three study sites, and neglecting minor fluctuations, nighttime HONO peak levels generally are higher for higher ambient  $\text{NO}_2$  concentrations, as expected from environmental chamber data. In the Glendora study, for example,  $\text{NO}_2$  levels of 60 to 75 ppb produced HONO peak concentrations between 2 to 4 ppb, whereas in Torrance, where the  $\text{NO}_2$  levels stayed nearly constant throughout the night at 120-150 ppb, HONO peaked at 6 to 11 ppb.

Ambient PAH and Nitroarenes. As we have observed previously, the most abundant nitroarene in the ambient POM analyzed was 2-nitrofluoranthene, observed at levels as high as  $1.7 \text{ ng m}^{-3}$ . Several other m/z 247 nitroarene isomers (i.e. the nitro-derivatives of three isomeric PAH present in ambient POM, namely fluoranthene, pyrene and acephenanthrylene) were also observed, most of these less abundant isomers being identified in ambient POM for the first time. The isomers observed in their typical order of abundance were: 2-nitrofluoranthene > 1-nitropyrene ~ 2-nitropyrene > 8-nitrofluoranthene > 3-nitrofluoranthene ~ 4-nitropyrene ~ 7-nitrofluoranthene ~ nitroacephenanthrylene.

The most abundant gas-phase PAH (observed on the Tenax-GC cartridges) at Torrance were naphthalene, the 1- and 2-methylnaphthalenes and biphenyl, together with lesser amounts of  $\text{C}_2$ -naphthalenes, fluorene and phenanthrene. On the first of the PUF plugs (sampling gas-phase PAH and those "blown-off" the particles collected by the filter), phenanthrene was the most abundant PAH. The PAH more volatile than phenanthrene were not quantitatively collected on the PUF plugs. As expected, quantification of ambient concentrations of fluoranthene and pyrene based solely on extracts from the filter-collected POM were significantly low, but a single PUF

plug was adequate to retain these PAH at the sampling temperatures encountered during this study.

An important observation made at Torrance was that the most abundant nitroarenes were the more volatile species. In particular, levels of 1- and 2- nitronaphthalene and 3-nitrobiphenyl as high as 3.0, 2.9, and 6.0  $\text{ng m}^{-3}$ , respectively, were measured, and several methylnitronaphthalenes were also observed. Clearly, the health implications of these abundant, largely gas-phase, nitroarene species must be evaluated.

Formation Routes to the Nitroarenes. There is strong evidence that the volatile nitroarene species we observed in ambient air at Torrance are atmospheric transformation products of the parent aromatic species. Thus the particular isomers observed, for example 3-nitrobiphenyl and 2-nitronaphthalene, are often not the species found in primary POM emissions. Additionally, in chamber studies we have observed these nitro-species to be products of the gas-phase reactions of the parent aromatic species with the OH radical in the presence of  $\text{NO}_x$  and/or with  $\text{N}_2\text{O}_5$ .

These summer and winter field studies allowed us to examine the m/z 247 nitroarenes present in ambient POM which had been exposed to different reactive atmospheric species, including key nitrogenous compounds. Thus, the POM collected in Claremont had been exposed to the reactive species  $\text{N}_2\text{O}_5$  (since concurrent DOAS measurements of  $\text{NO}_3$  and  $\text{NO}_2$  indicated the presence of  $\text{N}_2\text{O}_5$ ), while  $\text{N}_2\text{O}_5$  was not present in Torrance, although high levels of  $\text{NO}_x$  and OH radicals were present.

The studies we conducted in this program to assess the possibility for nitroarene formation during Hi-vol sampling of ambient air showed that any artifact formation of the m/z 247 nitroarenes during sampling would affect only 1-nitropyrene, but this contribution would be insignificant relative to ambient levels of 1-nitropyrene. However, in experiments carried out to assess the importance of the formation of nitroarenes arising from transformations of fluoranthene and pyrene from adsorbed phase reactions, we observed the formation of all eight possible nitroisomers, although only in low yields during the 12-hr ambient exposures conducted.

In summary, utilizing the findings from this research program concerning the formation of nitroarenes in the adsorbed phase during atmospheric transport and sampling (together with our knowledge of the

nitroarene products formed from the gas-phase reactions of fluoranthene, pyrene and acephenanthrylene with  $N_2O_5$  and with the OH radical in the presence of  $NO_x$ ) we suggest that the  $m/z$  247 nitroarene species we observed in ambient samples can be explained by the following major formation routes:

- 1-nitropyrene is a direct emission from combustion sources, with a small amount being formed in the atmosphere from adsorbed phase reactions of pyrene.

- 2-nitropyrene is formed in the atmosphere, predominantly via the gas-phase OH radical-initiated reaction with pyrene.

- 4-nitropyrene is formed in the atmosphere, both from the gas-phase reaction of pyrene with  $N_2O_5$  (when present) during nighttime hours and from the adsorbed-phase reaction of pyrene during atmospheric transport from source to receptor.

- 2-nitrofluoranthene is formed in the atmosphere, both from the gas-phase reactions of fluoranthene with OH radicals, in the presence of  $NO_x$ , during daytime hours and with  $N_2O_5$  (when present) during nighttime hours.

- 3-nitrofluoranthene is a minor direct emission from combustion sources, and can also be formed from adsorbed-phase reactions during atmospheric transport.

- The 7- and 8-nitrofluoranthenes can be formed from both the gas-phase reactions of the OH radical with fluoranthene and from adsorbed phase reactions of fluoranthene during atmospheric transport conditions, although it appears likely that 7-nitrofluoranthene is formed mainly via OH radical-initiated reaction.

Ambient Mutagenicity. The contributions of the  $m/z$  247 nitroarenes to the overall direct mutagenicity of the dichloromethane extracts of several ambient POM samples from Claremont and Torrance were calculated to range from 1 to 10%. In one Claremont sample, 2-nitrofluoranthene alone contributed as much as 5% to the observed mutagenicity. In the Torrance sample in which 10% of the mutagenicity could be attributed to these nitroarene species, 8-nitrofluoranthene, 3-nitrofluoranthene and 2-nitrofluoranthene each contributed comparable amounts. 1-Nitropyrene, the only  $m/z$  247 isomer well documented to be present in several direct particulate

emissions, contributed a maximum of only 0.2% to the observed mutagenicity.

Thus, in the South Coast Air Basin, a significant portion of ambient particulate mutagenicity can be accounted for by a relatively few highly mutagenic nitroarenes which are largely atmospheric reaction products, rather than directly-emitted species. This bears critically on any risk assessments which are based solely on mutagenic testing of primary emissions. It should be noted that, although the observed levels of 4-nitropyrene did not contribute significantly to the ambient mutagenicities, this isomer has recently been found to be a potent tumorigen in the newborn mouse assay (Wisocki et al. 1986) and its detection in ambient air is of major relevance in the evaluation of the human health risks of atmospheric nitroarenes.

We did not find evidence for mutagenicity artifacts occurring on TIGF filters, but the results for the GF filters indicated that the uncoated glass fiber surface was more reactive. For this reason, we will continue to use TIGF filters for the Hi-vol collection of ambient POM for mutagenicity determinations.

Of particular importance was our observation that the method of POM extraction has a considerable effect on its mutagenicity. Specifically, we have established that the Soxhlet extraction of POM with acetonitrile produces artifactual mutagenicity, and we recommend that acetonitrile not be used to extract POM for mutagenicity testing.

Since we were the first researchers to report the presence of 2-nitrofluoranthene in ambient POM and additionally successfully used  $N_2O_5$  to produce mg quantities of 2-nitrofluoranthene in solution, we investigated the in vitro hepatic metabolism of 2-nitrofluoranthene and have identified 8- and 9-hydroxy-2-nitrofluoranthene as the in vitro hepatic metabolites.

#### E. Recommendations for Future Research

- In conducting the FT-IR measurements described above, we chose operating parameters with the objective of attaining the best sensitivity for  $HNO_3$ ,  $NH_3$  and HCHO in order to ensure a successful comparison with the other analytical methods during the CARB-sponsored methods intercomparison studies. This was not entirely compatible with our original objective of

attempting to detect  $N_2O_5$  for the first time in a polluted airshed. We have previously noted that for the detection of  $N_2O_5$ , the use of a path-length about half of that used in the present study, i.e., ~500 meters, might be advantageous since it would reduce  $H_2O$  interferences. Due to the demanding schedules of both the Claremont and Glendora intercomparison studies and the need to preserve the continuity of the data sets being taken, no experimentation on the optimum detection of  $N_2O_5$  could be conducted at Claremont or Glendora. The limited number of such experiments conducted in the 1986 Torrance study yielded no data on  $N_2O_5$ , as expected from the presence of high concentrations of NO. Obviously, several appropriately chosen air pollution episodes must be examined with optimum parameterization of the FT-IR system in order to experimentally test the recent predictions (Atkinson et al. 1986) of significant nighttime  $N_2O_5$  levels, and this remains an important research goal.

o Although a substantial portion of ambient POM mutagenicity can be attributed to relatively few nitroarenes, much of the activity remains to be explained. From previous tests of HPLC fractions of ambient POM, we have seen that a substantial portion of the TA98 direct mutagenicity is due to compounds which are more polar than simple nitroarenes. Additionally, based in part on our chamber studies of the reactions of gas-phase PAH with the OH radical in the presence of  $NO_x$ , we can anticipate that more polar, possibly highly mutagenic, compounds (for example, hydroxy-nitroarenes) may be formed from the parent PAH during transport through the atmosphere. Thus, one important goal for future research designed to characterize atmospheric mutagenicity should be to investigate these more polar mutagenic species and assess their contribution to the total mutagenic activity of ambient POM.

• As we have observed in previous studies concerned with determining the mutagen burden to which populations in the South Coast Air Basin are exposed, there were substantial intra-day and inter-day variations in mutagen density (revertants  $m^{-3}$ ) during both the summer study at Claremont and the winter study at Torrance. Because of these wide short-term variations in mutagen density, an evaluation of the long-term trends in atmospheric mutagenicity in Southern California remains elusive, despite the accumulation of data over nearly a decade. In order to determine long-term trends in airborne particulate mutagenicity, which can then be

used to evaluate, for example, the effectiveness of certain pollutant control measures, it will be necessary to use a standardized low-cost sampling, extraction, and testing protocol. Such a protocol should be developed involving, for example, weekly integrated samples taken with a low volume sampler at specific locations in the air basin over the period of several years, with mutagenic testing conducted using a simplified and highly automated Ames assay.

## II. INTRODUCTION

### A. Background to Present Study

Over the past decade, attention has increasingly focused in California on the role which nitrogenous pollutants play in a wide range of air pollution phenomena, including photochemical oxidant formation, visibility reduction, atmospheric acidity, adverse effects on vegetation, formation of atmospheric mutagens and other impacts on human health. For example, the California Air Resources Board (CARB) has for many years been concerned with the effects of nitrogen oxides and the fact that  $\text{NO}_x$  emissions contribute to increased concentrations of three of the four pollutants for which national ambient air quality standards are exceeded in California (i.e., ozone, nitrogen dioxide and fine particulate). Thus, the CARB has initiated many nitrogen oxide emission control strategies, while continuing to support research designed to lead to a better understanding of this class of pollutants (CARB 1985).

While there is growing evidence in the scientific and health communities of the multitude of adverse air quality and health effects resulting from oxides of nitrogen (CARB 1985, SCAQMD 1986), questions continue to be raised about the need for further controls of nitrogen oxides (General Motors 1985, SCAQMD 1986). Therefore, it is important to continue to generate scientific information and to obtain additional ambient air quality data concerning nitrogenous air pollutants. It was in this context that the present program was initiated, with a focus on two aspects of air pollution which impact human health and welfare, and which have emerged in recent years as particular causes for concern in California and in the U.S. These are the observed mutagenicities of respirable particulate organic matter (POM) and the effects of acid deposition. While seemingly disparate phenomena, these two forms of air pollution share at least one important common link -- the key involvement of gaseous nitrogenous pollutants.

### B. Major Objectives

As originally proposed, this program was to have involved two carefully coordinated ambient air monitoring studies employing our in situ long pathlength spectroscopic techniques, our expertise in polycyclic

aromatic hydrocarbon (PAH) chemistry, and our experience in utilizing mutagenic assays as a tool for elucidating chemical transformations.

As discussed in detail in several sections of this report, nitroarenes, many of which are strong direct (not requiring metabolic activation) mutagens (Rosenkranz and Mermelstein 1983, Tokiwa and Ohnishi 1986), contribute to the observed mutagenicity of collected ambient POM (the PAH themselves are not direct mutagens, but rather require metabolic activation). These nitroarenes are not only emitted directly into the atmosphere, but have also been postulated to be formed from the reaction of PAH with gaseous nitrogenous co-pollutants during transport through the atmosphere and/or during collection of the particulate. In particular, at the time the present program was undertaken, we (Pitts et al. 1978, Pitts 1979) and other groups (Hughes et al. 1980, Jäger and Hanus 1980, Butler and Crossley 1981, Tokiwa et al. 1981, Brorström et al. 1983, Ramdahl et al. 1984) had demonstrated the formation of nitroarenes from the reactions of PAH with  $\text{NO}_2$  containing traces of nitric acid. However, the extent to which such reactions occur in the atmosphere or during high-volume (Hi-vol) sampling of POM was not well defined due to the difficulty in obtaining reliable and relevant data concerning this question.

Prior to the present program, we had also determined that gaseous dinitrogen pentoxide ( $\text{N}_2\text{O}_5$ ) is a potent nitrating agent for certain PAH, including gaseous naphthalene (Pitts et al. 1985a) and adsorbed fluoranthene and pyrene (Pitts et al. 1985b,c), the latter being common PAH constituents of POM. In the experiments involving adsorbed-phase PAH, a "passive" exposure technique was used to avoid passing large volumes of gas through the substrate on which the PAH were adsorbed. Thus, it was recognized that the role of  $\text{N}_2\text{O}_5$  in the atmospheric formation of nitroarenes during transport was an important question.

This evidence for potential atmospheric transformations of PAH has important regulatory implications from two different perspectives. First, reliable risk assessments should consider not just the mutagenicity/carcinogenicity of directly emitted material but also that of the actual POM which impacts human populations downwind from the primary sources. Such populations may be as little as a few feet to many tens of kilometers from the site of introduction of POM into the atmosphere. During the time such material is transported through the atmosphere it may undergo

substantial chemical modification, with resulting alterations in biological activity, due to reactions of POM constituents, such as the PAH, with gas phase pollutants or atmospheric species (e.g.,  $O_3$ , HONO,  $N_2O_5$ ,  $NO_2$ ,  $NO_3$  radicals, etc.).

The second aspect concerns the possibility of artifact formation of mutagens from PAH during the collection of ambient POM, leading to an increase in the direct mutagenicity. Indeed, any such artifact formation of mutagens during the collection of POM could lead to serious overestimates of the mutagenic burden impacting the human population. It is the overall issue of the relative importance of such transformations, and their implications for the mutagenic burden in California's atmospheres, that constituted one of the major concerns of the present research program.

The specific questions we put forth in our proposal to investigate and answer were:

- How much is the observed direct-acting mutagenicity of ambient POM enhanced due to artifactual formation of strongly mutagenic products during filter collections, and which nitrogenous and/or oxidative species cause these transformations?
- What is the potential for the mutagenicity of direct POM emissions to be enhanced due to chemical transformations resulting from reactions of PAH with gaseous nitrogenous species during the residence time for POM in the atmosphere?
- Are nitroarenes formed from the reactions of adsorbed PAH with ambient levels of nitrogenous species under "passive" conditions simulating atmospheric transport?

A significant finding in our previous CARB supported study (Contract No. A3-049-32) occurred prior to commencing work on the present program. This finding was the identification, for the first time, of 2-nitrofluoranthene in ambient POM (Pitts and Winer 1984, Pitts et al. 1985d). 2-Nitrofluoranthene and 2-nitropyrene were identified in ambient POM collected in southern California, and since these two nitroarenes had not been reported in direct particulate emissions, this provided strong evidence for the atmospheric transformation of PAH to nitroarenes (Pitts et al. 1985d). While both 2-nitropyrene and 2-nitrofluoranthene are

strong direct mutagens (see Section VII), at that time their contributions to ambient mutagenicity were unknown.

The identification of 2-nitrofluoranthene and 2-nitropyrene, in addition to 1-nitropyrene, in ambient POM collected in southern California had a major impact on our approach to answering the questions proposed above. In particular, the importance of measuring the nitroarenes present in ambient POM collected simultaneously with our proposed "active" (corresponding to Hi-vol sampling) and "passive" (corresponding to adsorbed-phase reactions occurring during transport) exposures of POM and deuterated PAH-doped POM was realized. This is reflected in this report in Section VI which details our ambient measurements of PAH and nitroarenes, and is critical to the conclusions drawn in Section XI.C.

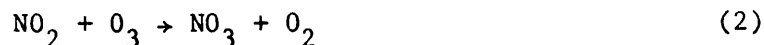
As noted above, assessing the importance of atmospheric transformations and sampling artifacts to the observed mutagenicity of collected POM bears importantly on obtaining reliable risk-assessments concerning the mutagenic constituents of ambient POM. Critical to these investigations is a complete characterization of the nitrogenous and other species present in urban atmospheres. In particular, it was recognized that the role of  $N_2O_5$  in the formation of mutagenic nitroarenes should be addressed, and measurement of the  $NO_3$  radical and  $NO_2$  concentrations (from which  $N_2O_5$  can be calculated) were undertaken, as discussed in Section IV.

With respect to acid deposition, it is now abundantly clear that the major emissions leading to acid deposition (both "wet" and "dry") are oxides of nitrogen and sulfur dioxide. In the atmosphere, these initially emitted species are transformed to sulfuric acid ( $H_2SO_4$ ) and nitric acid ( $HNO_3$ ) by homogeneous (Calvert and Stockwell 1983, Stockwell and Calvert 1983) and heterogeneous (Graedel and Weschler 1981, Chameides and Davis 1982, Heickes and Thompson 1983, Calvert 1984) processes. In California's atmospheres, oxides of nitrogen, and hence  $HNO_3$ , are usually dominant due to the greater emissions of  $NO_x$  than of  $SO_2$  [for example, in the California South Coast Air Basin the 1983 emission rates were reported to be  $\sim 1100$  tons  $day^{-1}$  for  $NO_x$  versus  $\sim 230$  tons  $day^{-1}$  for  $SO_2$  (SCAQMD 1984)].

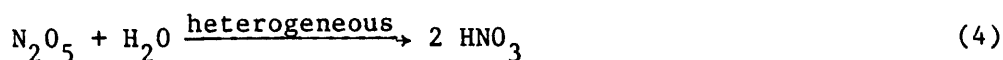
Until a few years ago the only reaction forming  $HNO_3$  from oxides of nitrogen which was considered in computer airshed models was that involving the gas-phase daytime reaction of OH radicals with  $NO_2$



However, it is now recognized that  $\text{N}_2\text{O}_5$ , which is formed in nighttime atmospheres via the reactions,



can react with water vapor by heterogeneous processes (Heikes and Thompson 1983).



This nighttime formation route to nitric acid can be an important loss process for  $\text{NO}_x$  as well as a significant route to acid deposition.

Although developed later than the longpath FT-IR system, the long pathlength DOAS system conceived by Platt and Perner (1979), and applied and extended by these workers and by researchers of the Statewide Air Pollution Research Center [SAPRC] (Platt et al. 1980a,b, 1981, 1982, 1984, Harris et al. 1982, Pitts et al. 1984a,b, 1985e), has provided a technique capable of sensitive, specific, and time-resolved measurements of the ambient concentrations of a number of critical nitrogenous atmospheric species, including nitrous acid, nitrate radicals and nitrogen dioxide (as well as formaldehyde). Moreover, the simultaneous measurement of  $\text{NO}_3$  radical and  $\text{NO}_2$  concentrations permits the calculation (Atkinson et al. 1986) of ambient concentrations of  $\text{N}_2\text{O}_5$ .

In this program, we have employed the DOAS and FT-IR systems for several purposes; (a) to expand the data base available concerning the ambient concentrations of  $\text{NO}_3$  radicals, HONO and  $\text{HNO}_3$ , particularly in the western end of the South Coast Air Basin and at mid-basin sites such as Glendora and Claremont, (b) to provide quantitative and time-resolved ambient concentration data for HONO,  $\text{NO}_2$ ,  $\text{HNO}_3$ ,  $\text{NH}_3$  and HCHO which could serve as benchmark data for comparison with other, less specific, analytical methods for those species, or for intercomparison with the

tunable diode laser spectrometer (TDLs) method, and (c) to provide a basis for evaluating the possible interferences of certain of these species in analytical techniques such as those employing filter packs and denuders.

Furthermore, the DOAS data obtained can provide further insights concerning the role of  $\text{NO}_3$  radicals and  $\text{NO}_2$  (and hence  $\text{N}_2\text{O}_5$ ) in the atmospheric transformations of PAH to form atmospheric mutagens such as the nitroarenes, as well as the role of HONO,  $\text{NO}_3$  radicals,  $\text{NO}_2$  and  $\text{N}_2\text{O}_5$  in the production of photochemical smog and acidic deposition.

To achieve these goals, early in this program we decided to switch the DOAS system from the single pass optical design, which we had previously employed over pathlengths ranging from  $\sim 0.5$  to  $\sim 17$  km, to a closed optical system. The major motivation for this change concerned observed inhomogeneities of  $\text{NO}_2$  concentrations in single-pass optical paths (Pitts and Winer 1984). Such inhomogeneities make it difficult to interpret observations which involve correlations with point monitors (such as chemiluminescence analyzers for  $\text{NO}$  and  $\text{NO}_x$ ).

This consideration was particularly important with respect to the role the DOAS system ultimately played in both the Nitrogen Species Measurement Methods Intercomparison and the Carbonaceous Aerosol Study, as well as our interest in correlating observations of ambient gaseous and particle-associated nitroarene concentrations with  $\text{NO}_3$  radicals and  $\text{NO}_2$  concentrations (and with calculated  $\text{N}_2\text{O}_5$  levels). Accordingly, two entirely new optical systems were designed to be interfaced to the SAPRC rapid-scanning ultraviolet/visible (uv/vis) absorption spectrometer and Michelson interferometer. These optical systems were 25 m basepath configurations, essentially of the three mirror White design (White 1943), but with an added corner reflector at the in-focus end of the Horn-Pimentel design (Horn and Pimentel 1971).

Details concerning the design, construction, and operation of the 25 m basepath DOAS system, the application of this system in three field studies and the results obtained during these measurement periods are given in Section IV. The corresponding operational details of and the measurements obtained by the long pathlength FT-IR system are described in Section V.

C. Changes in Program Emphasis to Meet CARB Objectives

At the time the proposal for the present program was submitted to the CARB in September 1984, plans for the CARB to sponsor two major measurement methods intercomparison studies had not been announced. However, after the present program began in January 1985, specific plans to hold a Nitrogen Species Measurement Methods Intercomparison Study in September 1985 at Claremont, CA, were finalized. At that time, the CARB staff expressed a strong interest in having the SAPRC long pathlength FT-IR spectrometer participate in the Claremont study, in part to serve as a benchmark measurement method for  $\text{HNO}_3$ . To allow us to participate in this intercomparison study, the process of disassembling the FT-IR and DOAS systems, transporting them to Claremont, and reassembling and testing them had to begin no later than early August. On August 5, 1985, agreement was reached between the SAPRC and CARB for full participation of the 25 m basepath FT-IR and DOAS systems at the Claremont study, and it was further agreed that we should also simultaneously conduct at Claremont those portions of our program concerned with ambient concentrations of nitroarenes and mutagenicity levels. Thus, the initial summer field study called for in this program took place on the campus of Pomona College in Claremont between September 11 and 19, 1985.

Following the winter field study as originally proposed, and held at El Camino College in Torrance at the western end of the South Coast Air Basin, a third field study, not originally planned as part of this program, was held on the Citrus College Campus in Glendora in August 1986. Again, this departure from our original proposal was at the request of the CARB staff, and again so that the DOAS and FT-IR long pathlength spectrometers could participate in a CARB-sponsored measurement method intercomparison study, in this case the Carbonaceous Aerosol Study.

As a result of these measurement protocol changes mutually agreed to by SAPRC and CARB, some lessening of emphasis on acid deposition studies per se and a corresponding increase in emphasis on providing a reliable and expanded data base of specific and quantitative spectroscopic data for the nitrogenous species  $\text{HNO}_3$ ,  $\text{NH}_3$ ,  $\text{HONO}$ ,  $\text{NO}_2$ , and  $\text{NO}_3$  radicals (as well as for  $\text{HCHO}$ ) is reflected in the final results and in the treatment of data in this report. Accordingly, a complete tabulation of the spectroscopic data obtained with the SAPRC long pathlength FT-IR and DOAS systems is

provided in this report for all three field studies (Claremont, Torrance and Glendora) carried out as part of this program. These data are reported in Sections IV and V and in Appendices B and D of the present report.

However, the corresponding PAH and nitroarene results, and related data, are furnished in this report only for one summer field study (Claremont) and one winter field study (Torrance), as specified in our original proposal. Data concerning gaseous and particle-associated PAH and nitroarenes obtained during the Glendora study will be presented and discussed in the final report to CARB Contract A5-185-32. Thus, by agreement with the CARB staff, the Glendora site will serve as the vehicle-impacted site for the investigation of mutagenicity and PAH and nitroarenes present at seven different locations in California which we are presently conducting for the CARB under Contract No. A5-185-32.

#### D. Organization of this Final Report

The present program was complex, involving a large number of instruments and the measurement and analysis of a broad spectrum of gaseous and particle-associated species, with extensive data reduction and interpretation. The location and nature of the three study sites and the measurement protocols employed are described in Section III. For purposes of reporting the results from these studies, we have grouped the DOAS data for HONO, NO<sub>2</sub>, NO<sub>3</sub> radicals and HCHO in Section IV, the FT-IR data for HNO<sub>3</sub>, NH<sub>3</sub> and HCHO in Section V and the ambient measurements of PAH and nitroarenes in Section VI. These ambient measurements include the first data we have obtained for gaseous, as well as particle-associated, PAH and nitroarenes (from the field study at Torrance in February, 1986):

Studies concerning the characterization of ambient mutagenicity, including determining the contribution of the nitroarenes to ambient mutagenicity, potential mutagenicity artifacts, and the mutagenicity of 2-nitrofluoranthene and its in vitro hepatic metabolites are described in Sections VII, IX and X, respectively, while measurements and research concerning nitroarene formation in the adsorbed phase during transport and sampling are presented and discussed in Section VIII.

Conclusions, and recommendations for further research, relevant to this entire program are presented at the end of the report in Section

XI. Supplementary data of various kinds which were too voluminous to be included in the body of the report are presented in the Appendices, together with a list of journal articles resulting from the research conducted under this program (Appendix A).



### III. MEASUREMENT SITES AND PROTOCOLS

#### A. Introduction

The proposed experimental program called for ambient atmospheric sampling and measurement periods to take place on the University of California, Riverside (UCR) campus during the summer of 1985 and at a site in the western end of the South Coast Air Basin during the winter of 1985/86. Accordingly, in the spring of 1985 all of the required instruments and apparatus, including the long pathlength FT-IR and DOAS systems, were set up at the UCR campus. Beginning in late June, meteorological conditions and South Coast Air Quality Management District air quality forecasts were monitored on a daily basis in order to determine the optimum periods for spectroscopic measurements and for particulate sampling.

However, the trend of steady and significant improvements in air quality experienced over the previous several years at the UCR campus area of Riverside continued in the summer of 1985. Indeed, air quality conditions were unusually favorable during the entire month of July, with maximum ozone levels rarely exceeding 150 to 180 parts-per-billion (ppb) and often being lower. Under these conditions, we were not able to detect nitric acid or the nitrate ( $\text{NO}_3$ ) radical. After discussions with the CARB staff it was agreed that continuing measurements under the prevailing air quality conditions at UCR would not yield the data needed to meet the research objectives of this program.

As noted in the preceding section, a further consideration in these discussions was the desire of the CARB staff to have the SAPRC's long pathlength optical spectrometers participate in the Nitrogen Species Measurement Methods Intercomparison Study, which was scheduled to occur in early September at Pomona College in Claremont. Thus, the initial summer field study under this program took place on the campus of Pomona College in Claremont between September 11 and 19, 1985.

Subsequently, the winter field study portion of our program was conducted on the campus of El Camino Community College in Torrance during January and February of 1986. A second summer measurement period, involving both of the long pathlength spectroscopic systems and collections of gaseous and particle-associated PAH and nitroarenes, took place in August

1986 on the Citrus College campus in Glendora, in conjunction with the CARB-sponsored Carbonaceous Aerosol Study. The PAH and nitroarene data from Citrus College will not be reported here, but rather will be reported in a separate final report for the Carbonaceous study. The locations of the three studies we conducted are shown in Figure III-1.

In the remainder of this section, details of the sites at which our three ambient air monitoring studies took place are given, together with an overview of the sampling protocols and study designs employed. Further details concerning the measurement protocols are given in the specific chapters of this report dealing with the individual spectroscopic measurements or sample collections and analyses.

1. Pomona College Study (Claremont)

The Pomona College campus is located ~2 km north of the Interstate 10 freeway, ~1 km east of Indian Hill Boulevard and ~1 km south of Foothill Boulevard. The site for all investigators participating in the Nitrogen Species Methods Intercomparison Study was an unused parking lot near the southeastern corner of the campus. Buildings bordered the parking lot to the west and south, with an open field to the east, as shown in Figure III-2. The specific orientation of the various instruments involved in the intercomparison study are shown in Figure III-3.

An important requirement for the study was that all analytical techniques sample at a common height of 2.4 m (8 ft) above the ground in order to minimize influences of dry deposition of nitric acid and other nitrogenous species. This requirement necessitated a major restructuring of the FT-IR and DOAS instrument supports. In order to augment the 1.2 m (4 ft) height initially designed into the optical axes of both of the long pathlength mirror assemblies, while at the same time preventing extraneous vibrations, the spectrometers, mirror systems and their housings were set on massive concrete blocks.

Six 4 ft x 4 ft x 10 ft concrete structures were rented from the Pyramid Precast company, which provided the necessary machinery to position the blocks on premarked areas at the study site. Three of these blocks constituted the support platform for the FT-IR and DOAS assemblies at each end of the optical path (see Figure III-3). New 9 ft x 12 ft sheds were procured and constructed on these platforms during the last week of August and the first week of September. Subsequent assembly and

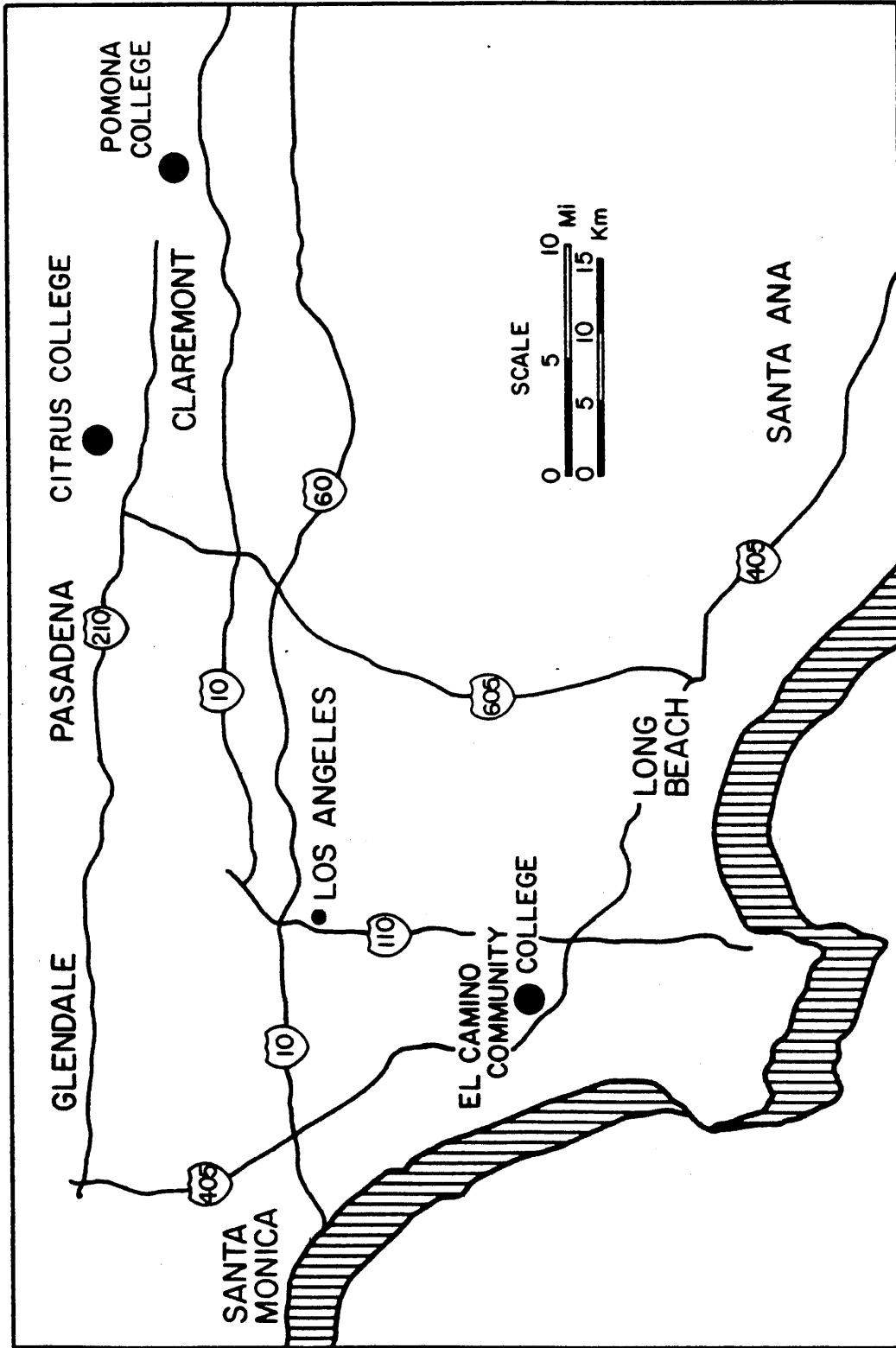


Figure III-1. Locations of the three study sites used in this program.



Figure III-2. Location of September 1985 field study on Pomona College campus. ★ - Field study site.

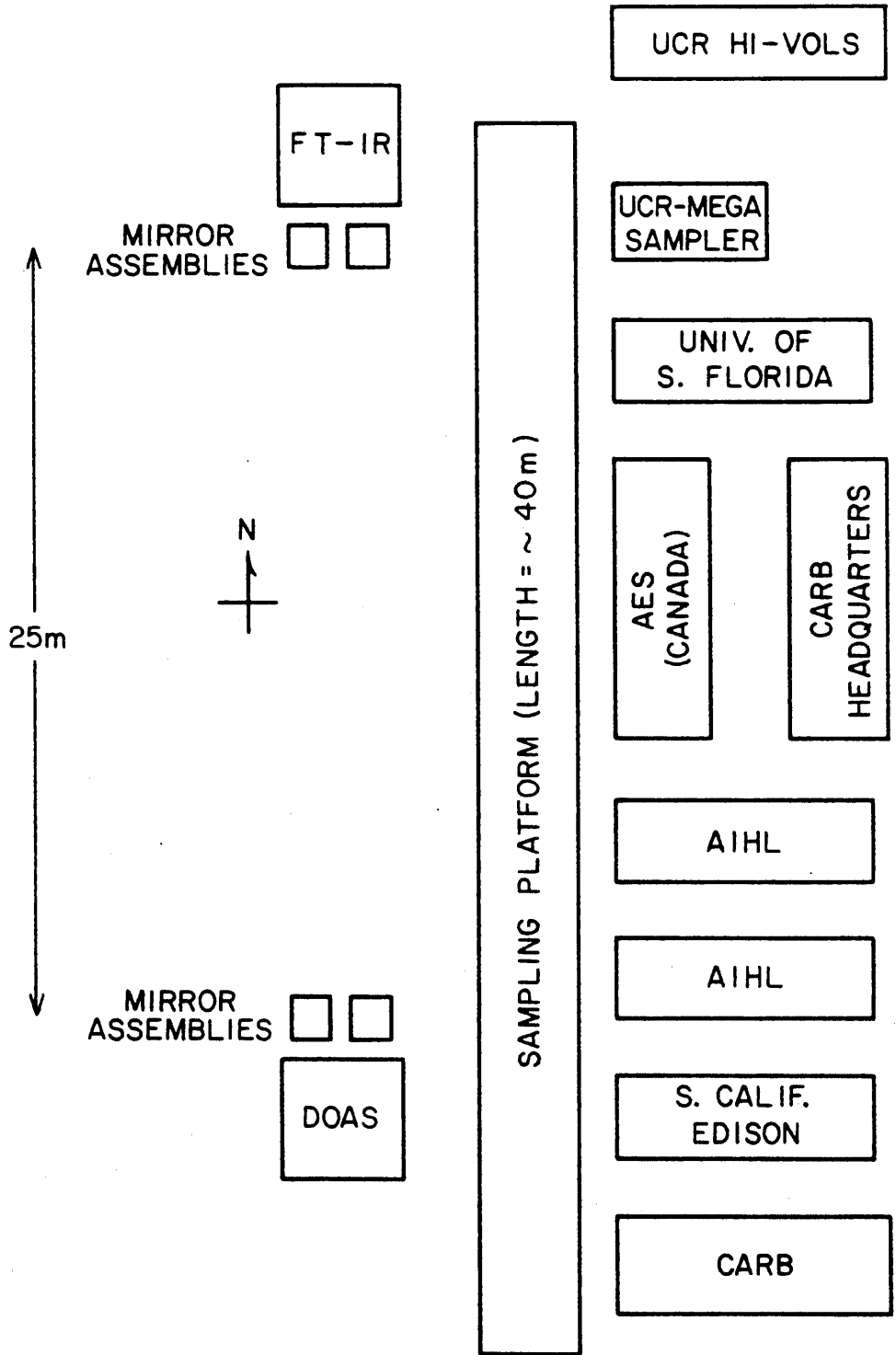


Figure III-3. Layout of the Claremont study site illustrating the positions of the longpath FT-IR and DOAS systems and other SAPRC instruments relative to the instruments of the other participants on the Pomona College campus, September 1985.

testing of the spectrometers and optical systems was completed in time for the scheduled start of the field study on September 11, 1985.

As shown in Figure III-3, the two SAPRC 25 m basepath optical systems were set up parallel to each other and to the scaffolding which supported most of the samplers from other groups participating in the intercomparison study. The optical systems were aligned in a north-south orientation to minimize scattered light problems at sunrise and sunset, and positioned due west of the scaffolding and various mobile vans and trailers.

In addition to the longpath spectrometers, SAPRC's ultra-high volume "mega-sampler" was moved to the study site and located at the north end and just to the east of the scaffolding. Two Hi-volume samplers were also employed and these were placed north of the mega-sampler.

The study began at 0800 PDT on Friday September 11 and continued for a nine-day period through 0600 PDT on September 19. Five sampling blocks per day, consisting of 4 to 6 hours each, were designated in the sampling protocol. However, the FT-IR and DOAS systems were operated continuously throughout this entire period, while the particulate sample collections took place in 6-hr intervals as described in Sections VI, VII and IX. This field study period was generally characterized by low pollution days, consistent with our experience earlier in the summer at Riverside. However, elevated pollution levels were encountered on several days, notably on Saturday, September 14.

## 2. El Camino Community College (Torrance)

Site Selection and Installation of Equipment. A major effort was expended in the fall of 1985 to identify a suitable site for the winter field study at the west end of the South Coast Air Basin. The candidate locations were chosen on the basis of previous records of high NO<sub>x</sub> levels in the winter made available to us by the South Coast Air Quality Management District. Other criteria used in site selection included security, availability of sufficient area to accommodate the FT-IR and DOAS systems, and the availability of adequate electrical power. Examples of the sites investigated included 20th Century Fox Studios in Beverly Hills, the Federal Building in Westwood, the Pepperdine University campus, Garrett Air Research Corporation, the California State University at Dominguez Hills, Northrup Corporation, the Getty Oil field north of Hollywood Park, the Long Beach Water Treatment Plant grounds, and Loyola

Marymount College. Many of the sites evaluated did not meet one or more of the criteria noted above. Others were unavailable due to, for example, security restrictions imposed by defense contractors.

The site ultimately chosen was the campus of El Camino Community College in Torrance, CA, which is ~20 km southwest of downtown Los Angeles and ~8 km east of the coast. Permission to use the roof of a two-story building at the north side of the campus (see Figure III-4) was officially granted during the second week of January 1986. This specific location was judged best with respect to air parcel sampling criteria, security, and non-interference with campus activities.

All instruments and major pieces of equipment, including two assembled instrument sheds, were transported from the UCR campus to El Camino Community College on Tuesday, January 14. Since the only access to the roof was via a narrow spiral staircase, the equipment was lifted to the roof using a rented scissors-type lift. The long pathlength FT-IR and DOAS systems were installed in the same configuration as employed in the Claremont study except that the concrete platforms were not used. At the El Camino Community College site the east-west optical axes of both the FT-IR and DOAS systems were 1.2 m from the roof surface and ~9 m above the ground.

An array of support instrumentation was installed inside the sheds which housed the spectrometers. This included dedicated monitors for NO and NO<sub>x</sub>, O<sub>3</sub>, SO<sub>2</sub>, CO, peroxyacetyl nitrate (PAN), temperature/relative humidity, as well as a nephelometer and anemometer, all of which (except for PAN) were directly inputted into a common data acquisition system. A total of sixteen Hi-vol samplers for collection of particulate organic matter were assembled at one end of the FT-IR and DOAS spectrometers. These included six standard Hi-vol samplers with 10 μm cut-off inlets run at 40 SCFM and utilizing Teflon-impregnated glass fiber (TIGF) and glass fiber (GF) filters for particulate collection; five Hi-vol samplers without inlets run at 40 SCFM; five Hi-vol samplers equipped with three polyurethane foam (PUF) plugs downstream of TIGF and GF filters, run at flow rates of ~30 SCFM; and two Tenax-GC sampling cartridges in series, each packed with 0.1 g of the solid adsorbent and run at 1 liter min<sup>-1</sup>.

Measurement Periods. Full power for all equipment and instrumentation, which required installation of special electrical outlets, did not



become available until Saturday, January 18, 1986. However, optical alignment of the two longpath spectrometers, partial calibration of support instrumentation, and flow calibration of the Hi-vol samplers were carried out with the available power prior to the first filter sampling, which began on Sunday, January 19. On the basis of moderately high levels of  $\text{NO}_x$  on that day, and predicted stagnant air conditions in the coastal region, the Hi-vol samplers were operated from 1700 hr on Sunday, January 19 to 1700 hr on Tuesday, January 21. Hi-vol particulate samples were collected over 12-hr daytime (0500-1700 hr in January and 0600-1800 hr in February) and 12-hr nighttime (1700-0500 hr and 1800-0600 hr, respectively) periods. Due to a faulty cooling system for the infrared light source, no FT-IR data were obtained during the January 19-21 period. However, the DOAS system was operational on a continuous basis from January 18 to February 8.

An additional filter sampling period began at 1700 hr on January 27, and continued until 1700 hr on January 28. The period between January 28 and February 22 was characterized by numerous days of heavy rains and coastal storms. Thus, after January 28 measurements were limited to the last week of February. The long pathlength FT-IR spectrometer was operated continuously from 1800 hr, February 23, to 1800 hr, February 27. The long pathlength DOAS system was operated continuously from the morning of February 23 to the evening of February 26. Measurement periods during this winter study were characterized by low inversion heights with daytime clear-sky conditions: approximately constant nighttime temperatures around  $15^\circ\text{C}$  ( $60^\circ\text{F}$ ) with maximum daytime temperatures as high as  $35^\circ\text{C}$  ( $95^\circ\text{F}$ ) were encountered.

### 3. Citrus Community College (Glendora)

As noted earlier, this monitoring program was conducted in conjunction with the Carbonaceous Aerosol Study. As shown in Figure III-5, the CARB selected a site adjacent to the football stadium on the campus of Citrus College for this study. The orientation and relationship to other investigators of the long pathlength FT-IR and DOAS systems was similar to that for the Claremont study, as shown in Figure III-6. The SAPRC Hi-volume samplers were located just north of the mobile vans and trailers of other investigators and again the optical spectrometers were elevated on concrete blocks to achieve a 2.4 m (8 ft) height for the optical beams.

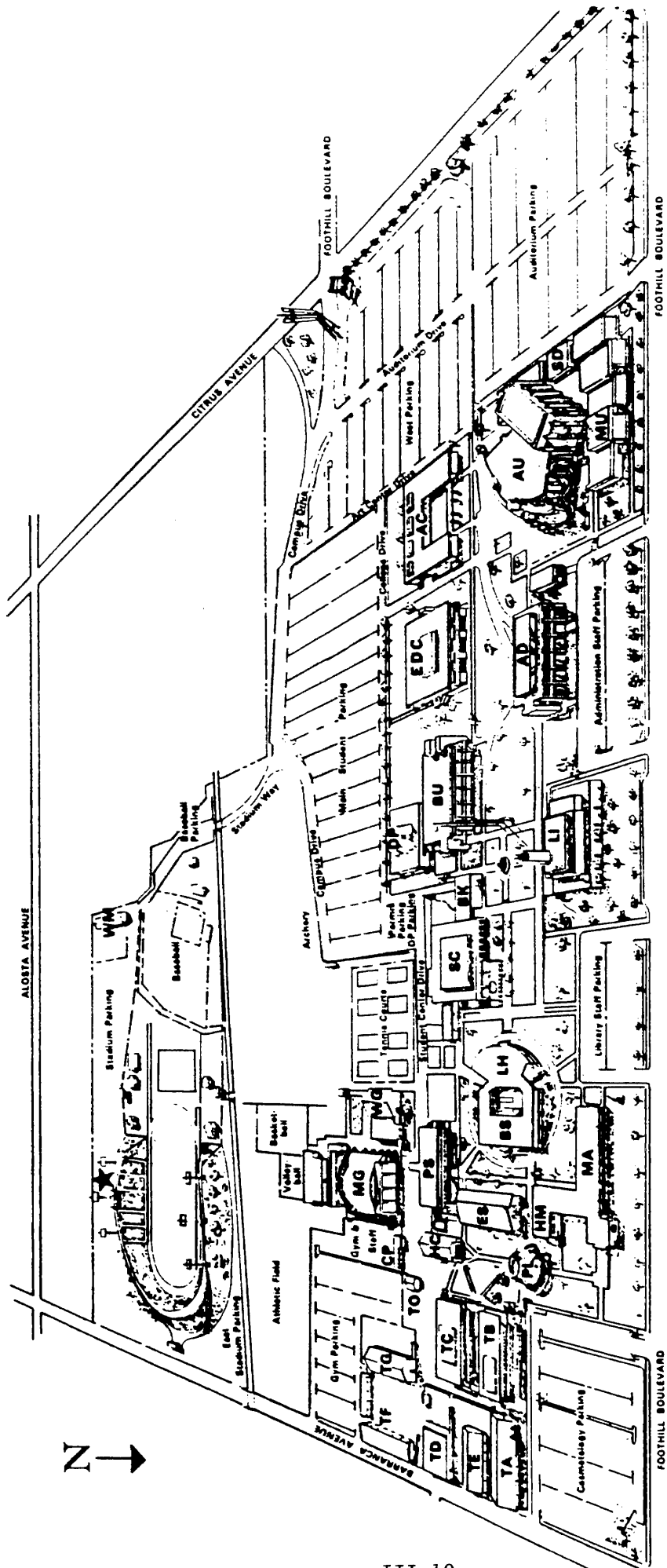


Figure III-5. Citrus College campus showing location of August 1986 field study adjacent to football stadium. ★ - Field study site.

FOOTBALL STADIUM

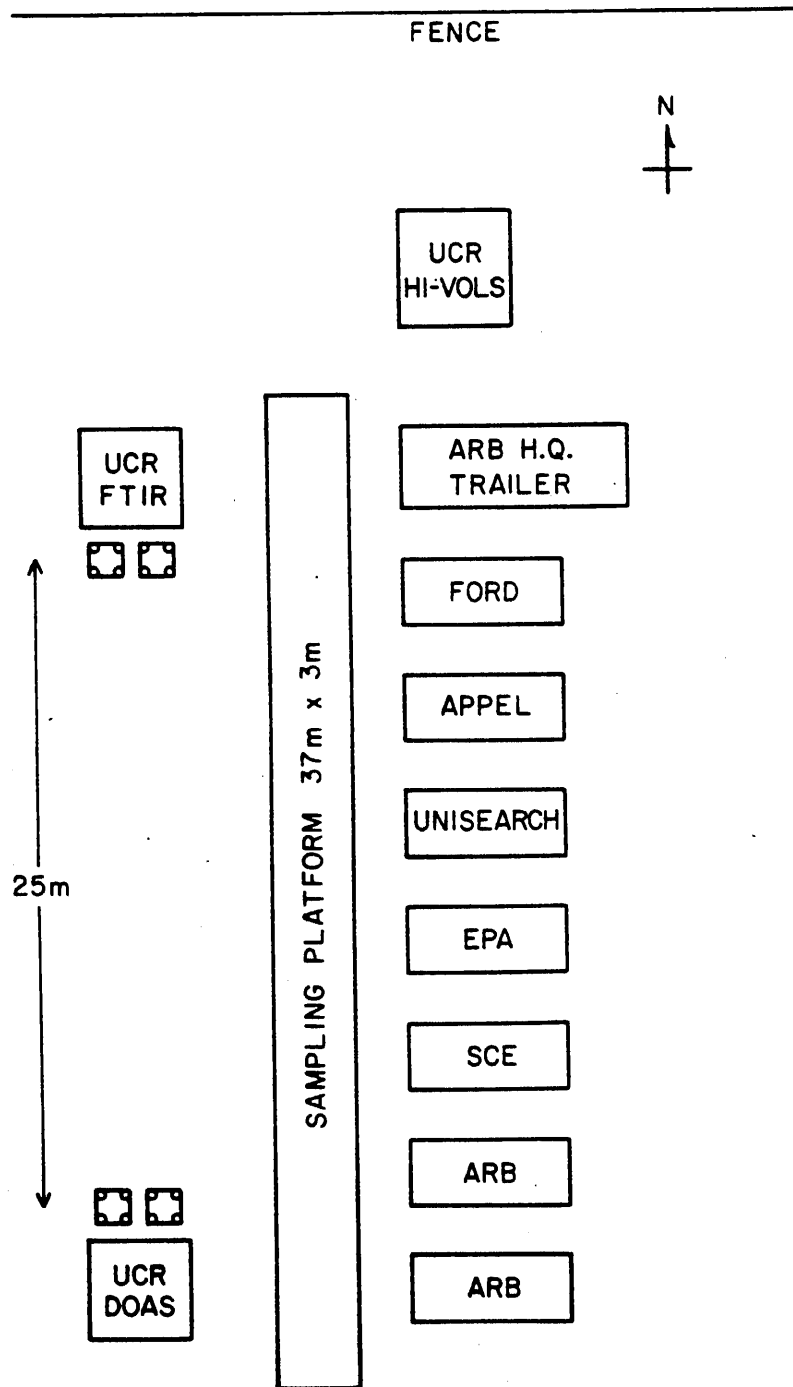


Figure III-6. Positions of the longpath FT-IR and DOAS systems and UCR Hi-vols relative to the instruments of the other participants in the Carbonaceous Aerosol Study on the Citrus College campus, August 1986.

The study period began at 0800 PDT on Tuesday, August 12 and continued until 0800 PDT on August 21. The FT-IR and DOAS systems operated essentially continuously during this period, with FT-IR spectra being acquired every 12-15 minutes during the day and every 20 minutes at night; DOAS spectra were acquired approximately every 15 minutes day and night. While data from particulate samples collected in this study will be given in the final report for our Carbonaceous Aerosol Study program, we note the Hi-vol samplers and other associated experiments operated on the 12-hr time periods 0800-2000 hr and 2000-0800 hr.

#### IV. MEASUREMENTS OF HONO, NO<sub>2</sub>, NO<sub>3</sub> RADICALS AND HCHO BY DIFFERENTIAL OPTICAL ABSORPTION SPECTROSCOPY

##### A. Introduction

The development of a long pathlength DOAS system by Perner and Platt (1979) and its application and extension by these workers and by SAPRC researchers (Platt et al. 1980a,b, 1981, 1982, 1984, Harris et al. 1982, Pitts et al. 1984a,b, 1985e) has provided a technique capable of sensitive, specific, and time-resolved measurements of the ambient concentrations of a number of important atmospheric species, including nitrous acid, formaldehyde, the nitrate radical and nitrogen dioxide. Moreover, the simultaneous measurement of NO<sub>3</sub> radical and NO<sub>2</sub> concentrations permits the calculation (Atkinson et al. 1986) of ambient concentrations of dinitrogen pentoxide (N<sub>2</sub>O<sub>5</sub>), which we have shown (Pitts et al. 1985a, Sweetman et al. 1986, Zielinska et al. 1986b, Atkinson et al. 1987) to react with polycyclic aromatic hydrocarbons to form nitroarenes (Section XI.C), many of which are potent mutagens. N<sub>2</sub>O<sub>5</sub> can also play an important role in the nighttime formation of nitric acid and hence contributes to acidic deposition (Atkinson et al. 1986, Russell et al. 1986).

In this section, we describe in detail the design, construction, and operation of the 25 m basepath DOAS system, the application of this system to the measurement of ambient levels of NO<sub>3</sub> radicals, HONO, NO<sub>2</sub> and HCHO at the three sites detailed in Section III, and the results obtained during these measurement periods.

##### B. Experimental Methods

###### 1. Design and Construction of 25 m Basepath DOAS System

The design of the multiple-reflection optical system was finalized during February 1985, and details of its fabrication were discussed with Brunache Instrument Optics (Carlsbad, CA). Three sets of optics were subsequently ordered: one each for the FT-IR and DOAS systems, plus a back-up set. Figure IV-1 shows a schematic diagram of the DOAS optical system.

The 25 m basepath optical system was of the three-mirror White design, but with an added corner reflector at the in-focus end which effectively doubled its maximum pathlength capability. The mirrors were

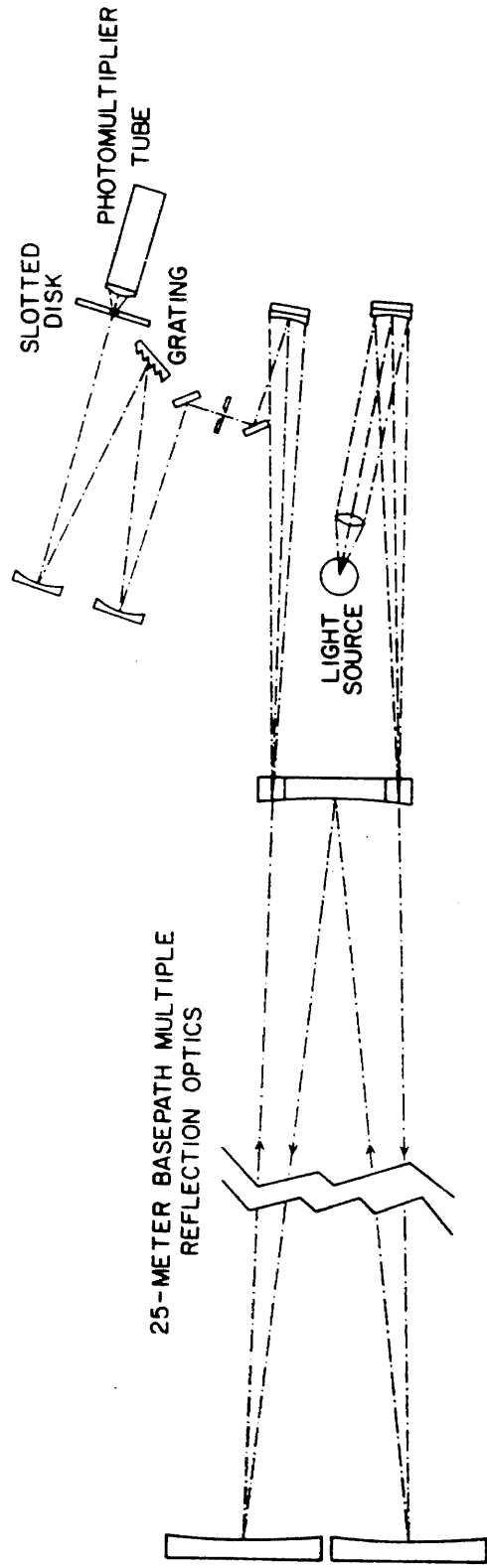


Figure IV-1. Schematic diagram of the longpath DOAS system.

fabricated from 30 cm dia. x 5 cm thick Pyrex blanks. The DOAS optics were initially furnished with an aluminum coating with an  $MgF_2$  overcoating, but were subsequently coated with a custom dielectric coating, as discussed below.

Mirror Mounts: Drawings for the kinematic mounts were also finalized in February 1985 and fabrication of mounts were completed by the UCR Chemistry Department Machine Shop. Concurrent fabrication of the steel base frames by SAPRC machinists allowed the complete mirror support system to be assembled prior to June 1985.

The kinematic mounting system chosen employs a design in which the weight of the mirror is totally supported by its central pivot. The latter consists of a socket attached to the center of the mirror backing plate, which rests and pivots on a ball end whose stem is secured to the support frame. The orthogonal adjustments are provided by micrometer screws which track on V-grooves and work against the positive action of a single compression spring.

Instrument Shed: Assembly of a 3 m x 4.3 m shed to house the DOAS was completed with addition of indoor insulation, air conditioning, and the requisite electrical power outlets.

Basic Spectrometer Design and Operation: The DOAS system measures the ambient concentrations of trace components which have distinct vibronic structures by their light absorption in the near-ultraviolet (uv) and visible spectral regions. White light from a 75 W high pressure Xenon lamp was imaged by a spherical mirror into the plane of the nesting (in-focus) mirror of the White cell and then propagated through the multiple reflection optics until it emerged from the system and was imaged onto the entrance slit of the monochromator (SPEX 1870 0.5 m). The light intensity was monitored by a photomultiplier (EMI 9659Q) and the signal acquired and averaged by a DEC MINC 11/23 minicomputer.

With the DOAS, a rotating slotted disk was used to allow rapid scanning. The slotted disk was formed by etching a set of exit slits (100  $\mu\text{m}$  wide, 10 mm spacing) radially into a thin metal disk. This disk was rotated in the focal plane of the dispersed spectrum. As each slit moved across the opening between the masks that block the two adjacent slits, it scanned a spectral range of ~30-60 nm, depending on the rotation frequency of the slotted disk. The orientation of the spectrometer grating

determined which specific spectral region was scanned. As employed in its final form in this program the slotted disk rotated at  $\sim 4$  Hz, resulting in a scan rate of  $\sim 100$  Hz, well above the frequency distribution of atmospheric turbulence (which otherwise would introduce unwanted structure into the spectra).

As a slit became visible at the edge of the mask, it was detected by an infrared photodiode. A trigger signal was sent to the computer which continuously recorded digitized samples of the light intensity as the slit scanned across the spectrum. Since several tens of thousand such scans were acquired and added in the computer memory within a few minutes, this improved the signal-to-noise ratio of the resulting spectrum. The rotational speed of the slotted disk was maintained constant to within  $\pm 0.1\%$  to preserve the spectral resolution while superimposing the scans. The computer was also used for spectral deconvolution and for the calculation of optical densities.

Since a single scan required only  $\sim 10$  msec, atmospheric scintillation effects had little effect on the signal. Moreover, since typically  $(2-8) \times 10^4$  individual scans were recorded and signal-averaged over each several minute measurement period, even complete, but momentary, interruption of the light beam had no appreciable effect on the final spectrum. Except under the haziest conditions, stray light effects were negligible due to the instrument's narrow field of view [ $\sim 8 \times 10^{-5}$  steradians] and in any case stray light could be taken into account by means of appropriate background spectra.

The concentrations of atmospheric species were derived from Beer's Law. However, since the light intensity ( $I_0$ ) in the absence of any absorption cannot be obtained with this technique, the differential optical density was employed and thus only those compounds which have structured absorption spectra could be measured. For such compounds

$$\log \frac{I_0'}{I} = \alpha C l$$

where  $I$  is the light intensity at the center of the absorption band (at wavelength  $\lambda_2$ ) due to the compound of interest,  $I_0'$  is the intensity in the absence of absorption by that compound,  $\alpha$  is the "differential" absorption coefficient at  $\lambda_2$  for the compound of interest,  $l$  is the

optical path and C is the concentration of the absorbing molecule.  $I_0'$  is interpolated linearly from the intensities at wavelengths  $\lambda_1$  and  $\lambda_3$  at which there is no absorption due to the compound of interest, according to

$$I_0' = I(\lambda_1) + [I(\lambda_3) - I(\lambda_1)] \left( \frac{\lambda_2 - \lambda_1}{\lambda_3 - \lambda_1} \right)$$

Table IV-1 gives the characteristic absorption bands and detection limits for a number of atmospheric species of interest, based on a 1 km pathlength. It can be seen that the detection limits range from 3 ppb for HCHO down to ~10 ppt for the  $\text{NO}_3$  radical.

Mirror Coatings. As noted earlier, the set of mirrors for the DOAS optical spectrometer were initially coated with aluminum with a  $\text{MgF}_2$  overcoating for high reflectivity, and these were installed in the 25 m base path optical system. Our first goal was to determine the optimum absorption pathlength in the uv/vis spectral region for this configuration. Starting with 4 passes (100 m), and then increasing the pathlength in 100 m increments, we obtained two separate air spectra for each pathlength and ratioed them. We then defined the detection limit for a given pathlength as three times the noise level of the ratioed spectrum.

Table IV-1. Calculated Detection Limits for 25-m Basepath Multiple-Reflection Cell DOAS System Operated at 1 km Pathlength

Compound	Differential Absorption Coefficient ( $\text{atm}^{-1} \text{cm}^{-1}$ )	Absorption Wavelength (nm)	Detection Limit (ppb) for 1 km and $2.5 \times 10^{-4}$ O.D. (base 10)
$\text{NO}_2$	2.7	365	2.3
HONO	11	354	0.6
$\text{NO}_3$ Radical	480	662	0.01
$\text{SO}_2$	15	300	0.4
HCHO	2.1	339	3.0

These tests showed that up to a pathlength of  $\sim 400$  m the noise level was equal to the digitizing noise of an equivalent optical density of  $1 \times 10^{-4}$ . For greater pathlengths, the noise level increased approximately linearly with the pathlength up to  $\sim 700$  m. Above that, an exponential growth in noise level led to a rapid decrease in the detection sensitivity. The decay in the light intensity due to the multiple reflections was more severe than anticipated, and limited the useful absorption pathlength to  $\sim 500$  m, with corresponding limits for quantitative measurement of HONO and  $\text{NO}_3$  radicals of 1.1 ppb and 26 ppt, respectively.

This limitation in useful pathlength was due to the overall reflectivity of this aluminum plus  $\text{MgF}_2$  coating being  $< 90\%$ . New coatings were ordered from two manufacturers, with specified maximum reflectivities at either 350 nm (for HONO) or 600 nm (for  $\text{NO}_3$  radicals). In each case the detection limits for the compounds for which the coating was optimized improved by a factor of  $\sim 3$  over the original mirror system, due to the greater pathlength possible. However, the sensitivity for detection of the other compound for which the coating was not optimized decreased by almost an order of magnitude.

Finally, to improve the light throughput of our multipath system at the wavelengths of interest, we decided to employ dielectric coatings which offer a much higher reflectivity (although limiting the useful spectral width), and the Newport Thin Film Company designed a custom coating for our special needs (i.e., high reflectivity around 350 and 660 nm). From the attached test sheet (Figure IV-2), it can be seen that in the region of the HONO and  $\text{NO}_3$  radical absorption bands the reflectivity of this dielectric coating was better than 99%. With this dielectric coating the pathlength was no longer limited by the light losses, but rather by the stacking limit for the images on the mirror surface while preserving their separation from neighboring images. Furthermore, at high image densities, minute changes in the positioning of the mirror mounts due to large temperature changes at sunrise and sunset caused misalignment of the optical system, unless the system was under constant operator observation. For automatic scanning of spectra, 32 or 40 reflections (corresponding to pathlengths of 800 and 1000 m, respectively) were generally employed, and the corresponding detection limits for quantitative analyses were then 0.6-0.7 ppb for HONO and 13-16 ppt for  $\text{NO}_3$  radicals.

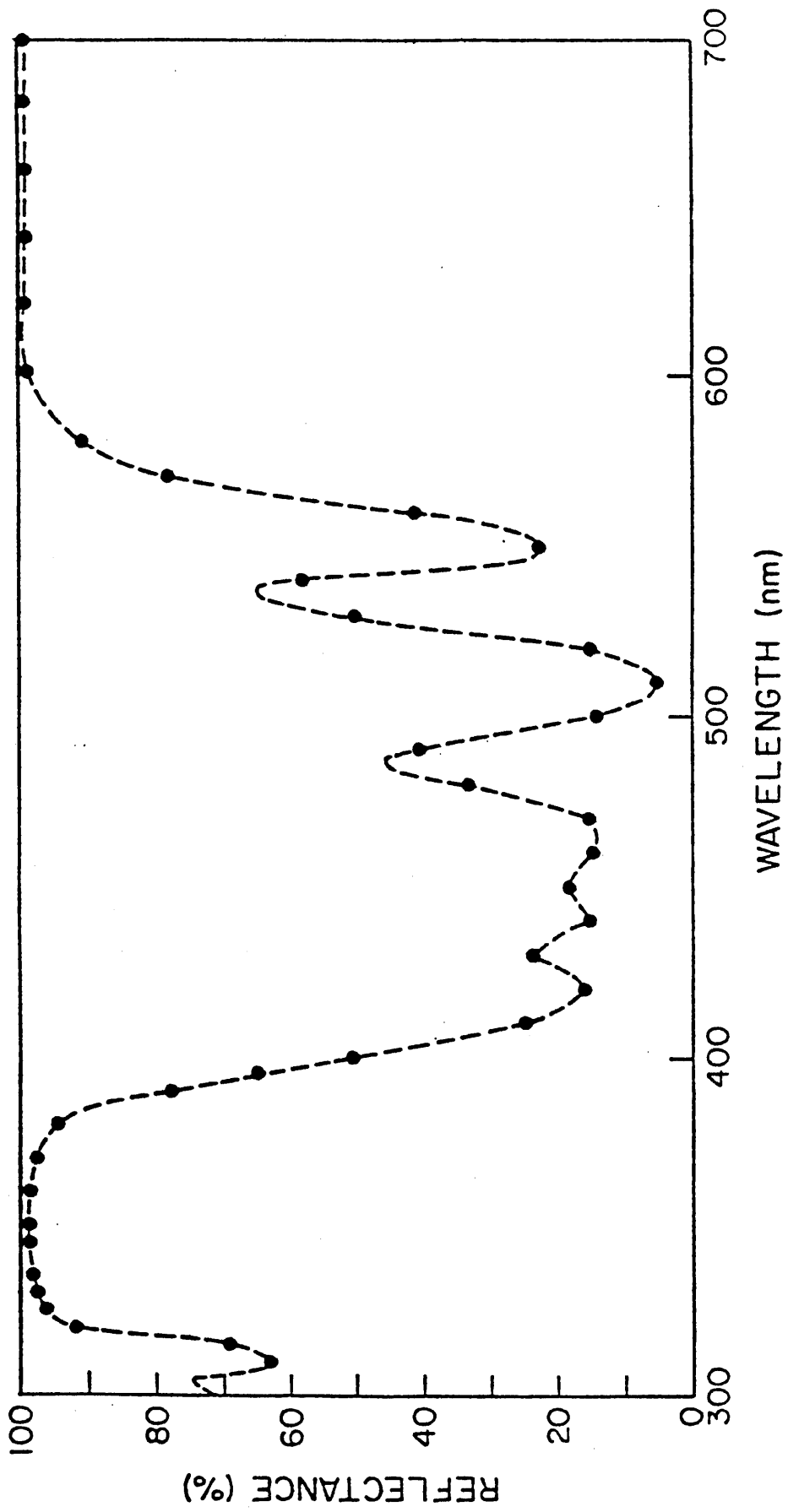


Figure IV-2. Reflectance properties of 37-layer dielectric coating employed in DOAS multiple reflection optical system.

## C. Results and Discussion

### 1. Pomona College Study (Claremont), September 1985

Prior to the beginning of this study, the spectrometer was overhauled and modified by decreasing the number of slits on the rotating wheel. The result of this modification was to double the useful scanning range of the system from ~30 nm to ~60 nm without compromising either the resolution or the signal-to-noise ratio of the data. This doubling of the scan range allowed us, for the first time, to scan the spectral range 320-370 nm and hence simultaneously quantify the species HONO, NO<sub>2</sub> and HCHO from their absorption features at 354, 365 and 339 nm, respectively. Previously, two separate scans, one centered at ~360 nm and the other at ~330 nm, were needed to quantify these species. Examples of reference spectra for NO<sub>2</sub>, HONO and HCHO over the 300-370 nm wavelength range are shown in Figure IV-3.

The conditions which led to the participation of the DOAS system in the Nitrogen Species Measurement Methods Intercomparison, the nature of the Claremont site, and the specific configuration of the DOAS system at this site have been discussed in detail in Section III, and are not repeated here. It should be noted, however, that the Claremont study represented the first application of the 25 m basepath DOAS optical system.

The overall performance of the DOAS system during this study was totally satisfactory. However, temperature changes between day and night caused slight movements in the metal mountings which in turn caused small shifts of the light beam. This effect became more serious for a larger number of passes (40 or greater), when the angle of reflection was of the same order as that induced by the temperature change. In this case the number of passes could change with temperature and a quantitative evaluation of the data became impossible.

Because of these temperature effects, the alignment of the light beam needed to be checked regularly, especially around sunrise and sunset (every 20 min at those times, otherwise every 1 to 2 hours), and this problem limited the usable pathlength to 800 m. However, the high reflectivity (>99%) of the new multilayer coating on the multipass optics yielded an improved light throughput compared to the straight line paths of similar length previously employed. Together with several improvements in the DOAS software, this allowed us to reduce the practical detection

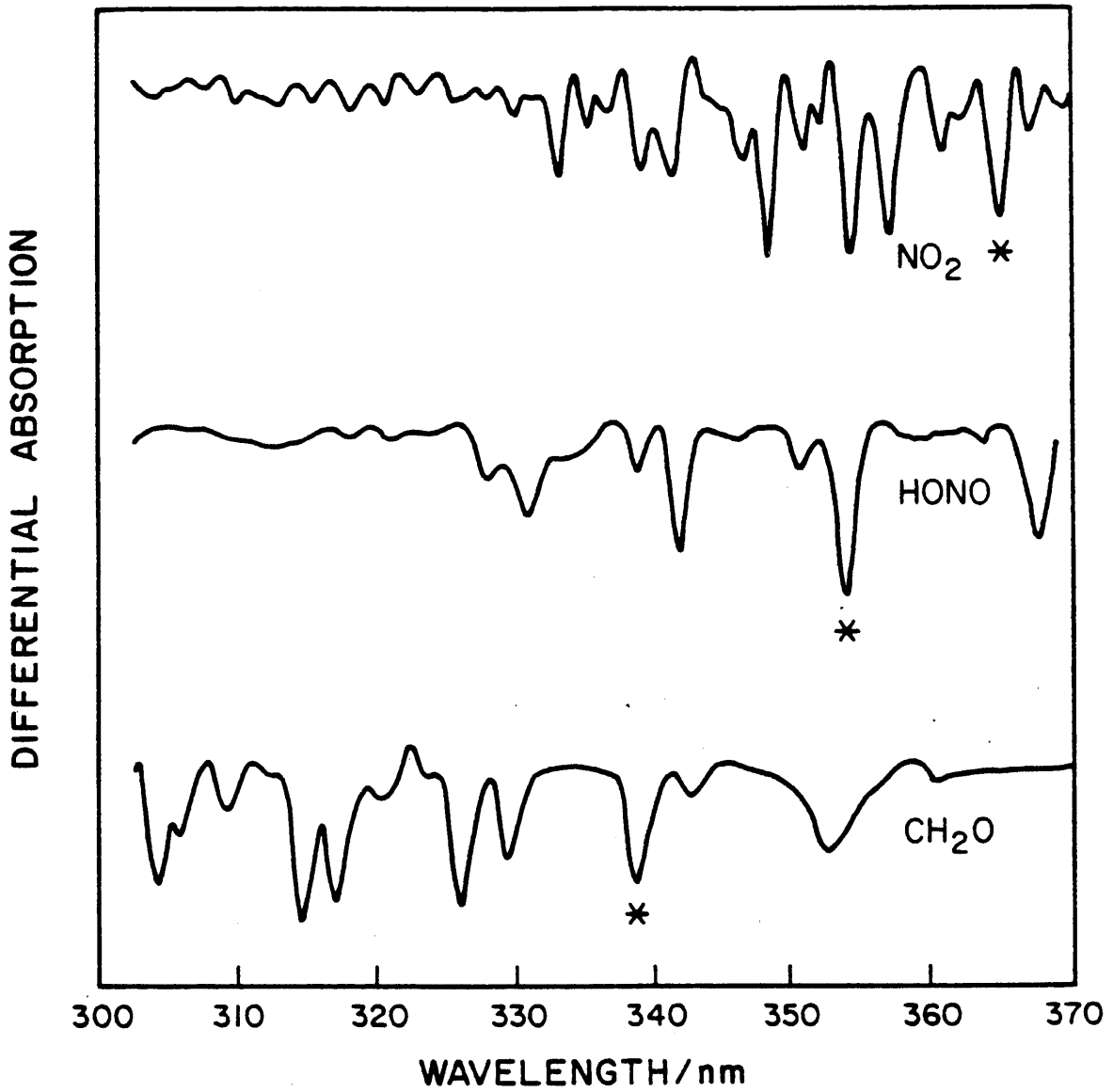


Figure IV-3. DOAS reference spectra generated for nitrogen dioxide, nitrous acid and formaldehyde, indicating principal absorption bands used for quantitative atmospheric measurements.

limit to an optical density of  $\sim 2 \times 10^{-4}$  (base 10); at a pathlength of 800 m this corresponded to detection limits of: 2.3 ppb for  $\text{NO}_2$ , 0.6 ppb for  $\text{HNO}_2$  and 0.01 ppb for  $\text{NO}_3$ .

Sampling Schedule. The intercomparison study began at 0800 PDT, September 11 and lasted until 0600 PDT, September 19, 1985. For the majority of the analytical techniques used for nitrogenous species in this intercomparison (e.g., denuders and filter packs), there were five sampling time periods for each day: 0000-0600 hr, 0800-1200 hr, 1200-1600 hr, 1600-2000 hr, and 2000-2400 hr, with the period 0600-0800 hr being utilized for maintenance and calibration. Both the FT-IR and DOAS techniques, which acquired four to five spectral records per hour, were considered "continuous" techniques for the purpose of this study.

Calibration and Treatment of DOAS Data. In order to determine the differential absorptions of  $\text{NO}_2$ , HONO and  $\text{NO}_3$  from ambient air spectra, the background envelope was first removed. A background spectrum was synthesized from the original spectrum by a sequence of Fourier analyses, with truncation after approximately five frequency elements and consecutive Fourier syntheses. After removal of the broad-band contour the residual spectra were successively fitted to the reference spectra using a least squares method.

Figure IV-4 gives an example of this data analysis procedure and the system performance. The top trace (a) is an actual, full-scale air spectrum obtained during the night of September 15 (the zero intensity line overlaps trace (b)]. The broad, large-scale structure is due to a superposition of spectral response curves resulting from mirror reflectivity, lamp intensity, photomultiplier sensitivity, and other instrumental characteristics. Trace (b) shows the residual trace after the synthetic background was subtracted as described above. Trace (c) is the same spectrum magnified by a factor of 16 to depict more clearly the low optical densities involved. The predominant structure can be immediately recognized as being due to  $\text{NO}_2$ , a reference spectrum of which is shown in (d). After subtraction of the  $\text{NO}_2$  features and further magnification by a factor of 4, the residual structure in trace (e) is unambiguously identified as HONO by comparison with its reference spectrum (f).

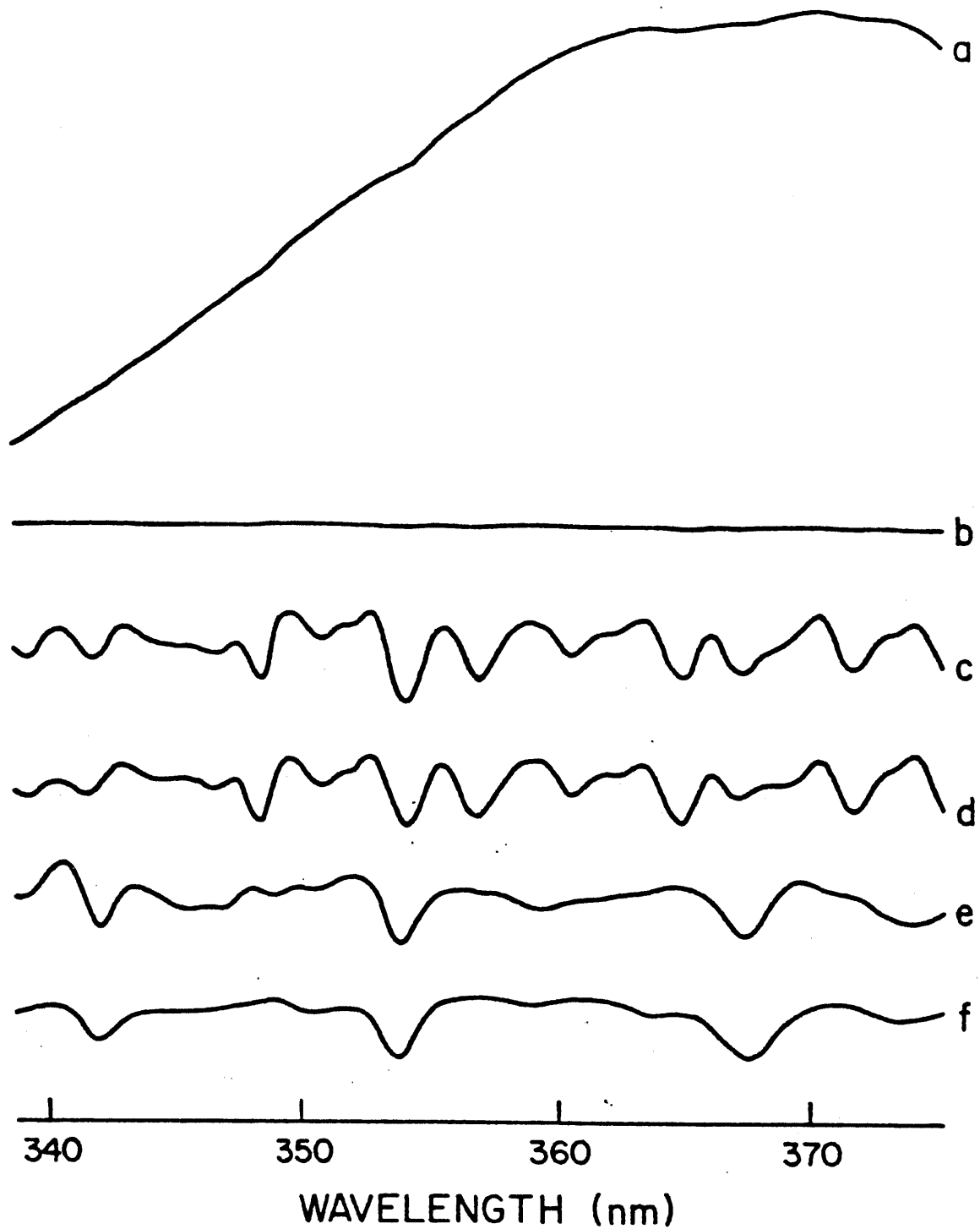


Figure IV-4. DOAS spectrum of ambient air covering the wavelength region ~340-375 nm from the night of September 15-16, 1985: (a) full scale air spectrum [the zero intensity line overlaps trace (b)]; (b) after removal of background curvature; (c) same as (b), magnified by a factor of 16; (d)  $\text{NO}_2$  reference; (e) after  $\text{NO}_2$  subtraction, magnified by a factor of 4; (f) HONO reference spectrum.

These optical densities were converted to concentrations using recommended literature values (DeMore et al. 1985) for the differential absorption cross-sections for NO<sub>2</sub> and HONO of  $1 \times 10^{-19} \text{ cm}^2 \text{ molecule}^{-1}$  at 365 nm and  $4.2 \times 10^{-19} \text{ cm}^2 \text{ molecule}^{-1}$  at 354 nm, respectively. We also determined the NO<sub>2</sub> differential absorption cross section using known concentrations of NO<sub>2</sub> in 10 cm and 25 cm cells under actual operating conditions of the DOAS system, and obtained agreement with the literature absorption cross-sections to within 10%. Based on the literature cross-sections, an 800 m pathlength, and the actual noise levels in the spectra, we calculated detection limits of 4 ppb for NO<sub>2</sub> and 0.6 ppb for HONO. The error limits for the NO<sub>2</sub> data were estimated at  $\pm 15\%$ , while the corresponding errors for HONO were  $\pm 30\%$ , reflecting the more complex data deconvolution.

DOAS Data. Hourly average NO<sub>2</sub> concentrations during the study period, as measured by DOAS, are given in Table IV-2. Throughout this measurement period, NO<sub>2</sub> levels were always above the detection limit of 4 ppb, with a minimum value of 9 ppb being observed during the early afternoon hours of September 15, and a maximum of 135 ppb being recorded during the evening hours of September 12. A comparison of NO<sub>2</sub> data obtained with other methods (Lawson 1987) show good agreement with the DOAS results. NO<sub>3</sub> radical concentrations only exceeded the detection limit of 20 ppt on September 13 and 14 for an approximately one-hour period on each day around 2000 hr, when the concentrations peaked at  $\sim 70$  ppt. From these NO<sub>3</sub> and NO<sub>2</sub> data, N<sub>2</sub>O<sub>5</sub> concentrations can be calculated (Atkinson et al. 1986) by use of the appropriate equilibrium constant (Kircher et al. 1984). These calculations yield N<sub>2</sub>O<sub>5</sub> concentrations of  $\sim 5$  ppb at the times of these NO<sub>3</sub> maxima.

HONO concentrations (in ppb), as measured by our long pathlength DOAS system, are provided in Table IV-3. These data are hourly averages computed from the original measurements, which cover 12-minute sampling intervals. When concentration levels were detectable only for part of the hour, they are quoted as upper limits. For example, based on a detection limit of 0.6 ppb, if during the first 48 minutes (four 12-minute samples) no HONO was detected and for the last 12 minutes a concentration of 1.0 ppb was measured, an upper limit of  $[(4 \times 0.6) + 1.0]/5$  or 0.68 ppb would be quoted.

Table IV-2. Hourly Average NO<sub>2</sub> Concentrations (ppb)<sup>a</sup> Measured During the 1985 Claremont Study by the Long Pathlength DOAS System

Hourly Period (PDT)	Sept 11	Sept 12	Sept 13	Sept 14	Sept 15	Sept 16	Sept 17	Sept 18	Sept 19
0000-0100		46	83	82	85	56	50	41	22
0100-0200		48	38	54	39	32	47	38	20
0200-0300		40	31	55	52	21	28	42	18
0300-0400		36	23	48	37	38	16	43	16
0400-0500		40	21	42	45	40	18	39	24
0500-0600		42	25	44	29	41	15	39	33
0600-0700		47	52	41	18	36	21	41	33
0700-0800		50	73	40	42	27	22	38	34
0800-0900	23	47	72	75	41	49	21	37	36
0900-1000	21	50	59	97	60	61	28	34	
1000-1100	20	46	53	62	40	47	33	36	
1100-1200	17	46	40	36	23	29	28	26	
1200-1300	15	26	15	39	11	21	24	25	
1300-1400	13	13	32	23	11	18	24	41	
1400-1500	15	12	26	17	9	16	20	24	
1500-1600	15	34	28	19	11	17	22	33	
1600-1700	18	33	37	27	13	21	32	39	
1700-1800	22	38	48	26	16	30	35	36	
1800-1900	29	50	58	37	34	33	46	33	
1900-2000	43	78	73	50	47	36	48	47	
2000-2100	52	123	99	58	56	40	64	45	
2100-2200	53	135	128	80	69	56	62	43	
2200-2300	52	103	119	90	73	64	57	37	
2300-2400	45	96	110	91	63	59	51	30	

<sup>a</sup>Estimated errors:  $\pm 4$  ppb or  $\pm 15\%$ , whichever is larger.

Table IV-3. Hourly Average HONO Concentrations (ppb)<sup>a,b</sup> Measured During the 1985 Claremont Study by the Long Pathlength DOAS System

Hourly Period (PDT)	Sept 11	Sept 12	Sept 13	Sept 14	Sept 15	Sept 16	Sept 17	Sept 18
0000-0100		0.74	1.56	1.25	1.31	2.55	0.83	BD
0100-0200		0.75	0.97	0.94	0.69	1.89	0.68	BD
0200-0300		0.73	0.74	0.88	0.89	1.37	≤0.63	≤0.66
0300-0400		0.85	0.61	0.94	0.87	1.40	BD	≤0.80
0400-0500		0.75	0.63	0.98	0.94	1.31	BD	BD
0500-0600		1.00	≤0.62	1.03	0.78	1.37	BD	BD
0600-0700		1.04	BD	0.85	0.66	1.27	BD	BD
0700-0800		≤0.82	BD	≤0.70	≤0.66	≤0.79	BD	BD
0800-0900	BD							
0900-1000	BD							
1000-1100	BD							
1100-1200	BD							
1200-1300	BD							
1300-1400	BD							
1400-1500	BD							
1500-1600	BD							
1600-1700	BD							
1700-1800	BD							
1800-1900	BD							
1900-2000	BD	≤0.62						
2000-2100	BD	≤0.63	BD	BD	BD	BD	BD	≤0.80
2100-2200	BD	0.88	≤0.79	≤0.79	≤0.61	BD	BD	≤0.91
2200-2300	≤0.62	1.53	1.16	1.28	0.95	≤0.66	BD	≤0.64
2300-2400	0.75	1.76	1.43	1.48	1.76	1.01	BD	BD

<sup>a</sup>BD: below detection limit (0.6 ppb).

<sup>b</sup>Digits beyond 2 significant figures are retained only for the sake of format. See text for a discussion of errors.

Tables IV-4 and IV-5 list the NO<sub>2</sub> and HONO concentrations measured by DOAS as averaged over the sampling periods designated for non-spectroscopic methods in the sample protocol for the Nitrogen Species Measurement Methods Intercomparison Study. These data were derived from the hourly averages given in Tables IV-2 and IV-3.

Table IV-4. Average NO<sub>2</sub> Concentrations (ppb) Measured by the Long Pathlength DOAS System for the Designated Sampling Periods at Claremont (1985)

Sampling Period (PDT)	Sept 11	Sept 12	Sept 13	Sept 14	Sept 15	Sept 16	Sept 17	Sept 18	Sept 19
0000-0600		42	37	54	48	38	29	40	22
0800-1200	20	47	56	68	41	47	28	33	
1200-1600	15	21	25	25	11	18	23	31	
1600-2000	28	50	54	35	28	30	40	39	
2000-2400	51	114	114	80	65	55	59	39	

Table IV-5. Average HONO Concentrations (ppb) Measured by the Long Pathlength DOAS System for the Designated Sampling Periods at Claremont (1985)<sup>a</sup>

Sampling Period (PDT)	Sept 11	Sept 12	Sept 13	Sept 14	Sept 15	Sept 16	Sept 17	Sept 18	Sept 19
0000-0600		0.8	0.9	1.0	0.9	1.6	≤0.7	≤0.6	BD
0800-1200	BD								
1200-1600	BD								
1600-2000	BD								
2000-2400	≤0.6	≤1.2	≤1.0	≤1.0	≤1.0	≤0.7	BD	≤0.9	

<sup>a</sup>BD: below detection limit (0.6 ppb).

Significant levels of HONO were observed during the nights of September 12-13, 13-14, 14-15 and 15-16. The highest HONO concentration of 2.7 ppb was observed at 0038 hr on September 16. In the case of HONO, large discrepancies between the various methods employed in this intercomparison study were evident, with the DOAS system yielding the lowest concentrations by at least a factor of three. For our spectroscopic technique, the only steps between data acquisition and the final calculated HONO levels consisted of the determination of the minimum and adjacent maxima of an absorption band and subsequent conversion to the equivalent concentration. The factors which enter this calculation are the pathlength and the absorption cross-section. The pathlength can be determined from the basepath by visually counting the number of reflections in the multipass system; the absorption cross-sections are taken from the literature (DeMore et al. 1985).

Because the information concerning  $\text{NO}_2$  and HONO concentrations is contained in the same spectrum, any error occurring during data acquisition and analysis involved both species. Considering the good agreement between our data and other measurements of  $\text{NO}_2$  concentrations, there could only be two possible sources for systematic errors in our HONO data: either an interference from another compound or an error in the literature value of the absorption cross-section. The former problem always implies an overestimate of the concentrations, whereas our data are already lower than the results from other methods. For a discussion of the likely error limits of the absorption cross-section, we refer the reader to the original literature (Stockwell and Calvert 1978, DeMore et al. 1985). In their publication (Stockwell and Calvert), the authors conclude that "the accumulated error in these estimates which could result from the absorbance measurement and equilibrium data employed should be less than 10% at the maxima in the HONO absorption spectrum." Additionally, it should be noted that in simultaneous DOAS and FT-IR measurements of HONO concentrations in our environmental chamber, concentrations obtained from the two techniques agreed to within ~10%. Thus, it appears unlikely that the HONO data reported here are in error by more than ~30%.

The hourly  $\text{NO}_2$  and HONO averages as measured at Claremont are plotted as a function of time in Figures IV-5 through IV-8. Each time-concentration profile covers a period of two days, starting and ending at noon.



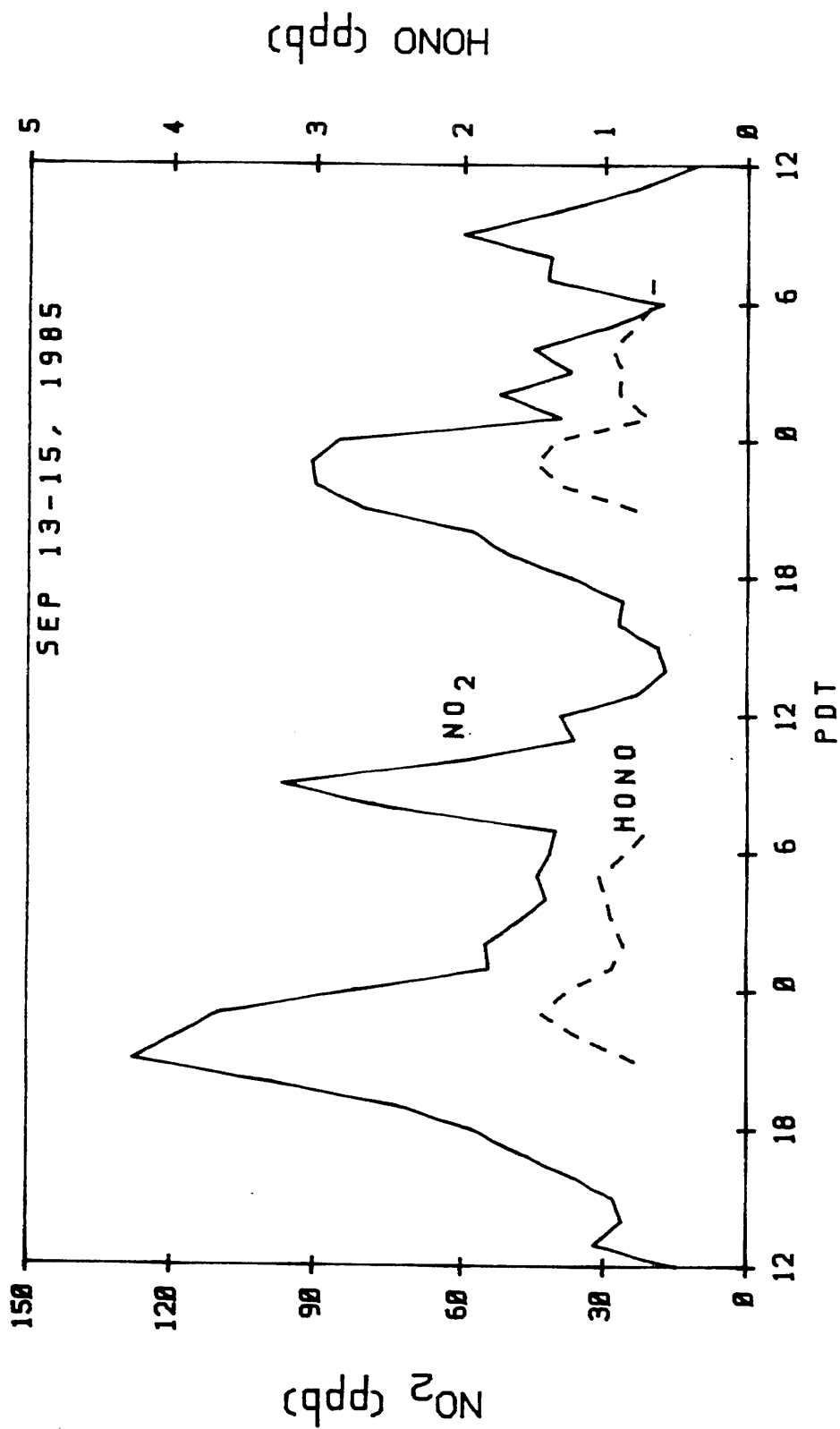


Figure IV-6. Nitrous acid and NO<sub>2</sub> time-concentration profiles for September 13-15, 1985, measured by DOAS system at Claremont, CA.

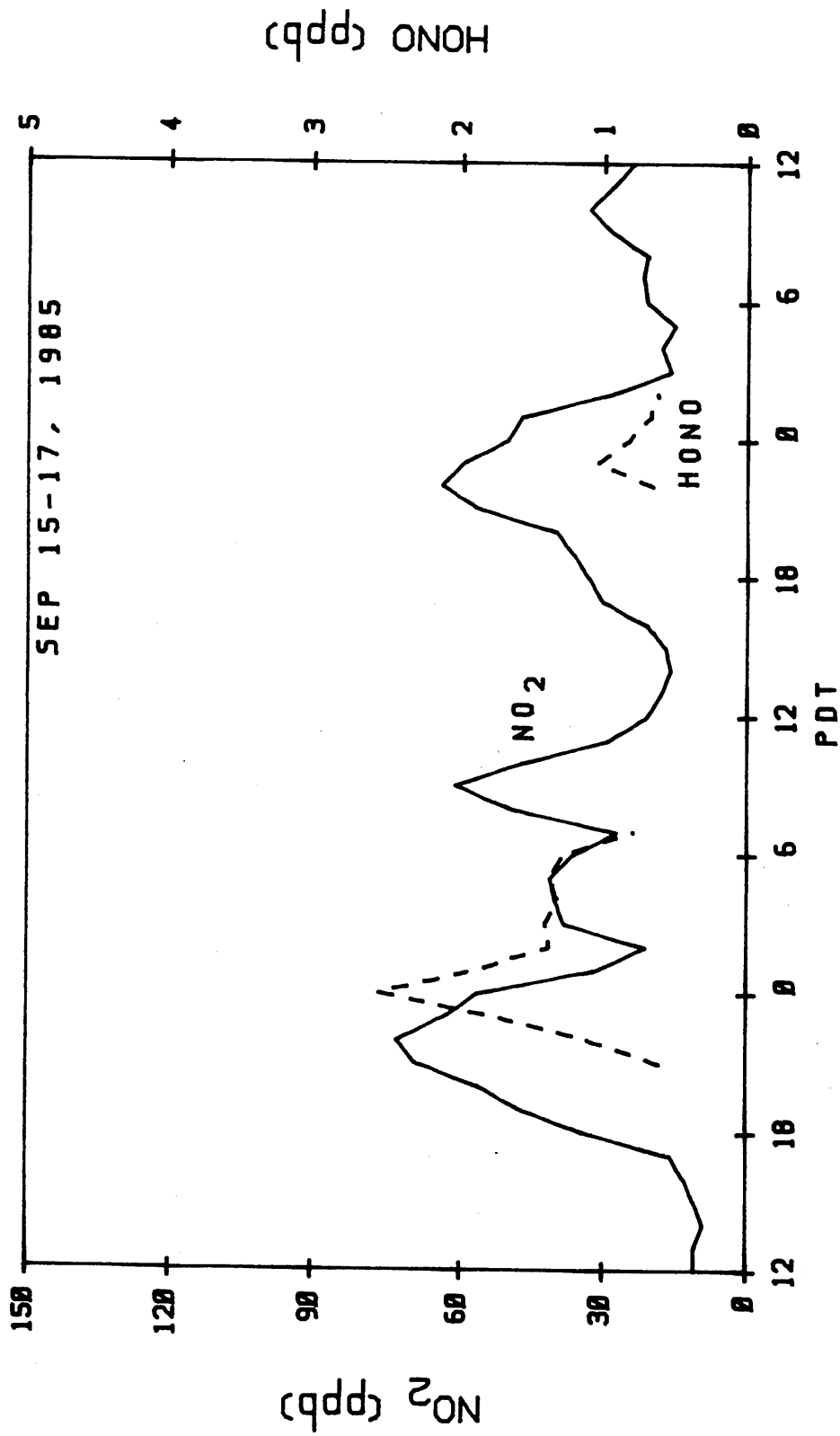


Figure IV-7. Nitrous acid and NO<sub>2</sub> time-concentration profiles for September 15-17, 1985, measured by DOAS system at Claremont, CA.

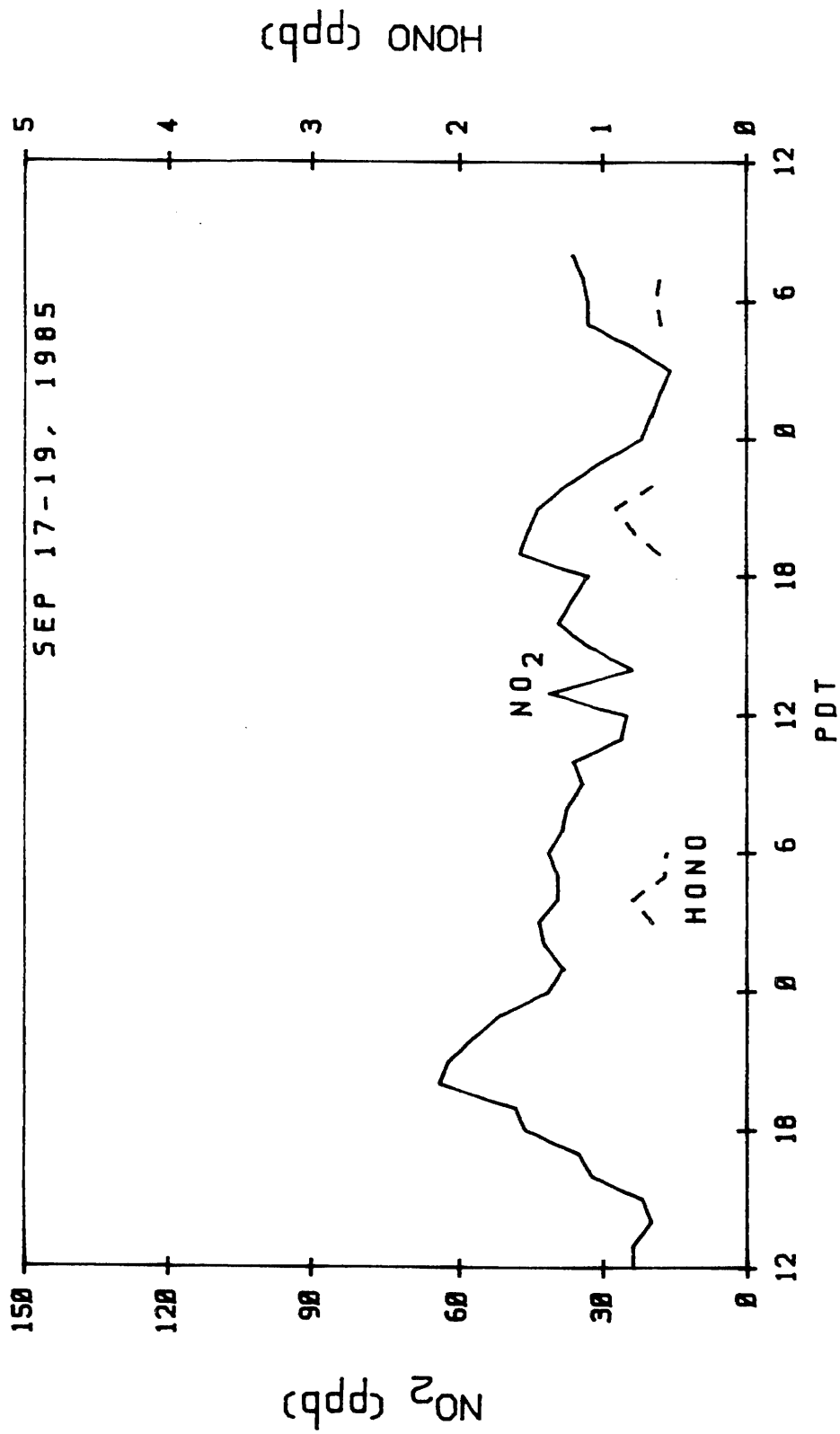


Figure IV-8. Nitrous acid and NO<sub>2</sub> time-concentration profiles for September 17-19, 1985, measured by DOAS system at Claremont, CA.

The most striking feature is that, with the exception of the night of September 15-16, the HONO profiles obtained at Claremont are different from all previous measurements obtained at Riverside (Pitts et al. 1984a). For the this first night at Claremont the profile conformed to the typical Riverside pattern of a steady increase during the night followed by a quite rapid decay after sunrise due to photolysis. This is consistent with the observation that this night was the only one that showed an NO<sub>2</sub> profile comparable to those observed in Riverside (Pitts et al. 1984a), i.e., a constant NO<sub>2</sub> level of between 25 to 30 ppb throughout the night.

During the other nights for which DOAS measurements were made at Claremont, NO<sub>2</sub> concentrations exhibited much larger fluctuations, typically peaking at 2100 to 2200 hr (well after the evening traffic peak). For those nights the HONO concentration profiles appear to follow the NO<sub>2</sub> changes, with a time lag of ~1-2 hr. Also noticeable is a shoulder, or secondary peak, in the early morning hours before sunrise comparable to the early morning peak usually observed in our previous studies (Harris et al. 1982, Pitts et al. 1984a).

The higher HONO peaks observed just before midnight are a new phenomenon, attributable to the higher NO<sub>2</sub> levels in the early part of the night. In previous SAPRC chamber studies concerning the formation of HONO from NO<sub>2</sub>-air mixtures, we observed a HONO production rate of about 6 ppb hr<sup>-1</sup> per ppm of NO<sub>2</sub>. Applying this production rate to ambient conditions, we obtain rates of HONO formation of ~0.5 ppb hr<sup>-1</sup> for Claremont and ~0.2 ppb hr<sup>-1</sup> for Riverside. These HONO production rates fit the observed increases in HONO with time quite well. One would expect, however, that in Claremont HONO should continue to rise throughout the night. The fact that the HONO profile instead follows the NO<sub>2</sub> profile may be attributed to transport phenomena; Claremont is closer to the major NO<sub>x</sub> sources than is Riverside, and thus responds to changes in the less well-mixed pollutant levels.

## 2. El Camino Community College Study (Torrance)

The selection of the El Camino Community College site, the nature of this site, and the configuration of the DOAS system have been discussed in Section III. In this section selected DOAS results from this winter high-NO<sub>x</sub> episode study during January and February of 1986 are presented.

The period between January 28 and February 22 was characterized by numerous days of heavy rains and coastal storms. Thus, after the January monitoring periods measurements were limited to the last week of February. The long pathlength DOAS system was operational during each of the three sampling periods in January and February. From January 21 until January 25 the system was operated at 700 m total optical pathlength. From January 27 until the end of the study a pathlength of 600 m was employed.

Figure IV-9 shows the NO<sub>2</sub> and HONO profiles observed during the January 27-28 sampling period, and the HONO concentration of ~11 ppb measured during this period is the highest value measured to date by SAPRC researchers using the DOAS system. The HONO time-concentration profiles observed for several other nights during this winter field study are shown in Figures IV-10 through IV-14.

In these experiments the DOAS system was operated automatically, generally signal-averaging the spectra over 30 minute time periods, and Table IV-6 lists the resulting half-hourly average NO<sub>2</sub> and HONO concentrations. The detection limits for the DOAS configuration employed at El Camino Community College were 3 ppb for NO<sub>2</sub> and 0.8 ppb for HONO. No HONO was detected during those nights (January 19-20 and February 7-8) when the NO<sub>2</sub> concentration remained below ~50-60 ppb. As expected from chamber experiments (Pitts et al. 1985e), HONO levels increased with higher ambient NO<sub>2</sub> concentrations. The HONO time-concentration profiles observed in this study differed from those observed at Riverside in the eastern end of the basin during summertime periods. In those studies, with NO<sub>2</sub> levels not exceeding ~50 ppb, HONO usually built up gradually to reach peak values of 1-2 ppb just before sunrise (see, for example, Pitts et al. 1984a, Pitts and Winer 1984). With the high NO<sub>2</sub> concentrations at Torrance, however, HONO concentrations increased rapidly after sunset and stayed reasonably constant during the middle part of the night, presumably indicating that an equilibrium was reached. Furthermore, on some nights a slight increase in the HONO concentration was observed in the morning hours before sunrise (being most pronounced on January 28). This probably resulted from direct emissions of HONO from cars or from rapid conversion of NO<sub>2</sub> to HONO in the high concentration conditions of exhaust gases.

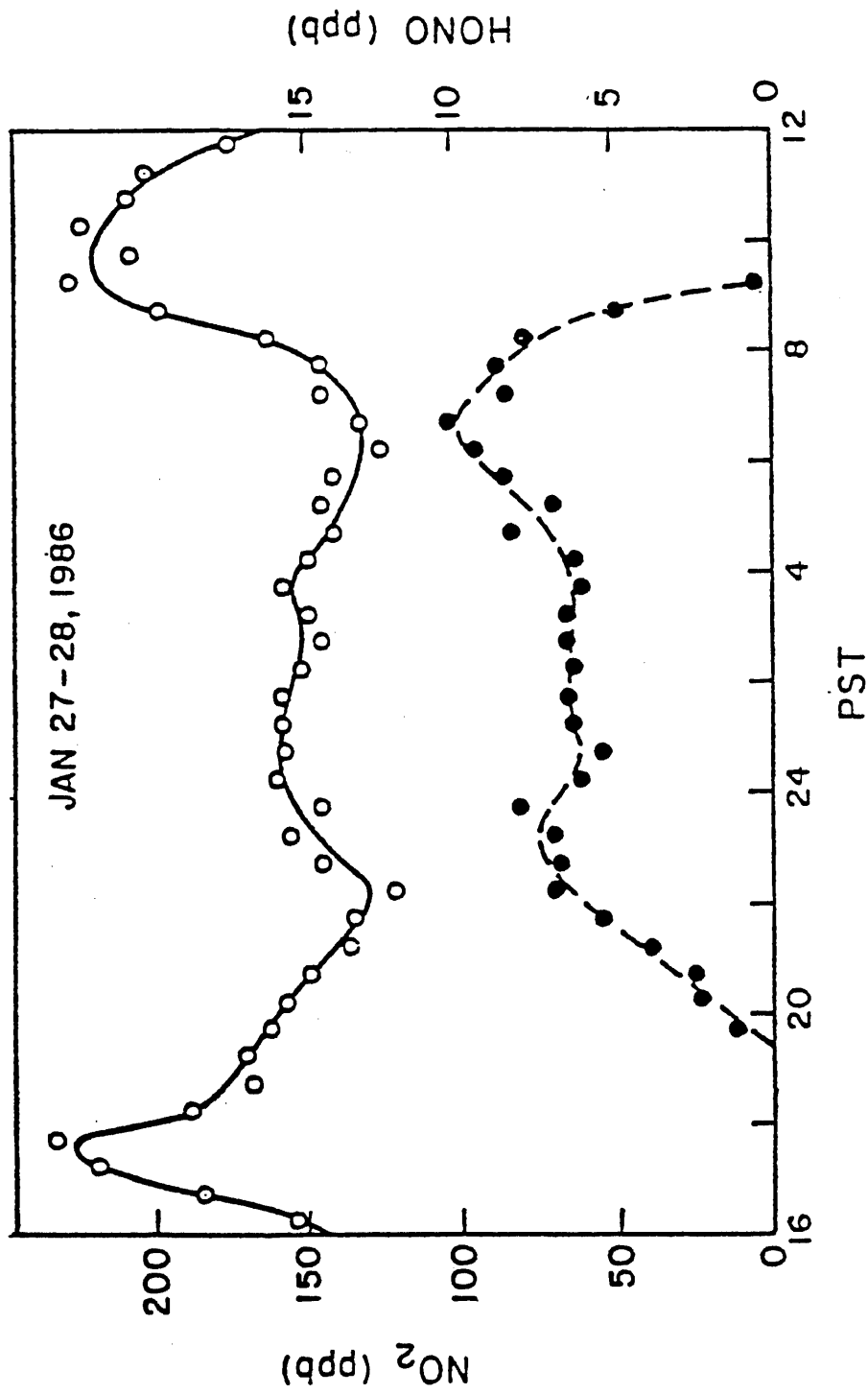


Figure IV-9. NO<sub>2</sub> (O) and HONO (●) profiles on January 27-28, 1986, at El Camino Community College, Torrance, CA. Measured by longpath (600 m) DOAS.

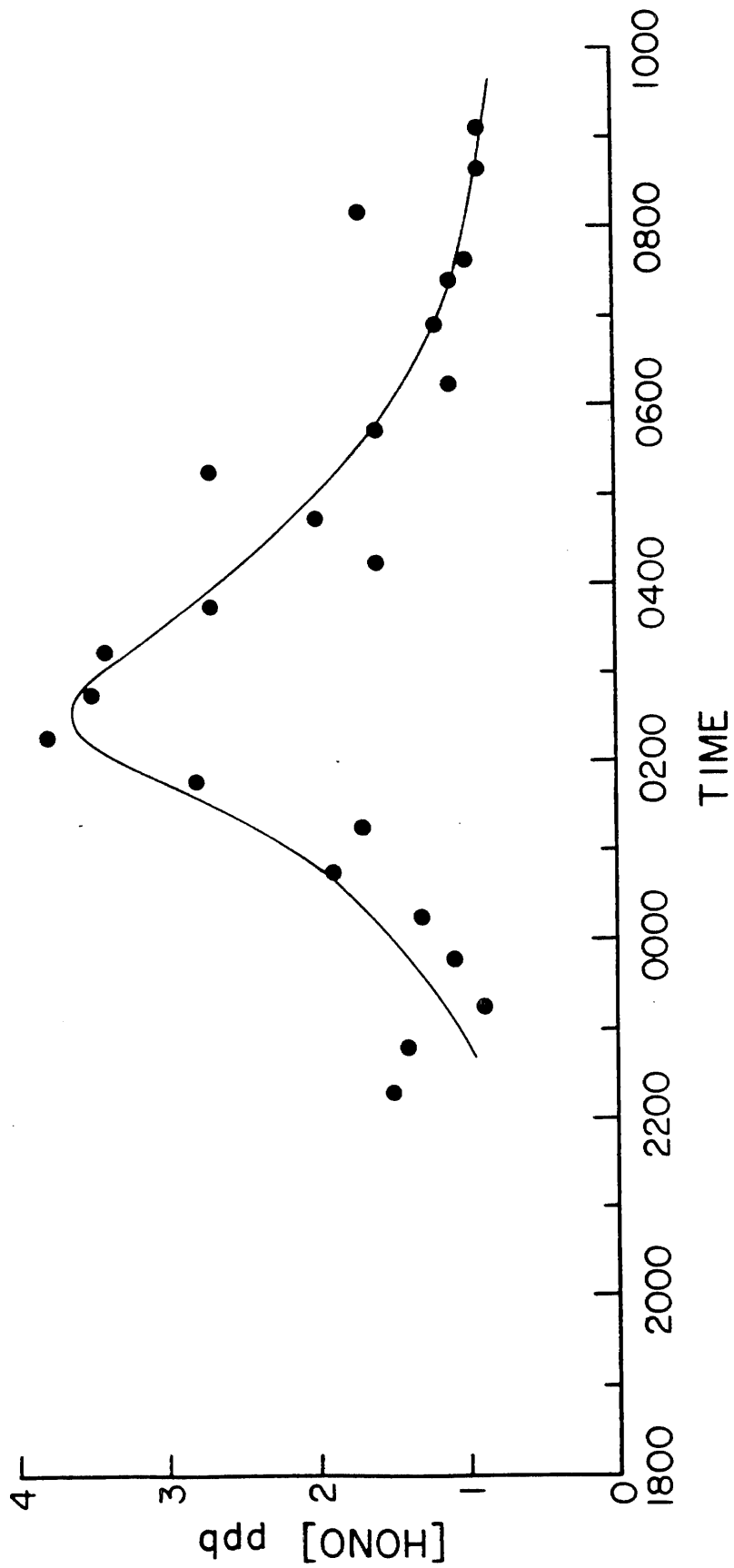


Figure IV-10. Nitrous acid time-concentration profile measured with long pathlength DOAS system during the evening of January 21-22, 1986, at El Camino Community College, Torrance, CA.

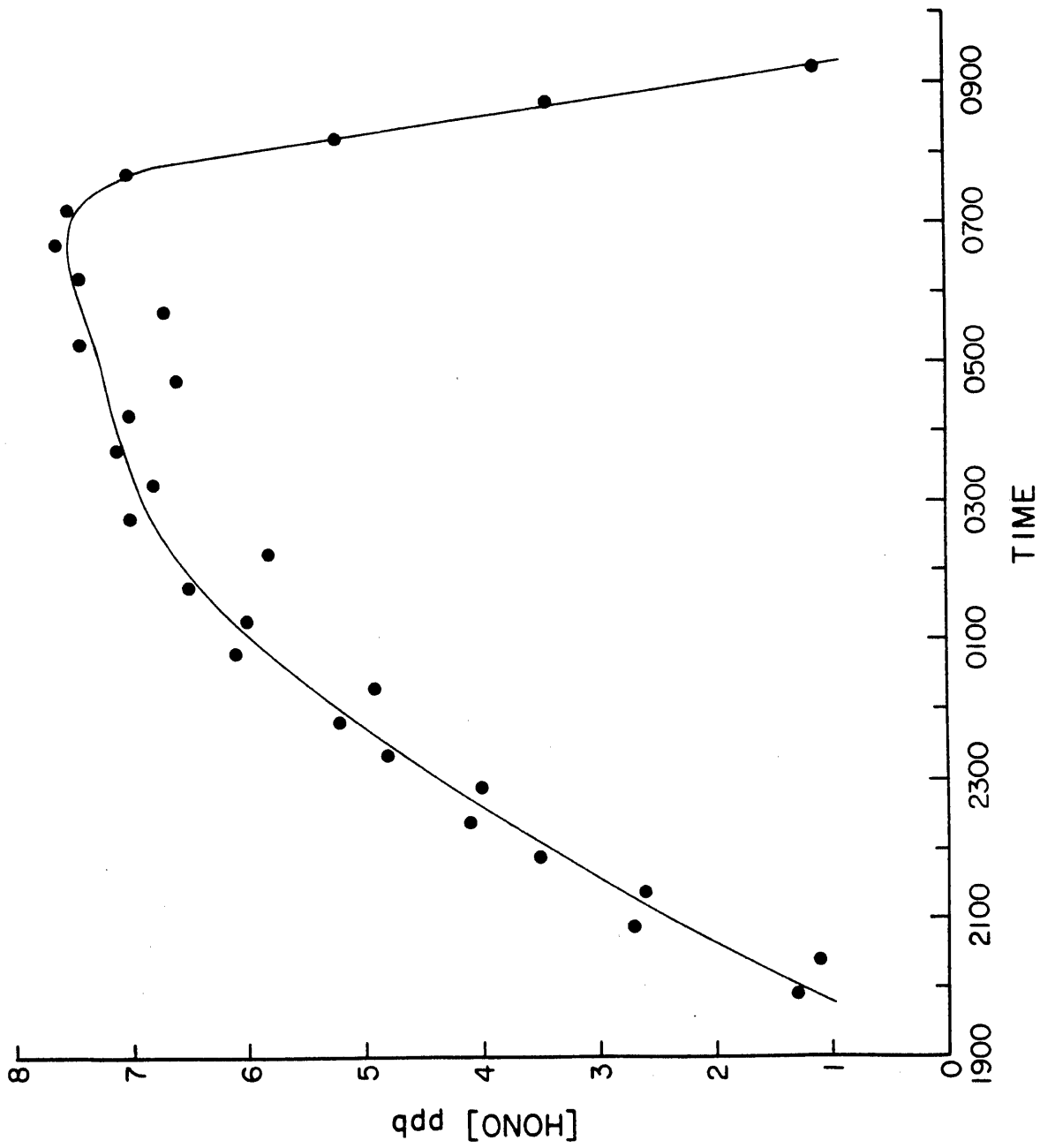


Figure IV-11. Nitrous acid time-concentration profile measured with long pathlength DOAS system during the evening of January 23-24, 1986, at El Camino Community College, Torrance, CA.

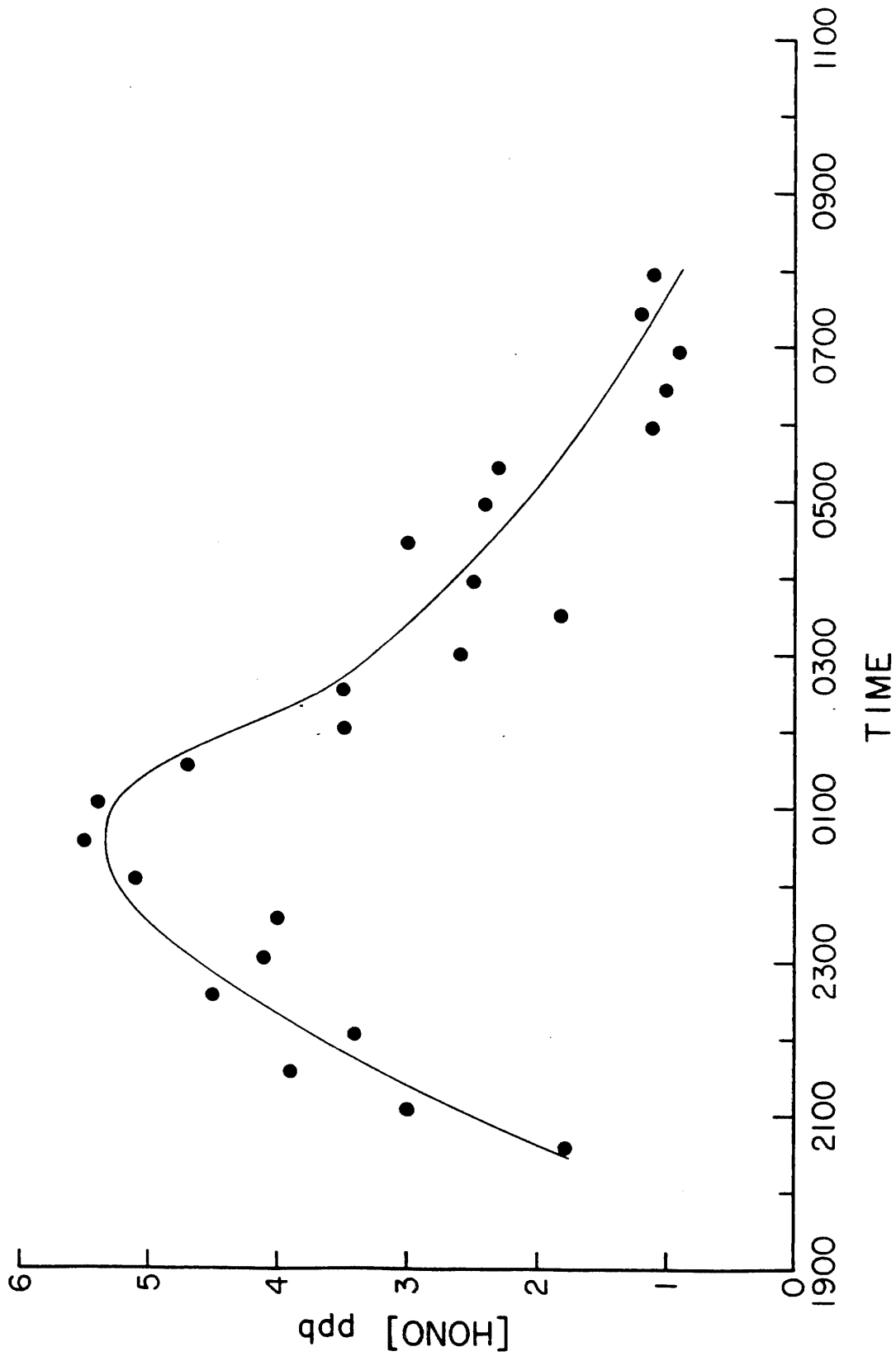


Figure IV-12. Nitrous acid time-concentration profile measured with long pathlength DOAS system during the evening of January 24-25, 1986, at El Camino Community College, Torrance, CA.

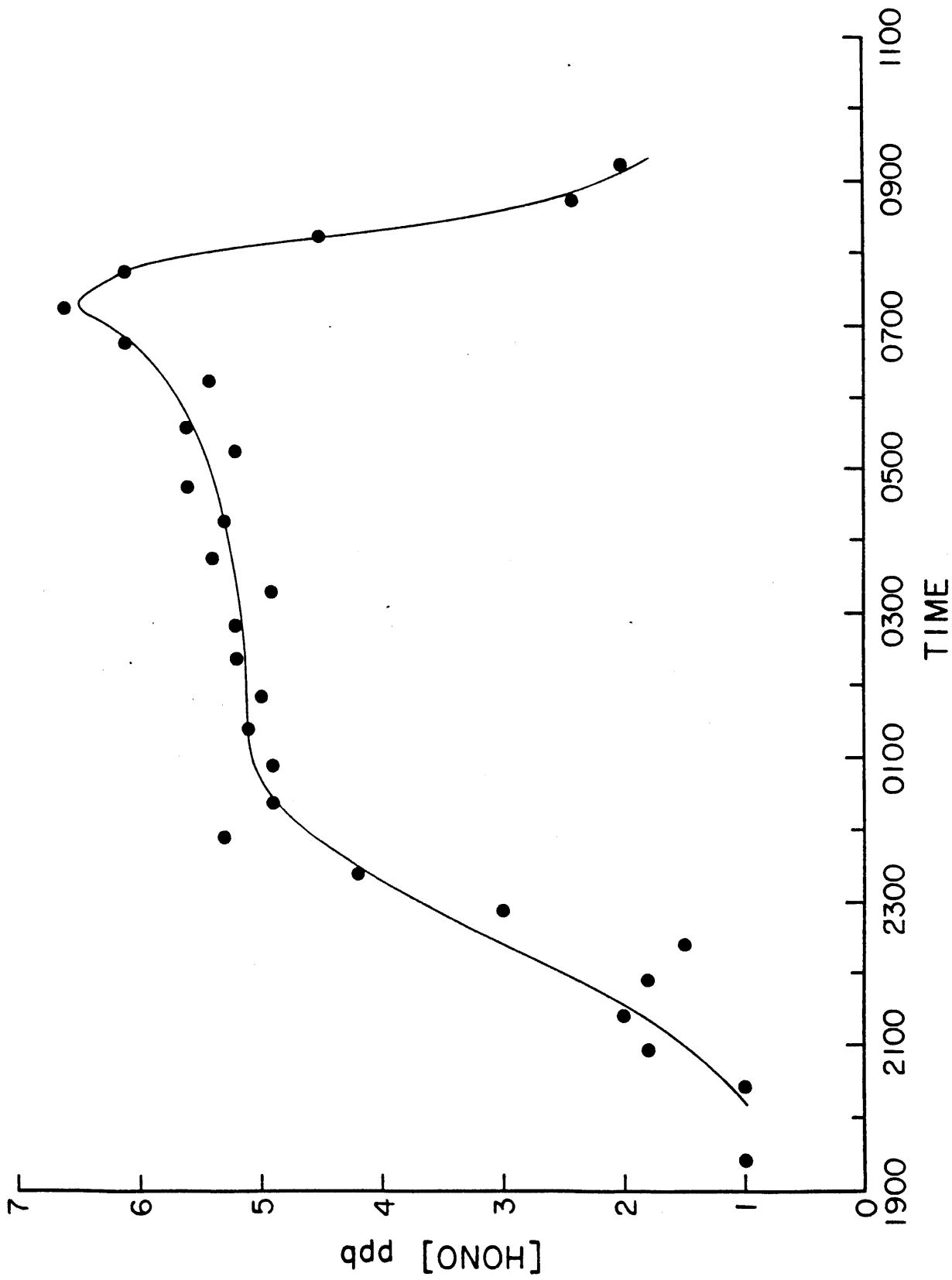


Figure IV-13. Nitrous acid time-concentration profile measured with long pathlength DOAS system during the evening of January 28-29, 1986, at El Camino Community College, Torrance, CA.

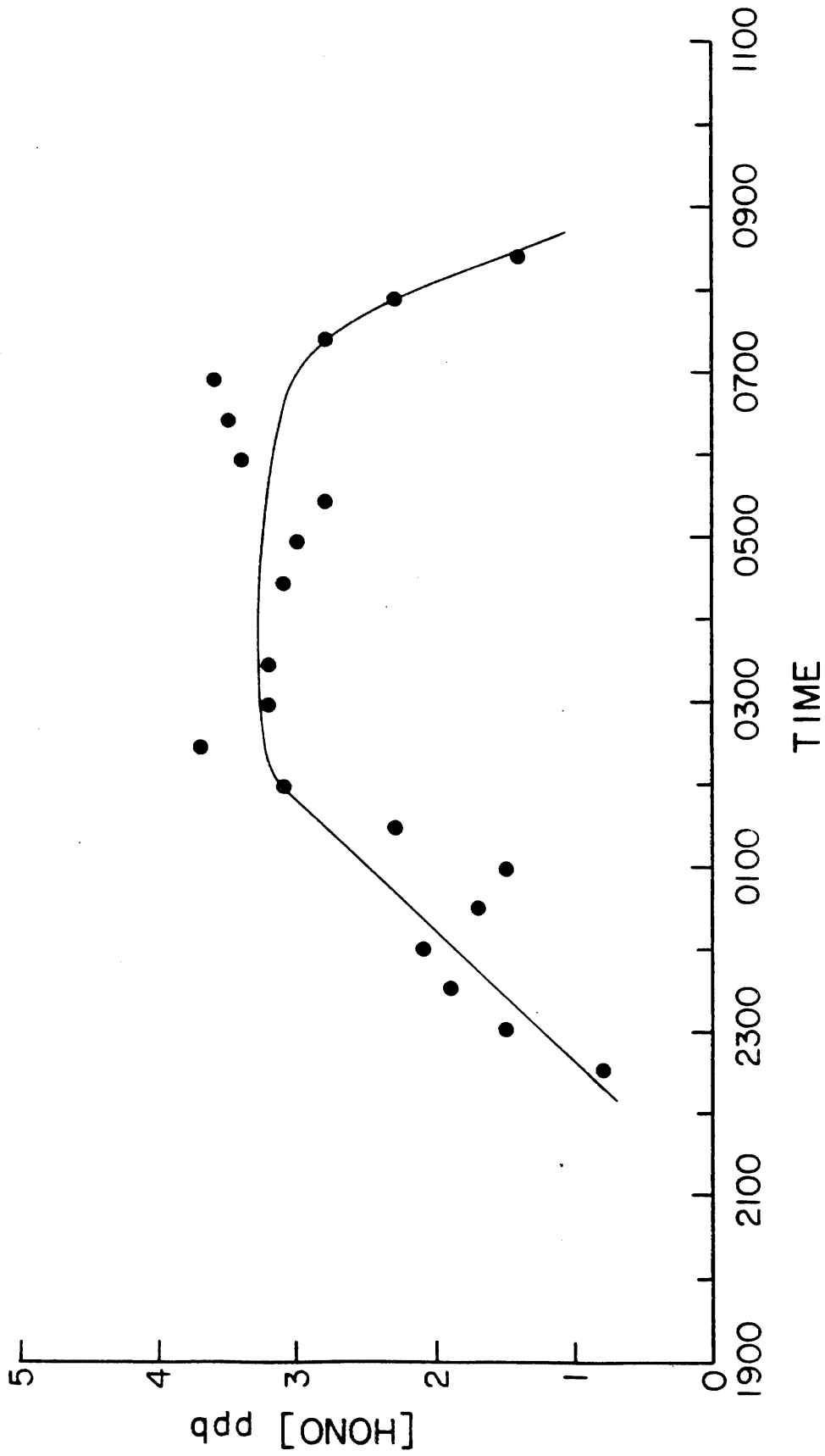


Figure IV-14. Nitrous acid time-concentration profile measured with long pathlength DOAS system during the evening of February 5-6, 1986, at El Camino Community College, Torrance, CA.

Table IV-6. Half-Hour Average NO<sub>2</sub> and HONO Concentrations (ppb)<sup>a</sup> at El Camino Community College, Torrance, CA

Time	HONO	NO <sub>2</sub>	Time	HONO	NO <sub>2</sub>
<u>January 21-22, 1986</u>			<u>January 23-24, 1986</u>		
16:54	ND	24	16:56	ND	21
17:23	ND	25	17:26	ND	28
17:53	ND	41	17:55	ND	55
18:22	ND	55	18:25	ND	72
18:52	ND	47	18:55	ND	94
19:21	ND	62	19:24	ND	100
19:51	ND	71	19:54	1.3	98
20:21	ND	101	20:23	1.1	96
20:51	ND	101	20:53	2.7	94
21:20	ND	100	21:23	2.6	100
21:50	ND	120	21:52	3.5	99
22:19	1.5	124	22:22	4.1	101
22:49	1.4	119	22:51	4.0	105
23:18	0.9	98	23:21	4.8	99
23:48	1.1	72	23:50	5.2	102
0:17	1.3	79	0:20	4.9	108
0:47	1.9	112	0:50	6.1	99
1:16	1.7	119	1:19	6.0	104
1:46	2.8	108	1:49	6.5	99
2:16	3.8	105	2:18	5.8	109
2:45	3.5	109	2:48	7.0	102
3:15	3.4	109	3:18	6.8	97
3:44	2.7	97	3:47	7.1	97
4:14	1.6	72	4:17	7.0	104
4:43	2.0	81	4:46	6.6	115
5:13	2.7	89	5:16	7.4	112
5:42	1.6	82	5:46	6.7	115
6:12	1.1	65	6:15	7.4	113
6:41	1.2	68	6:45	7.6	114
7:11	1.1	71	7:14	7.5	124
7:40	2.0	87	7:44	7.0	132
8:10	2.7	108	8:13	5.2	150
8:40	0.9	102	8:43	3.4	161
9:09	0.9	102	9:13	1.1	170
9:39	ND	93	9:42	ND	176
			10:12	ND	180
			10:41	ND	151
			11:11	ND	123
			11:41	ND	97

Table IV-6 (continued) - 2

Time	HONO	NO <sub>2</sub>	Time	HONO	NO <sub>2</sub>
<u>January 24-25, 1986</u>			<u>January 25-26, 1986</u>		
16:37	ND	38	17:48	ND	79
17:06	ND	55	18:17	ND	120
17:36	ND	50	18:47	ND	131
18:05	ND	66	19:16	ND	127
18:35	ND	51	19:46	1.3	127
19:05	ND	65	20:16	2.2	120
19:34	ND	80	20:45	3.4	123
20:04	--	--	21:15	3.9	118
20:36	1.8	95	21:44	5.3	118
21:05	3.0	95	22:14	5.4	129
21:35	3.9	97	22:43	6.7	122
22:04	3.4	94	23:13	3.5	102
23:34	4.5	93	23:43	2.4	85
23:04	4.1	99	0:12	2.1	84
23:33	4.0	103	0:42	2.0	86
0:03	5.1	129	1:11	3.5	91
0:32	5.5	131	1:41	3.6	88
1:02	5.4	110	2:11	3.8	88
1:32	4.7	95	2:40	4.9	81
2:01	3.5	99	3:10	3.8	76
2:31	3.5	90	3:39	2.8	74
3:00	2.6	86	4:09	3.1	76
3:30	1.8	83	4:38	2.8	74
3:59	2.5	73	5:08	3.5	68
4:29	3.0	70	5:38	3.0	70
4:59	2.4	72	6:07	2.7	67
5:28	2.3	71	6:37	2.0	63
5:58	1.1	72	7:06	2.1	61
6:27	1.0	74	7:36	1.3	60
6:57	0.9	72	8:06	ND	54
7:26	1.2	70	8:35	ND	49
7:56	1.1	75	9:05	ND	44
8:26	ND	76			
8:55	ND	80			
9:25	ND	90			

Table IV-6 (continued) - 3

Time	HONO	NO <sub>2</sub>	Time	HONO	NO <sub>2</sub>
<u>January 26-27, 1986</u>			<u>January 27-28, 1986</u>		
18:27	ND	68	18:10	ND	189
18:57	ND	93	18:39	ND	173
19:26	ND	104	19:09	ND	175
19:56	ND	105	19:38	ND	166
20:25	3.8	104	20:08	2.1	164
20:55	4.0	108	20:39	2.1	152
21:25	4.3	101	21:09	3.9	141
21:54	5.1	94	21:39	4.8	138
22:24	5.2	88	22:08	5.9	131
22:53	4.2	82	22:38	6.8	151
23:23	3.0	79	23:10	7.1	160
23:53	2.4	75	23:39	8.0	151
0:22	1.8	74	0:09	7.3	165
0:52	1.6	73	0:39	7.0	164
1:21	1.5	72	1:08	7.5	162
1:51	2.3	66	1:38	7.7	162
2:11	2.2	63	2:07	7.2	156
2:50	1.8	63	2:37	7.0	150
3:20	2.2	62	3:07	7.0	153
3:49	2.2	62	3:36	6.7	162
4:19	1.8	62	4:06	6.7	153
4:49	1.8	63	4:35	8.5	145
5:18	1.9	65	5:05	7.5	150
5:48	2.5	63	5:35	8.9	142
6:17	2.7	62	6:04	10.1	129
6:47	2.7	61	6:34	11.0	135
7:17	2.9	65	7:03	10.5	150
7:46	3.2	76	7:33	9.8	150
8:16	3.4	108	8:02	6.2	168
8:45	1.5	116	8:32	5.5	203
9:15	ND	130	9:02	2.2	230
9:45	ND	112	9:31	ND	208
			10:01	ND	222
			10:30	ND	207
			11:00	ND	200
			11:30	ND	172

Table IV-6 (continued) - 4

Time	HONO	NO <sub>2</sub>	Time	HONO	NO <sub>2</sub>
<u>January 28-29, 1986</u>			<u>February 5-6, 1986</u>		
16:59	ND	67	17:00	ND	27
17:28	ND	64	17:30	ND	30
17:58	ND	99	18:00	ND	43
18:28	ND	91	18:29	ND	41
18:57	ND	110	18:59	ND	62
19:27	1.0	95	19:28	ND	61
19:57	ND	95	20:04	ND	58
20:26	1.0	114	20:33	ND	39
20:56	1.8	143	21:03	ND	51
21:25	2.0	138	21:32	ND	49
21:55	1.8	132	22:02	ND	56
22:24	1.5	129	22:32	0.8	60
22:54	3.0	129	23:01	1.5	71
23:23	4.2	131	23:31	1.9	88
23:53	5.3	127	23:31	1.9	88
0:22	4.9	135	24:00	2.1	84
0:52	4.9	142	0:30	1.7	74
1:22	5.1	134	0:59	1.5	76
1:51	5.0	130	1:29	2.3	71
2:21	5.2	128	1:59	3.1	73
2:50	5.2	128	2:28	3.7	77
3:20	4.9	131	2:58	3.2	80
3:49	5.4	124	3:27	3.2	77
4:19	5.3	120	4:26	3.1	72
4:48	5.6	110	4:56	3.0	68
5:18	5.2	116	5:26	2.8	66
5:48	5.6	111	5:55	3.4	64
6:17	5.4	112	6:25	3.5	64
6:47	6.1	113	6:54	3.6	61
7:16	6.6	120	7:24	2.8	67
7:46	6.1	131	7:53	2.3	76
8:15	4.5	145	8:23	1.4	90
8:45	2.4	161	8:52	ND	97
9:14	2.0	208	9:22	ND	100
9:44	ND	199	9:52	ND	56
10:13	ND	197	10:21	ND	38
10:43	ND	164	10:51	ND	27
11:13	ND	69			
11:42	ND	28			

<sup>a</sup>ND: not detected (less than 0.8 ppb HONO).

Data for other species measured using continuous analyzers during the El Camino College Study are given in Appendix C.

### 3. Citrus College Study (Glendora)

In conjunction with the CARB-sponsored Carbonaceous Aerosol Study, the SAPRC 25 m basepath FT-IR and DOAS systems were set up essentially as described for the Claremont study (Section III). The specific orientation of the DOAS system relative to other experiments conducted during this field study has also been described in Section III.

Essentially continuous DOAS measurements were conducted from August 13 until the morning of August 21, 1986. Maximum ozone levels and peak concentrations of  $\text{NO}_3$  radicals during this study are summarized in Table IV-7. Individual concentrations of HONO, HCHO and  $\text{NO}_2$  observed during this period are given in tabular form in Appendix B and are plotted in Figures IV-15 to IV-17. Hourly average data for these species are given in Tables IV-8 to IV-10. For the majority of the time the pathlength was set to 800 m with a detection limit equivalent to an optical density of  $3 \times 10^{-4}$ . The data reduction process was more automated than previously, and thus the detection limit was raised from  $2 \times 10^{-4}$  to  $3 \times 10^{-4}$  O.D. to offset the tendency of the software to interpret noise at the detection limit as a peak. The corresponding detection limits were  $\text{NO}_2$ , 3.5 ppb; HONO, 0.8 ppb; and HCHO, 4.5 ppb.

Because the HONO and HCHO bands are overlapped by  $\text{NO}_2$  bands and  $\text{NO}_2$  is more abundant in the Los Angeles basin, the DOAS spectra must be first analyzed for  $\text{NO}_2$  to enable its features to be quantitatively removed prior to determining HONO and HCHO concentrations. Figure IV-15 shows the time-concentration profile for  $\text{NO}_2$  from 0000 hr on August 13 to 0800 hr on August 21. The solid line shows the DOAS data, while the dashed line shows measurements made by our chemiluminescence oxides of nitrogen analyzer. The two curves track each other very well during the nighttime and early morning hours. In the afternoon the  $\text{NO}_x$  analyzer consistently read 10 to 30 ppb higher; since the DOAS values at those times were as low as 15-25 ppb this caused a discrepancy of a factor of two or more. The higher values measured by the chemiluminescence method are attributed to the known interferences of  $\text{HNO}_3$  and PAN in this detection method, consistent with the levels of  $\text{HNO}_3$  and PAN in the afternoon periods being approximately equivalent to this difference in the DOAS  $\text{NO}_2$  and chemiluminescence  $\text{NO}_x$ -NO readings.

Table IV-7. Maximum O<sub>3</sub> Levels and Observations of NO<sub>3</sub> Radicals at Citrus College, Glendora, CA, During August 13-20, 1986

Date	Maximum O <sub>3</sub> Concentration (ppm)	NO <sub>3</sub> Radical Peak Concentration (ppt)
8/13	0.185	72
8/14	0.27	<40
8/15	0.26	ND
8/16	0.24	ND
8/17	0.27	ND
8/18	0.28	ND
8/19	0.30	<40
8/20	0.27	<40

ND: Not detected.

After the quantitative removal of the NO<sub>2</sub> features from the DOAS spectra, the data reduction procedure utilized a simultaneous least-squares fit of HONO and HCHO reference spectra to the residual ambient air spectra. Figure IV-16 shows the time concentration profile for HCHO as determined by DOAS (solid line). For comparison, the FT-IR data from Section V are shown as the dashed line. The agreement between the two methods is very good, with the discrepancies being within the error limits. However, it appears that the DOAS results for the first four nights are consistently higher than the FT-IR data by about 1-3 ppb. This could be due to an overestimation of HCHO absorption features in the DOAS spectra, since the reported FT-IR HCHO levels were at or below the DOAS detection limit of 4.5 ppb (where the signal-to-noise ratio was near unity).

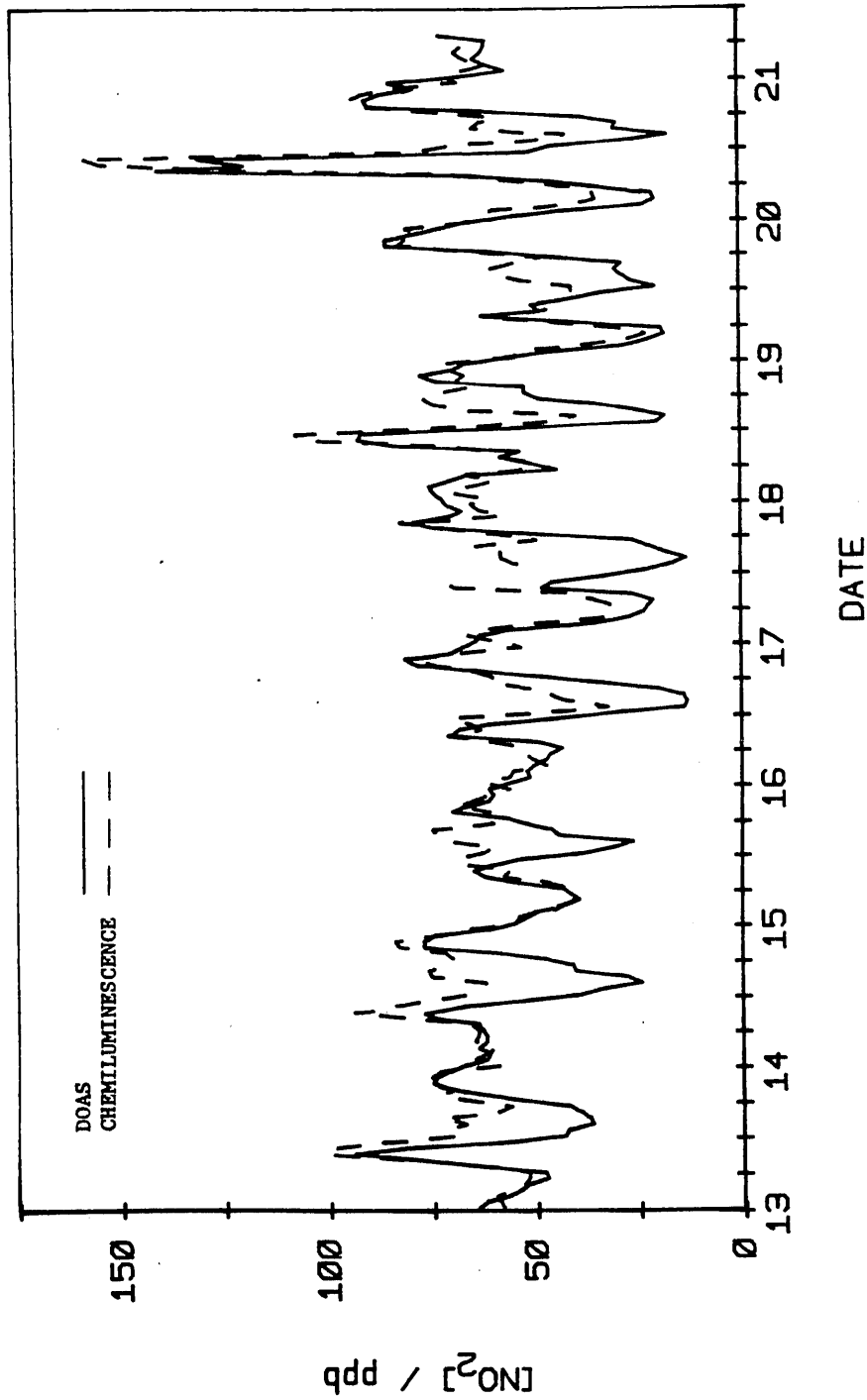


Figure IV-15. Time concentration profiles for nitrogen dioxide measured by DOAS and chemiluminescence ( $NO_x-NO$ ) at Citrus College (Glendora) in August 1986.

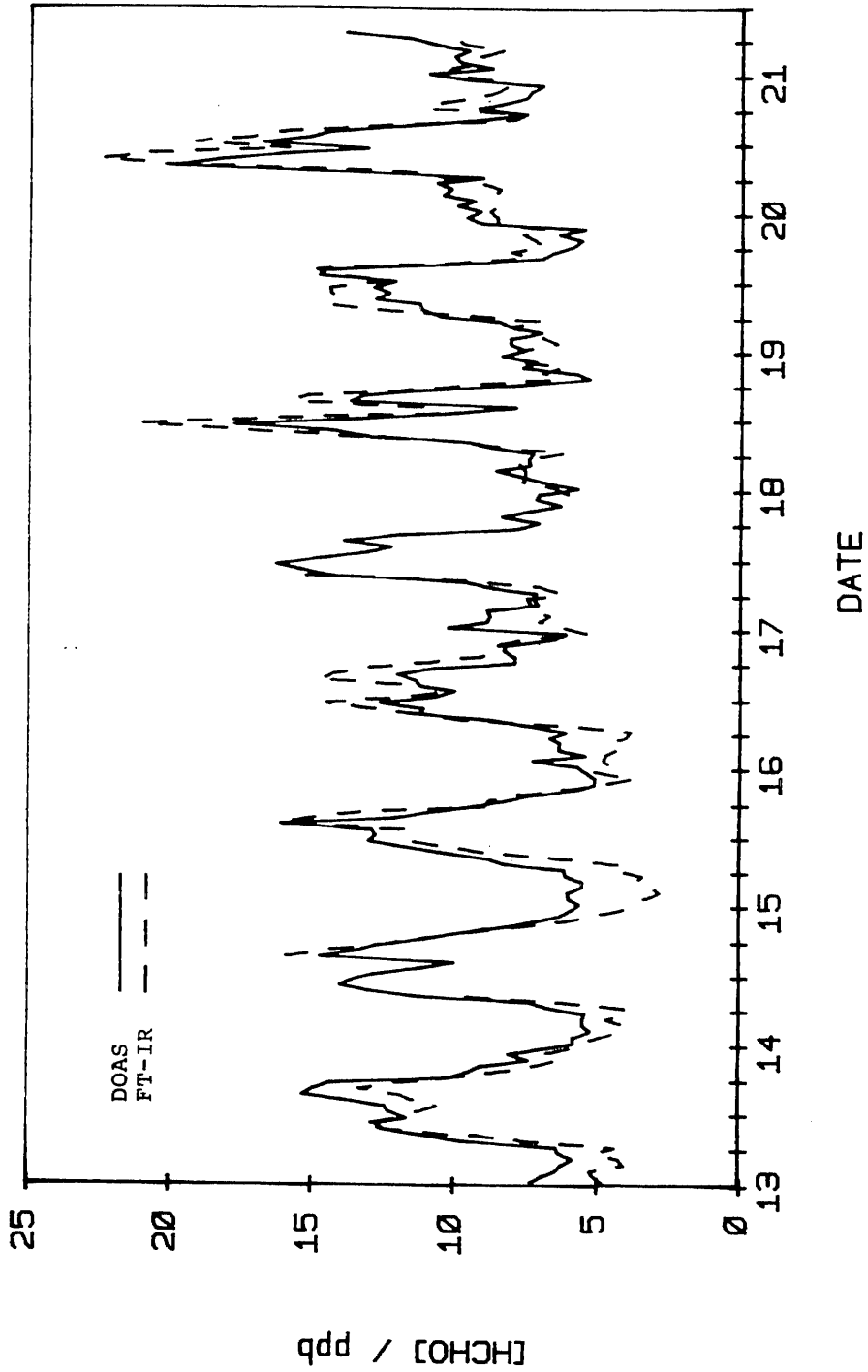


Figure IV-16. Time concentration profiles for formaldehyde measured by long pathlength DOAS and FT-IR spectrometers at Citrus College (Glendora) in August 1986.

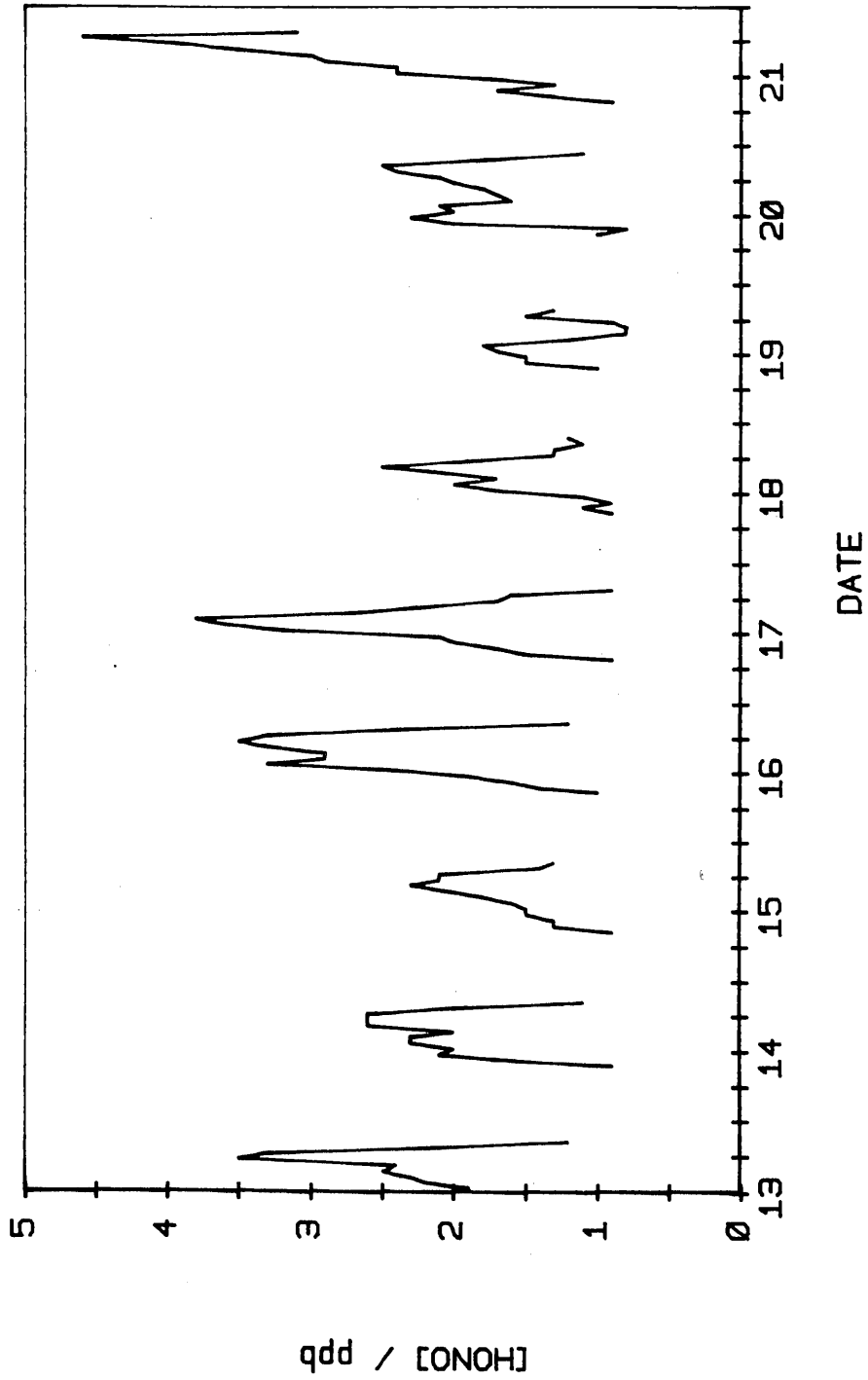


Figure IV-17. Nitrous acid time-concentration profiles measured by long pathlength DOAS system at Citrus College (Glendora) in August 1986.

Table IV-8. Hourly Average HONO Concentrations (ppb)<sup>a,b</sup>  
 Measured by the Long Pathlength DOAS System  
 During the 1986 Citrus College Study

Time Period (hr)	Date								
	8/13	8/14	8/15	8/16	8/17	8/18	8/19	8/20	8/21
00-01	1.9	2.0	1.5	2.4	3.2	1.7	1.7	2.0	2.4
01-02	2.2	2.3	1.6	3.3	3.6	2.0	1.8	2.1	2.4
02-03	2.3	2.3	1.8	2.9	3.8	1.7	1.2	1.6	2.9
03-04	2.5	2.0	2.0	2.9	2.7	2.1	BD	1.7	3.0
04-05	2.4	2.6	2.3	3.3	2.3	2.5	BD	1.8	3.5
05-06	3.5	2.6	2.1	3.5	1.7	1.9	0.9	2.0	3.9
06-07	3.3	2.6	2.1	3.3	1.6	1.3	1.5	2.1	4.6
07-08	2.2	2.0	1.4	2.4	0.9	1.3	1.3	2.4	3.1
08-09	1.2	1.1	1.3	1.2	BD	1.1	BD	2.5	
09-10	BD	BD	BD	BD	BD	1.2	BD	1.8	
10-11	BD	1.1							
11-12	BD								
12-13	BD								
13-14	BD								
14-15	BD								
15-16	BD								
16-17	BD								
17-18	BD								
18-19	BD								
19-20	BD	BD	BD	0.9	BD	BD	BD	0.9	
20-21	BD	0.9	1.0	1.5	0.9	BD	1.0	1.3	
21-22	0.9	1.3	1.4	1.7	1.1	1.0	BD	1.7	
22-23	1.6	1.3	1.6	2.0	0.9	1.5	2.0	1.3	
23-24	2.1	1.5	1.9	2.1	1.1	1.5	2.3	1.7	

<sup>a</sup>BD: Below detection limit (0.8 ppb).

<sup>b</sup>Estimated errors:  $\pm 0.8$  ppb or  $\pm 30\%$ , whichever is larger.

Table IV-9. Hourly Average NO<sub>2</sub> Concentrations (ppb)<sup>a</sup>  
 Measured by the Long Pathlength DOAS System  
 During the 1986 Citrus College Study

Time Period (hr)	Date								
	8/13	8/14	8/15	8/16	8/17	8/18	8/19	8/20	8/21
00-01	64.1	66.9	54.5	56.3	64.4	72.1	56.2	54.3	69.4
01-02	61.5	61.6	51.8	50.9	63.3	74.4	45.9	43.4	55.5
02-03	57.3	60.9	48.9	52.0	56.3	75.1	27.7	22.8	60.6
03-04	54.2	64.0	42.7	50.3	36.2	69.5	21.8	20.4	63.9
04-05	52.1	61.7	39.2	46.7	27.3	65.9	18.2	21.4	62.1
05-06	46.9	61.6	41.4	46.1	23.4	44.1	18.9	33.8	61.0
06-07	47.5	63.3	42.9	43.1	22.1	51.3	40.2	45.2	60.9
07-08	64.4	63.8	55.4	49.4	21.1	58.1	61.6	63.6	72.4
08-09	77.7	74.4	61.9	70.0	26.4	53.0	47.6	140.1	
09-10	93.6	76.8	65.0	68.3	48.3	82.8	49.5	118.5	
10-11	81.1	66.5	60.9	60.7	44.9	91.9	41.2	130.3	
11-12	57.1	50.8	53.0	47.1	33.3	90.6	32.5	50.7	
12-13	43.3	38.5	38.5	27.8	23.1	54.4	20.4	44.5	
13-14	42.2	33.2	31.1	14.4	16.8	20.2	26.3	25.7	
14-15	35.9	24.4	26.0	13.1	12.8	17.8	27.8	16.9	
15-16	36.8	28.4	43.8	14.2	17.7	25.0	29.8	29.9	
16-17	38.8	39.6	46.2	19.5	21.9	35.2	28.3	29.4	
17-18	42.4	41.1	51.6	33.2	26.0	47.7	42.7	37.6	
18-19	53.6	47.7	57.3	45.5	49.6	52.4	60.1	61.8	
19-20	62.1	59.6	70.3	62.6	74.3	52.1	85.2	88.7	
20-21	71.2	76.5	67.1	77.5	78.7	72.9	85.4	89.8	
21-22	75.3	77.4	60.6	81.3	70.3	77.3	77.7	85.5	
22-23	74.1	73.5	60.1	70.4	67.2	69.1	71.9	77.6	
23-24	70.8	61.1	60.5	66.9	70.6	65.7	66.0	83.7	

<sup>a</sup>Estimated errors: ±3.5 ppb or ±15%, whichever is larger.

Table IV-10. Hourly Average HCHO Concentrations (ppb)<sup>a</sup>  
 Measured by the Long Pathlength DOAS System  
 During the 1986 Citrus College Study

Time Period (hr)	Date									
	8/13	8/14	8/15	8/16	8/17	8/18	8/19	8/20	8/21	
00-01	7.3	5.8	5.6	5.7	10.3	5.7	7.6	9.2	11.0	
01-02	6.9	5.8	6.0	7.3	8.9	6.9	8.1	10.0	8.8	
02-03	6.4	5.2	6.0	5.4	8.8	7.8	8.1	9.4	9.9	
03-04	6.2	5.5	5.5	6.4	8.9	8.6	7.0	10.5	10.1	
04-05	5.8	5.5	5.5	6.3	7.1	7.4	8.1	10.2	9.6	
05-06	6.3	5.4	6.1	6.7	7.3	7.5	8.5	10.7	10.8	
06-07	6.4	6.7	6.2	6.1	7.2	7.3	10.5	9.1	11.6	
07-08	9.7	7.4	8.3	7.3	8.8	8.9	11.2	13.1	13.9	
08-09	11.0	11.2	8.9	8.7	9.7	9.6	11.3	19.9		
09-10	12.4	13.0	10.2	11.2	14.4	13.1	12.8	18.4		
10-11	12.7	14.0	11.7	11.1	15.4	14.3	12.3	16.1		
11-12	11.6	13.5	13.0	12.6	16.3	17.8	12.9	13.1		
12-13	12.2	12.8	12.7	10.7	14.8	13.8	12.1	16.8		
13-14	12.4	11.3	12.9	10.0	13.1	10.2	14.8	15.1		
14-15	13.8	10.0	16.1	11.2	12.2	7.9	14.6	14.4		
15-16	15.3	14.7	12.1	11.4	13.9	13.7	10.1	11.7		
16-17	14.9	13.5	10.9	12.0	12.0	13.2	7.0	9.2		
17-18	14.3	12.7	9.5	10.8	7.9	11.4	6.6	7.7		
18-19	10.2	11.1	8.3	7.9	7.1	7.8	5.9	9.3		
19-20	9.5	10.0	7.4	7.9	8.4	5.3	5.6	8.4		
20-21	9.1	8.5	5.7	8.3	7.5	5.8	6.4	7.6		
21-22	7.4	7.3	5.1	8.3	6.3	7.7	5.5	7.4		
22-23	8.1	6.3	5.1	6.5	7.2	7.2	9.2	7.0		
23-24	7.0	5.9	5.4	6.1	7.1	8.4	9.7	9.5		

<sup>a</sup>Estimated errors:  $\pm 4.5$  ppb or  $\pm 30\%$ , whichever is larger.

Finally, the HONO time-concentration profile for August 13-21 is presented in Figure IV-17. No comparison data are available for HONO for this study. However, as discussed above, the only source of a large systematic error would be the literature value for the HONO absorption cross-sections used in the calculations. During the Citrus College field study, nighttime HONO levels were higher than observed in the previous intercomparison study at Claremont, where the maximum HONO concentrations were in the range 1.5 to 2.5 ppb. For five of the nights at Citrus College, the HONO concentrations were also in the same range. However, for three nights HONO levels attained ~3.5 ppb, and during the last night of the study HONO reached a maximum of 4.5 ppb. There was, however, no correlation of the HONO concentrations to the nighttime NO<sub>2</sub> levels, which were relatively constant at 60-75 ppb. Since the heterogeneous formation of HONO from NO<sub>2</sub> involves moisture, correlations to other parameters such as relative humidity and particulate loading may prove interesting. Further interpretation of the observed HONO levels will be made when all supplementary data from this field study become available.



## V. LONG PATHLENGTH FT-IR MEASUREMENTS OF HNO<sub>3</sub>, NH<sub>3</sub> AND HCHO

### A. Introduction

Nitric acid is the dominant end product of the atmospheric transformations of oxides of nitrogen and is the species of particular interest with respect to acid deposition in southern California. It is well recognized that HNO<sub>3</sub> is predominantly formed in the daytime through the homogeneous reaction



However, a second mode of formation of HNO<sub>3</sub> involves the heterogeneous reaction of N<sub>2</sub>O<sub>5</sub> with water vapor,



and this reaction can be important at night when NO<sub>3</sub> radicals and N<sub>2</sub>O<sub>5</sub> are formed via the reactions:



Using the equilibrium constant for reactions (4,-4) [Tuazon et al. 1984] together with previously reported spectroscopic data for ambient concentrations of NO<sub>3</sub> radicals and NO<sub>2</sub> in the U.S. and Germany, the occurrence of nighttime N<sub>2</sub>O<sub>5</sub> concentrations as high as ~15 ppb was predicted (Atkinson et al. 1986). These estimates by Atkinson et al. (1986) emphasized that N<sub>2</sub>O<sub>5</sub> can be an important nighttime nitrogenous species and that its heterogeneous reaction with water vapor, via either wet or dry deposition pathways, can be an important route to HNO<sub>3</sub> during nighttime hours as well as being an important NO<sub>x</sub> removal process. Furthermore, as discussed in detail in Section XI.C, N<sub>2</sub>O<sub>5</sub> is known to react with PAH to form mutagenic nitroarenes (Pitts et al. 1985a, Sweetman et al. 1986, Zielinska et al. 1986a, Atkinson et al. 1987, Atkinson and Aschmann 1987).

The longpath FT-IR measurements were originally aimed primarily at providing temporal and diurnal  $\text{HNO}_3$  concentrations during selected episode days, which were also the days targeted for sampling of ambient air for PAH and nitroarene analyses. Attempts were also made to detect  $\text{N}_2\text{O}_5$  in ambient air by thorough examination of the spectra recorded in the late afternoon and evening hours. Ammonia ( $\text{NH}_3$ ) was included among the species measured since, in certain localities, it can profoundly affect the concentration of gaseous  $\text{HNO}_3$  by its reaction to form aerosol ammonium nitrate (Doyle et al. 1979, Tuazon et al. 1980).

As discussed earlier in this report (Sections II and III), the long pathlength FT-IR system was employed to provide benchmark data for the Nitrogen Species Methods Intercomparison Study held at Pomona College (Claremont) in September 1985. Following this, the FT-IR spectrometer participated in the winter field study at El Camino Community College (Torrance) as called for in our original proposal. Due to a need for more detailed comparison of  $\text{HNO}_3$  analysis between the FT-IR and tunable diode laser spectroscopic (TDLS) methods than had been possible during the 1985 Claremont study, the longpath FT-IR system was subsequently set up in Glendora on the Citrus College campus for more intensive measurements of  $\text{HNO}_3$  and  $\text{NH}_3$  between August 12-21, 1986. In this study, species coverage by the FT-IR method was extended to include the measurement of formaldehyde ( $\text{HCHO}$ ).

Prior to the studies conducted in this program, the longpath FT-IR method had already established a successful record of providing accurate measurements of pollutant species in polluted atmospheres, including  $\text{O}_3$ ,  $\text{HNO}_3$ ,  $\text{NH}_3$ , PAN,  $\text{HCHO}$  and  $\text{HCOOH}$ . Thus, following the exploratory work of Hanst and co-workers (Hanst et al. 1975), SAPRC researchers conducted kilometer pathlength FT-IR measurements in the South Coast Air Basin for the four consecutive summers of 1976-1979. In these studies we employed a Digilab Model FTS-14 spectrometer interfaced to a 22.5-meter basepath eight-mirror optical system (Hanst 1971) which was housed in a Teflon-walled sampling cell.

With the above instrumentation, our 1976 study in Riverside yielded the first spectroscopic detection of  $\text{HNO}_3$  and  $\text{HCHO}$  in the troposphere, with ~6 ppb detection sensitivity for both species (Tuazon et al. 1978). The more detailed simultaneous measurements of  $\text{HNO}_3$  and  $\text{NH}_3$  in 1977

strongly pointed to a negative correlation between the gaseous concentrations of these two species, presumably due to the formation of  $\text{NH}_4\text{NO}_3$  aerosol (Tuazon et al. 1980, Doyle et al. 1979).

Subsequently, in 1978 at Claremont, a mid-basin site, the first truly comprehensive set of simultaneous data for  $\text{O}_3$ ,  $\text{HNO}_3$ ,  $\text{NH}_3$ , PAN, HCHO and HCOOH was obtained during a five-day period of increasingly severe smog episodes, when daily maximum  $\text{O}_3$  concentrations ranged from 0.16 ppm to 0.45 ppm (Tuazon et al. 1981). In a U.S. Environmental Protection Agency-sponsored field study at the same site the following year (August 27 - September 3, 1979), our kilometer pathlength FT-IR measurements served as the standard for intercomparison of nitric acid analytical methods (Spicer et al. 1982).

## B. Experimental

### 1. Kilometer Pathlength FT-IR System

Measurements of ambient air pollutants by infrared spectroscopy were carried out using a recently constructed 25-m basepath, open multiple-reflection optical system interfaced to a Mattson Instruments, Inc., Sirius 100 FT-IR spectrometer. This spectrometer has a maximum resolution capability of  $0.125 \text{ cm}^{-1}$  and is equipped with a Motorola 68000-based data system. The long pathlength optics are of the three-mirror White design (White 1942), with provisions for adding a corner reflector at the in-focus end (Horn and Pimentel 1971), when desired, to effectively double the system's pathlength. The mirrors in this new optical system were fabricated from 30 cm diameter, 6 cm thick Pyrex blanks and gold-coated for the best reflectivity ( $\geq 99\%$ ) in the infrared. The optimum pathlength for monitoring was determined to be in the 1-1.5 km range during routine operation, although short-term use of optical paths greater than 2 km were possible.

As discussed in Section III, the long pathlength FT-IR spectrometer was operated alongside the long pathlength DOAS system, as shown in Figure V-1. The optical layout of the FT-IR system is presented in more detail in Figure V-2. The sets of mirrors of the two spectrometers were arrayed in opposite directions but aligned side by side in a compact arrangement which made possible simultaneous analyses of virtually the same air mass. The FT-IR spectrometer was housed in an air conditioned shed while

25m BASEPATH FT-IR AND DOAS SPECTROMETERS  
TOTAL OPTICAL PATHLENGTHS : 1-2 km

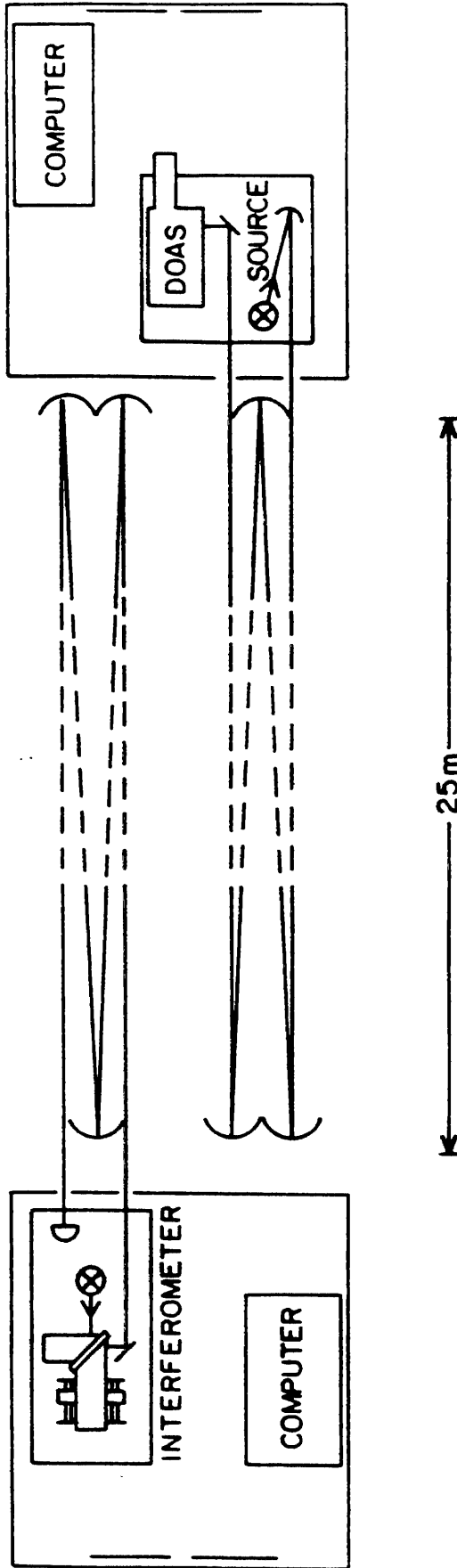


Figure V-1. Relative arrangement of the longpath FT-IR and DOAS systems.

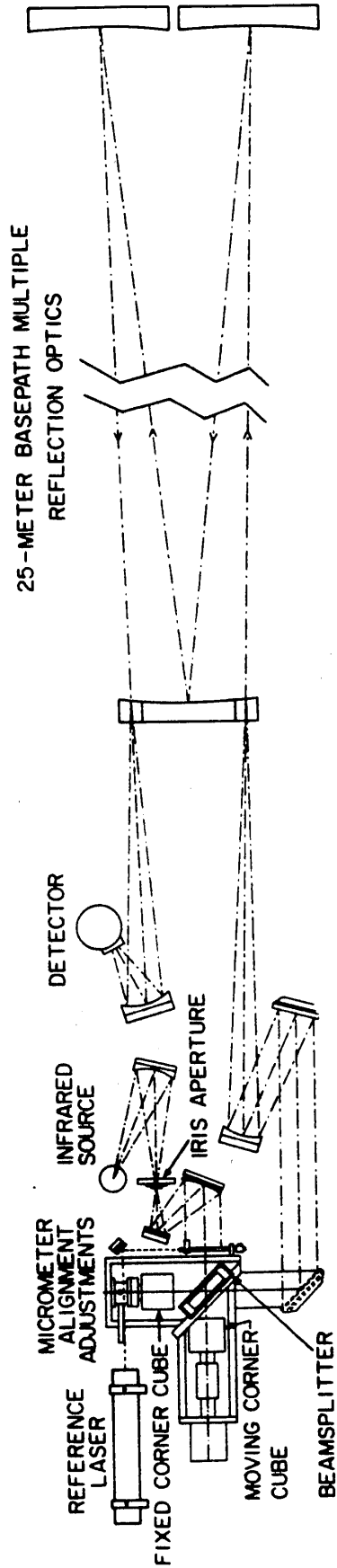


Figure V-2. Schematic optical diagram of the longpath FT-IR spectrometer.

the multiple reflection mirror assembly outside was shaded from direct sunlight by protective shields. The spectrometer system had an initial height of 1.2 m (above ground level) designed into the optical axis. In the Claremont study (as well as in the Glendora study) this was raised to a total of 2.4 m (8 ft), the common sampling height required for all analytical techniques being compared during these field studies. Massive concrete blocks were employed as support structures to attain this sampling height. No such modification was made during the winter study in Torrance since the spectrometer was located on the roof of a two-story building.

## 2. Acquisition of Spectra

Spectra were recorded at a pathlength of 1150 meters and  $0.125\text{ cm}^{-1}$  resolution (unapodized). Sixty-four scans (interferograms) were added during a 4.5-min period and then transformed (calculation time of  $\sim 2.5$  min) to a single beam spectrum. Each spectrum of 128 K points was truncated and only the spectral region from 400 to  $1600\text{ cm}^{-1}$ , which contained the absorption bands of  $\text{HNO}_3$  and  $\text{NH}_3$  used for analysis, was retained and archived. During the Citrus College Study, the spectral region up to  $3000\text{ cm}^{-1}$  was retained to allow data to be obtained for  $\text{HCHO}$ .

Four to five spectra per hour were collected. This rate of data collection permitted a real-time examination of the quality of spectra being recorded and such checks were consistently made during daytime and early evening hours (0800-2200 PDT). During the "noncritical" period of 2200-0600 hours when nitric acid was expected to be below the detection limit, the FT-IR spectrometer was programmed to conduct automatic monitoring.

## 3. Calibration

Figure V-3 illustrates the absorption features of  $\text{HNO}_3$  and  $\text{NH}_3$  in the region accessible to long pathlength FT-IR measurements. Asterisks mark the peaks which were employed to determine concentrations. A more expanded plot of the  $\text{HNO}_3$  spectrum in the range  $870\text{--}910\text{ cm}^{-1}$  is presented in Figure V-4, to which is added a qualitative single beam spectrum of "clean" ambient air at a pathlength of 1150 m. The Q-branch at  $896.1\text{ cm}^{-1}$  was the most appropriate one for quantitative measurement because of its favorable half-width and minimal interference by atmospheric water vapor. We restricted our measurements to the heights of the sharp absorption

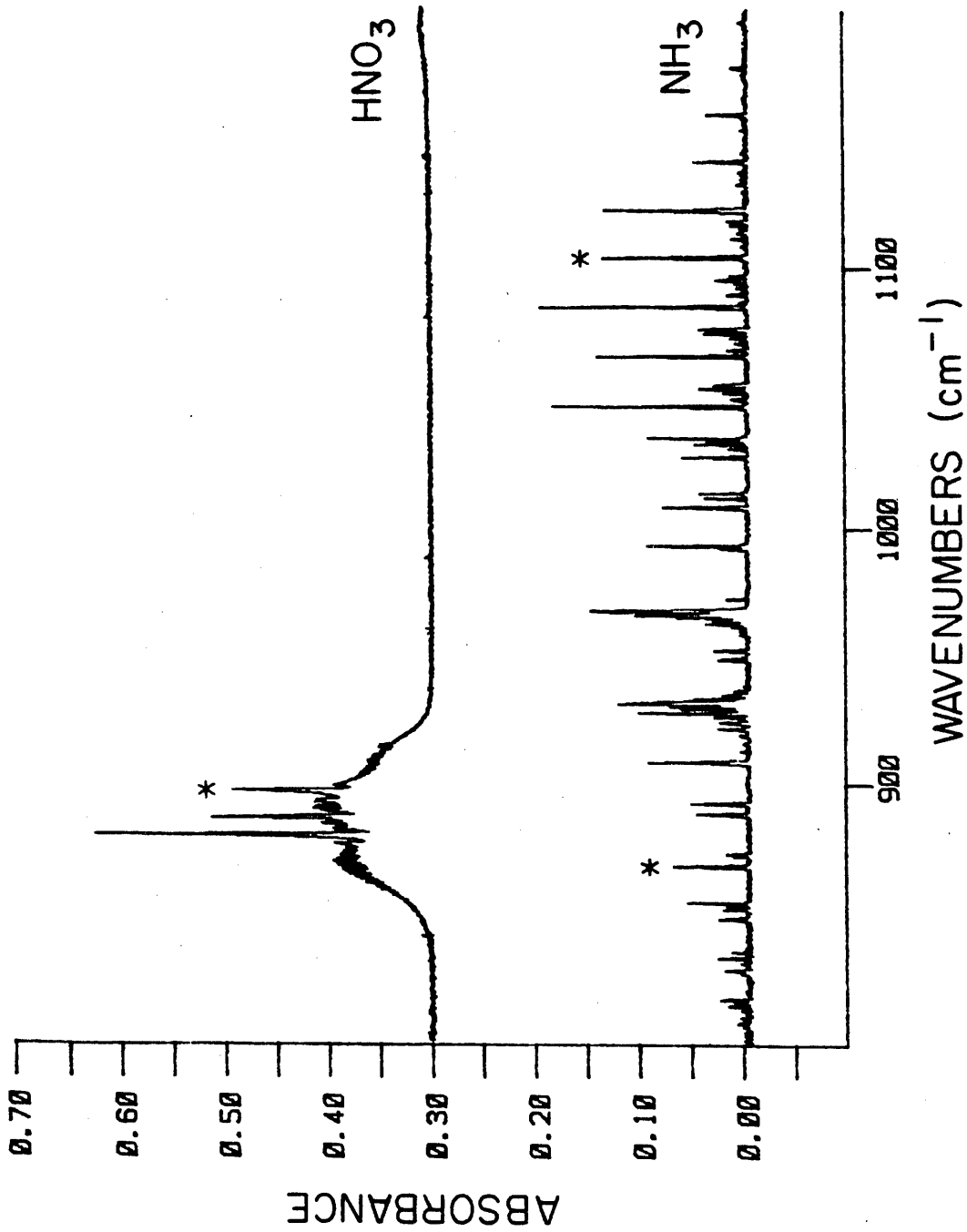


Figure V-3. Reference spectra of gaseous  $\text{HNO}_3$  (0.61 torr) and  $\text{NH}_3$  (0.23 torr) at spectral resolution of  $0.125\text{ cm}^{-1}$ , pathlength of 25 cm, total pressure with  $\text{N}_2$  of 740 torr. The  $\text{HNO}_3$  plot is offset by 0.30 absorbance (base 10) unit for clarity. Asterisks mark the absorption peaks used for analysis.

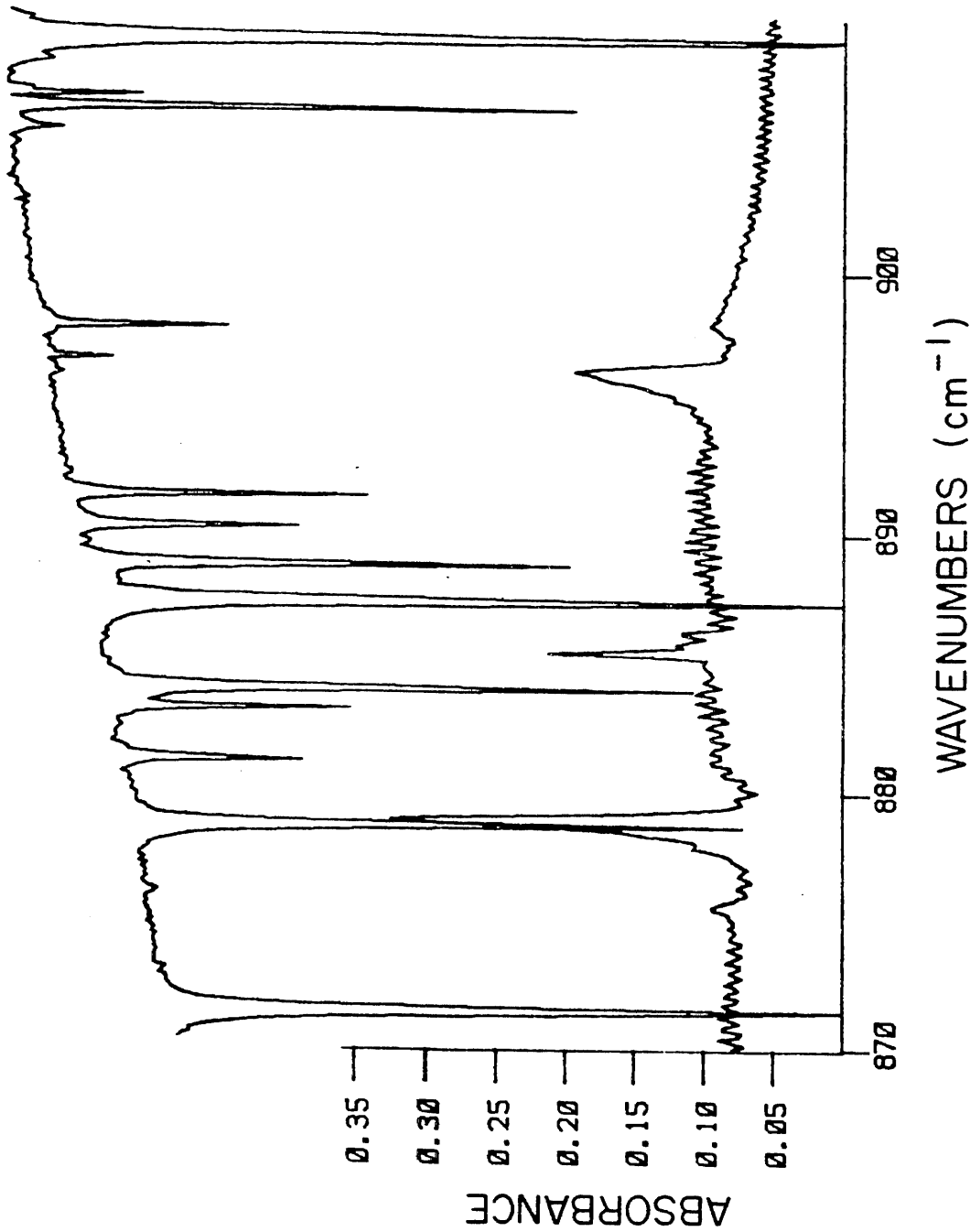


Figure V-4. Infrared absorption peaks of HNO<sub>3</sub> (lower trace) relative to atmospheric H<sub>2</sub>O absorptions (upper trace) in the 870-910 cm<sup>-1</sup> region.

(Q-branch) features only, since measurements which include the broad underlying envelope were more susceptible to unknown interferences. The  $885.4\text{ cm}^{-1}$  Q-branch was totally free of interferences but its relatively narrower line shape was more susceptible to distortion by noise, while the strongest Q-branch at  $878.9\text{ cm}^{-1}$  was severely overlapped by a strong water line.

Of the numerous sharp features of the  $\text{NH}_3$  spectrum depicted in Figure V-3, the lines at  $1103.4$  and  $867.9\text{ cm}^{-1}$ , though not the strongest, suffer the least interference by  $\text{H}_2\text{O}$  and  $\text{CO}_2$  absorption lines and were therefore the ones chosen for analysis. The line positions of  $\text{NH}_3$  relative to those of atmospheric  $\text{H}_2\text{O}$  (and  $\text{CO}_2$ ) in the  $1080$ - $1120\text{ cm}^{-1}$  region are shown in Figure V-5.

The calibration procedure for  $\text{NH}_3$  was straightforward. Spectra were recorded at  $0.125\text{ cm}^{-1}$  resolution for several  $\text{NH}_3$  pressures in the range  $0.2$ - $1$  torr, which were measured to within  $\pm 0.005$  torr accuracy with an MKS Baratron capacitance manometer. The  $\text{NH}_3$  samples were transferred to a  $25$ -cm cell with KBr windows and pressurized with  $\text{N}_2$  gas to atmospheric pressure. No measureable decay of  $\text{NH}_3$  concentration was observed within the  $15$ -minute period during which repeat spectra were recorded for each sample. These data yielded absorptivities (base 10) at  $23^\circ\text{C}$  and  $740$  torr total pressure of  $18.2\text{ cm}^{-1}\text{ atm}^{-1}$  for the  $1103.4\text{ cm}^{-1}$  peak and  $9.7\text{ cm}^{-1}\text{ atm}^{-1}$  for the  $867.9\text{ cm}^{-1}$  peak, with uncertainties of  $\pm 5\%$  (two standard deviations) for both values.

A similar calibration procedure was not possible for  $\text{HNO}_3$  because of its significant decay to the walls of the  $25$ -cm cell. We determined our high resolution absorptivity values relative to the data of Graham and Johnston (1978), who made an accurate determination of the absorptivity of the  $\text{HNO}_3\text{ } \nu_4$  ( $1325\text{ cm}^{-1}$ ) fundamental band at  $\sim 2\text{ cm}^{-1}$  resolution using two independent methods for generating  $\text{HNO}_3$  (for more details see also Graham 1975). We assigned Graham and Johnston's (1978) absorptivity value (peak-to-baseline) for the broad  $\nu_4$  P-branch at  $1315\text{ cm}^{-1}$  to the same feature in our  $0.125\text{ cm}^{-1}$  resolution spectrum after smoothing the latter to  $\sim 2\text{ cm}^{-1}$  resolution. The absorptivity for a Q-branch (e.g.,  $896.1\text{ cm}^{-1}$ ) at  $0.125\text{ cm}^{-1}$  resolution was then determined from the intensity ratio of the unsmoothed Q-branch to the smoothed P-branch.

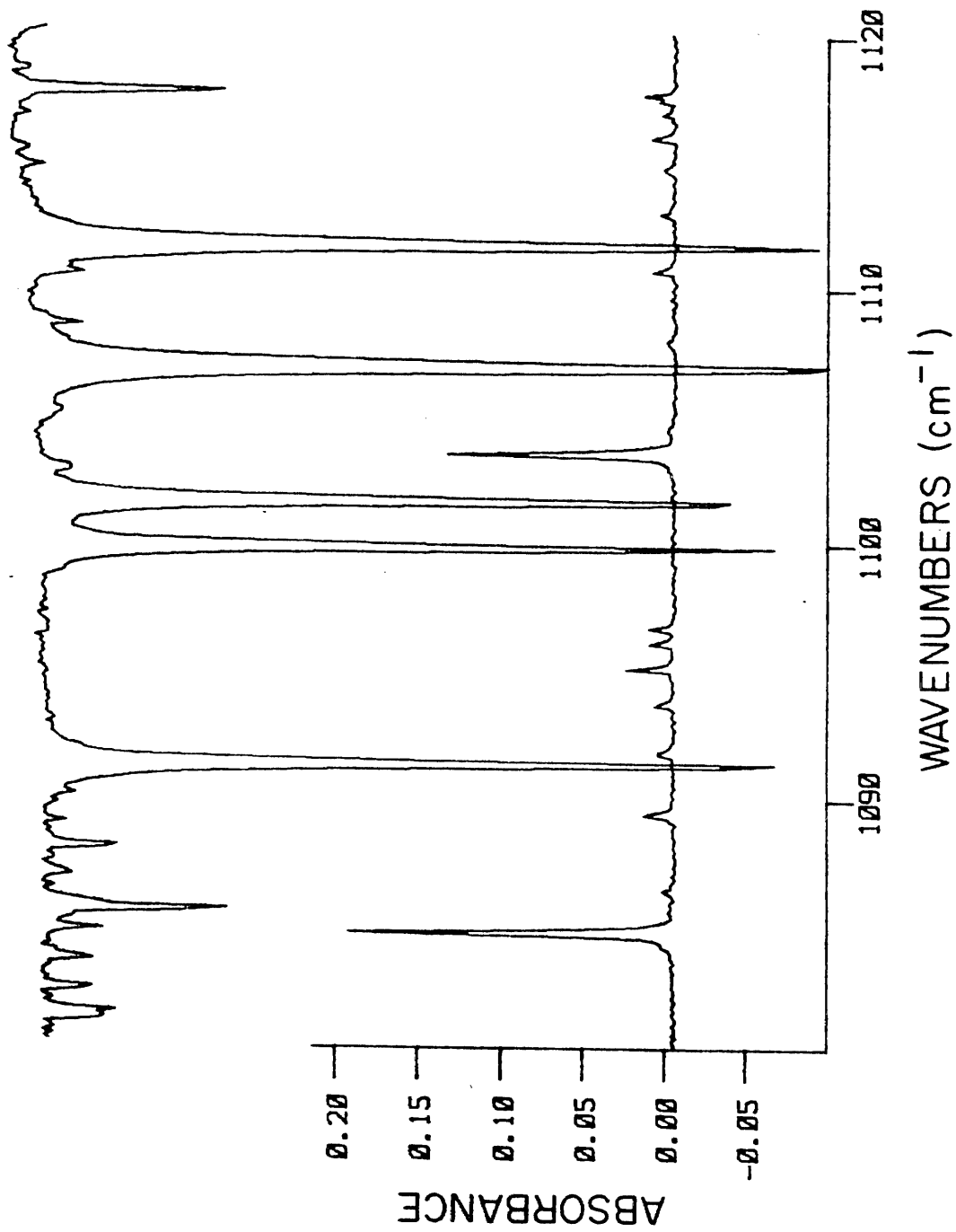


Figure V-5. Infrared absorption peaks of  $\text{NH}_3$  (lower trace) relative to atmospheric  $\text{H}_2\text{O}$  and  $\text{CO}_2$  absorptions (upper trace) in the 1080-1120  $\text{cm}^{-1}$  region.

Smoothing removes the fine structure superimposed on the  $\nu_4$  band envelope, and in order to test the adequacy of the smoothing function employed, measurements were carried out in which  $2\text{ cm}^{-1}$  and  $0.125\text{ cm}^{-1}$  resolution spectra were recorded alternately for an  $\text{HNO}_3$  sample. To take into account the  $\text{HNO}_3$  decay in the cell, the  $1315\text{ cm}^{-1}$  peak heights at  $2\text{ cm}^{-1}$  resolution were plotted against time, as were those of the  $0.125\text{ cm}^{-1}$  resolution spectra after having been smoothed to  $\sim 2\text{ cm}^{-1}$  resolution. The two curves were found to be indistinguishable, indicating the accuracy of the smoothing function applied. The above procedure yielded a value of  $5.2 \pm 0.4\text{ cm}^{-1}\text{ atm}^{-1}$  for the absorptivity (base 10) of the  $\text{HNO}_3$  peak at  $896.1\text{ cm}^{-1}$  (Q-branch height only) with the two standard deviation error including that reported by Graham (1975). This value is in fact the same as that we previously determined for this peak at  $0.5\text{ cm}^{-1}$  resolution (Tuazon et al. 1980). Following the same method, the absorptivity of the  $885.4\text{ cm}^{-1}$  Q-branch was found to be  $6.1 \pm 0.5\text{ cm}^{-1}\text{ atm}^{-1}$ .

The calibration procedure for  $\text{HCHO}$  was the same as that for  $\text{NH}_3$ . Formaldehyde samples were pre-distilled from paraformaldehyde and immediately used after collection in a liquid nitrogen cooled trap. The absorptivity value of the  $2781.0\text{ cm}^{-1}$  Q-branch, an absorption peak well isolated from  $\text{H}_2\text{O}$  absorptions, was determined to be  $8.9 \pm 0.5\text{ cm}^{-1}\text{ atm}^{-1}$ .

A summary of the absorptivities for the measurement peaks of the compounds studied here are presented in Table V-1, together with the estimated detection limits for the 1150 m pathlength employed.

#### 4. Treatment of Data

The quantitative analysis of species such as  $\text{NH}_3$ , which possess relatively narrow Q-branch features which are sufficiently resolved from atmospheric  $\text{H}_2\text{O}$  absorptions, was normally straightforward. The absorbance ( $\log I_0/I$ ) was derived directly from the single beam spectrum, and thus a ratio plot against an actual background spectrum was not necessary. Provided that the detector had a linear response,  $I_0$  and  $I$  as determined from a single beam spectrum had values on an arbitrary scale in which zero corresponded to zero signal on the detector. The appropriate differential absorption coefficient, such as those determined above, and the absorption pathlength had to be applied to the absorption intensity measured between  $I_0$  and  $I$  in order to convert to concentration units. This procedure was followed for the  $1103.4$  and  $867.9\text{ cm}^{-1}$  lines of  $\text{NH}_3$ .

Table V-1. Infrared Absorptivities and Calculated Detection Limits for Long Pathlength FT-IR Spectroscopic Measurements of Ambient Pollutants

Compound	Frequency ( $\text{cm}^{-1}$ )	Absorptivity <sup>a</sup> ( $\text{cm}^{-1}$ atm <sup>-1</sup> , base 10)	Resolution ( $\text{cm}^{-1}$ )	Reference	Detection Limit <sup>b</sup> (ppb) for 1150 m Pathlength
HNO <sub>3</sub>	896.1 <sup>c</sup>	5.2	0.125	This work	4
NH <sub>3</sub>	1103.4 <sup>c</sup>	18.2	0.125	This work	1
	867.9	9.7	0.125	This work	2
N <sub>2</sub> O <sub>5</sub>	1246 <sup>d</sup>	18.8	~2-4	Graham and Johnson (1978)	1 <sup>e</sup>
HCHO	2781.0 <sup>c</sup>	8.9	0.125	This work	3

<sup>a</sup>At 298 K, 760 torr.

<sup>b</sup>Based on a signal of 0.0025 absorbance unit (base 10).

<sup>c</sup>Differential height of the Q-branch or well-resolved structure only.

<sup>d</sup>Peak-to-baseline measurement.

<sup>e</sup>Actual attainable detection sensitivity may be several times higher than this value due to interferences by atmospheric absorptions.

Estimates of the  $\text{HNO}_3$  concentration could also be obtained from single-beam spectra by employing the  $885.4 \text{ cm}^{-1}$  Q-branch. However, the  $\text{HNO}_3$  analysis was more reliably carried out using the  $896.1 \text{ cm}^{-1}$  Q-branch by ratioing the sample spectrum with a clean background spectrum, a procedure which improved the baseline and resulted in essentially complete cancellation of a very weak  $\text{H}_2\text{O}$  interference. Background spectra were chosen from those recorded at around midnight during low pollution days, since previous measurements (Spicer et al. 1982) showed  $\text{HNO}_3$  levels that were much lower ( $<1$  ppb) than the FT-IR detection limit under these conditions.

The peak-to-peak noise level in the ratio spectrum was typically 0.0025 absorbance unit (base 10), corresponding to a 250:1 signal to peak-to-peak noise ratio for single spectral records. The absorption peaks used for the analyses were much wider than the frequency of random noise, such that peak heights as small as the noise level could be detected above the noise itself. Thus, the detection sensitivities were 3-5 ppb for  $\text{HNO}_3$ , 1-2 ppb for  $\text{NH}_3$  and 2-3 ppb for  $\text{HCHO}$ . The lower detection limit for each compound was realized when turbulence due to temperature gradients and/or wind were minimal (for example, during nighttime hours).

The possible detection of  $\text{N}_2\text{O}_5$  depended on how well its broad band, centered at  $1246 \text{ cm}^{-1}$  ( $\nu_{12}$ ), could be discerned from interfering  $\text{H}_2\text{O}$  absorptions. The  $\text{H}_2\text{O}$  interferences were reduced by ratioing the sample spectra against selected "background" spectra taken during those periods (mid-morning to noon) when  $\text{N}_2\text{O}_5$  was believed not to be present due to the rapid photolysis of  $\text{NO}_3$  radicals. Although exact cancellation of the  $\text{H}_2\text{O}$  absorptions was not possible, the "windows" between these absorptions were sufficient to define a baseline from which the presence of a broad absorption contour could be distinguished. From the literature value of  $18.8 \text{ cm}^{-1} \text{ atm}^{-1}$  for the absorptivity of the  $1246 \text{ cm}^{-1}$  peak (Graham 1975, Graham and Johnston 1978), it was calculated that 5 ppb  $\text{N}_2\text{O}_5$  at a pathlength of 1150 m would give a signal of  $\sim 0.01$  absorbance unit (base 10), approximately 4 times the peak-to-peak baseline noise of the ratio spectrum.

The largest source of uncertainty in the analyses was the noise level in the spectrum, with other errors being generally negligible. We assigned to each peak height measurement the maximum error, which was

equal to the peak-to-peak noise level. For  $\text{HNO}_3$  this error was  $\pm 4$  ppb. The uncertainty arising from the error in the absorptivity (of the  $896.1 \text{ cm}^{-1}$  Q-branch in this case) increased with the concentration. However, this contribution to the overall error limit was relatively small for the range of  $\text{HNO}_3$  concentrations encountered. For example, it increased the  $\pm 4$  ppb error by only 10% when included in the error calculation for an  $\text{HNO}_3$  concentration of 25 ppb.

For  $\text{NH}_3$  concentrations  $\leq 20$  ppb, the sum of uncertainties due to noise and error in the absorptivity of the  $1103.4 \text{ cm}^{-1}$  line was  $\pm 1.5$  ppb. At higher concentrations the contribution from the absorptivity error became relatively more important. A detailed plot of this error contribution as a function of concentration revealed that it is nearly linear in the concentration range 20 to 100 ppb, permitting the additional error to be calculated from the empirical formula  $(0.044)([\text{NH}_3]-20)$  ppb. Thus, for the measurement of 60 ppb  $\text{NH}_3$ , the total error can be calculated as  $[1.5 + (0.044)(60-20)] = \pm 3.3$  ppb.

For the range of  $\text{HCHO}$  concentrations encountered in the 1986 Glendora study, the measurement errors were within  $\pm 3$  ppb.

### C. Results and Discussion

#### 1. The 1985 Summer Field Study at Pomona College (Claremont, CA)

The kilometer pathlength FT-IR facility was operated as part of the Nitrogen Species Methods Intercomparison Study, which began at 0800 PDT, September 11 and lasted until 0600 PDT, September 19, 1985.

Nitric Acid. The field study period was characterized mainly by low pollution days with  $\text{HNO}_3$  levels mostly below the detection limit of 4 ppb. The lack of sufficiently high levels of  $\text{HNO}_3$  for FT-IR detection was compounded by intermittent noise problems (of unknown origin) which plagued the FT-IR measurements during four of the eight days of the study. Fortunately, no severe noise interferences occurred on September 14, when the highest daily maximum ozone level observed during the study ( $>0.2$  ppm) was recorded. Consistent with the strong correlation between  $\text{HNO}_3$  and  $\text{O}_3$  concentrations (Tuazon et al. 1981, Spicer et al. 1982), the highest levels of  $\text{HNO}_3$  were indeed observed on this day, and  $\text{HNO}_3$  concentrations were above the FT-IR detection limit for most of the daytime hours. The detailed time-concentration data for September 14 are presented in Table

V-2 and represent the best FT-IR measurements during the study for comparison with other continuous methods such as the TDLS.

Table V-2.  $\text{HNO}_3$  and  $\text{NH}_3$  Concentrations (ppb)<sup>a,b,c</sup> vs. Time in Claremont, CA, on September 14, 1985, by Long Pathlength FT-IR Spectroscopy

PDT	$\text{HNO}_3$	$\text{NH}_3$	PDT	$\text{HNO}_3$	$\text{NH}_3$
0927	<4	4.6	1354	10.9	3.9
0937	<4	5.5	1410	11.7	4.7
0950	<4	4.0	1423	11.7	4.8
1009	6.3	4.2	1439	13.9	5.3
1023	7.0	3.4	1452	13.4	4.2
1035	6.7	3.9	1507	18.4	5.3
1049	7.5	4.0	1520	20.0	3.6
1101	8.4	4.6	1531	21.7	4.7
1112	8.7	4.2	1545	25.9	1.9
1124	12.0	2.7	1559	21.4	4.0
1141	10.9	4.2	1615	20.0	3.8
1154	14.2	2.6	1629	20.0	3.9
1208	14.0	4.9	1649	16.7	4.1
1224	15.0	5.0	1703	15.5	4.8
1239	13.7	4.2	1717	8.4	4.6
1251	11.7	5.2	1729	8.4	5.1
1304	11.4	4.6	1744	6.7	5.4
1316	13.4	4.3	1816	<4	3.1
1329	15.9	3.9	1827	<4	4.2
1342	11.7	3.4	1840	<4	5.2

<sup>a</sup>At 23°C and 740 torr.

<sup>b</sup>Digits beyond two significant figures are retained only for the sake of format.

<sup>c</sup>Error:  $\pm 4$  ppb for  $\text{HNO}_3$  and  $\pm 1.5$  ppb for  $\text{NH}_3$ .

For compactness in the presentation of data, but more importantly because the co-existing concentrations of  $\text{HNO}_3$  and  $\text{NH}_3$  have been of interest in the past (Doyle et al. 1979), the simultaneously measured  $\text{NH}_3$  concentrations are also included in Table V-2. A similar tabulation of simultaneous  $\text{HNO}_3$  and  $\text{NH}_3$  concentrations is given in Table V-3 for September 17, a day which had lower pollution levels than September 14 but was also characterized by spectra which were free of the problem interferences mentioned above.

Table V-3.  $\text{HNO}_3$  and  $\text{NH}_3$  Concentrations (ppb)<sup>a,b</sup> vs. Time in Claremont, CA, on September 17, 1985, by Long Pathlength FT-IR Spectroscopy

PDT	$\text{HNO}_3$	$\text{NH}_3$	PDT	$\text{HNO}_3$	$\text{NH}_3$
1208	<3	28.9	1518	8.7	1.7
1219	<3	30.7	1532	5.8	3.3
1231	<3	18.5	1542	3.4	4.9
1245	<3	15.7	1554	7.5	3.3
1257	4.6	6.5	1606	3.3	2.1
1309	<3	7.9	1619	3.3	3.0
1331	4.3	5.8	1632	6.0	4.5
1343	5.0	5.3	1653	3.7	3.8
1356	6.2	4.2	1706	4.2	5.7
1418	8.0	3.3	1723	<3	0.5
1431	6.7	3.2	1735	<3	3.1
1442	9.2	4.1	1753	<3	2.1
1453	8.4	4.0	1803	<4	1.3
1505	8.3	1.6			

<sup>a</sup>At 23°C and 740 torr.

<sup>b</sup>Error:  $\pm 4$  ppb for  $\text{HNO}_3$  and  $\pm 1.5$  ppb for  $\text{NH}_3$ .

Figure V-6 illustrates the detection of  $\text{HNO}_3$  on September 14, which includes the highest value of 26 ppb recorded at 1545 hr, nearly coincident with the peak  $\text{O}_3$  level. To facilitate comparison on the same scale, the spectra were ratioed against a common background of "clean" air, in this case a spectrum recorded at 0026 hr of September 18 when pollution levels were known to be low. Nitric acid concentrations were primarily determined from absorbance spectra such as those illustrated in Figure V-6, primarily using the  $896.1 \text{ cm}^{-1}$  Q-branch. Estimates of concentrations were often possible also with the  $885.4 \text{ cm}^{-1}$  peak in single-beam spectra, and the  $878.9 \text{ cm}^{-1}$  peak provided qualitative verification of the presence of  $\text{HNO}_3$  when the overlapping  $\text{H}_2\text{O}$  absorption could be sufficiently well ratioed out. Measurement errors were well within  $\pm 4$  ppb for these spectra, which were not affected by the unusual interference problems mentioned earlier.

The generally low levels of photochemical pollution, and the consequence of the instrumental difficulties encountered, are reflected in the inventory of hourly average  $\text{HNO}_3$  concentrations presented in Table V-4. To facilitate comparison with time integrated techniques such as filter packs, denuder difference methods, and annular denuders, the average concentrations for the designated sampling blocks were derived from the hourly averages (where sufficient data were available) and are presented in Table V-5. Values below the FT-IR detection limit are represented as  $<4$  ppb and accounted for the majority of the data for the study period.

The data for September 14 and 17 comprised our best measurements since the noise interferences mentioned above were not experienced on those days. Of the sampling blocks for these two days, only for the period 1200-1600 hr on September 14 were the  $\text{HNO}_3$  concentrations consistently above the detection limit. The calculation of the 15.2 ppb average for this sampling period (Table V-5) was therefore straightforward. For the other sampling blocks, the number of hourly  $\text{HNO}_3$  values above the detection limit was at least equal to the number of hourly values below the detection. For these sampling blocks, lower and upper limit averages were calculated by substituting 0 and 4 ppb, respectively, for those hourly values below the detection limit of 4 ppb. Thus, for example, a narrow range of 4.5-5.5 ppb was calculated for the ambient  $\text{HNO}_3$  concentrations for the period 1200-1600 hr on September 17.

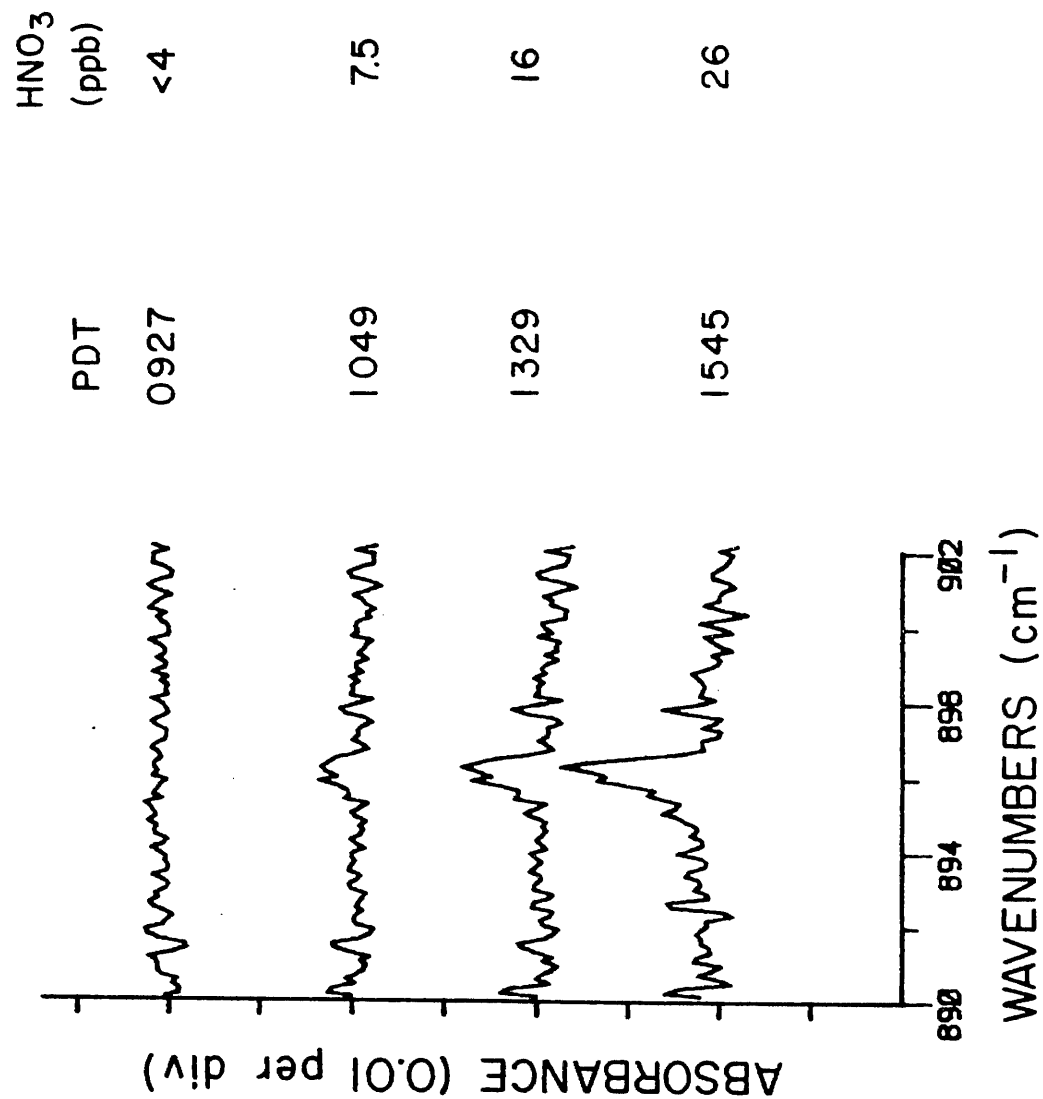


Figure V-6. FT-IR spectroscopic detection of HNO<sub>3</sub> during the pollution episode of September 14, 1985 in Claremont, CA.

Table V-4. Hourly Average HNO<sub>3</sub> Concentrations (ppb)<sup>a,b,c</sup> at Claremont, CA, During September 1986, Measured by Long Pathlength FT-IR Spectroscopy

Hourly Period (PDT)	Sept 11	Sept 12	Sept 13	Sept 14 <sup>d</sup>	Sept 15	Sept 16	Sept 17 <sup>d</sup>	Sept 18
0800-0900	BD	BD	BD	BD	BD	BD	BD	BD
0900-1000	BD	BD	BD	BD	BD	BD	BD	BD
1000-1100	BD	BD	BD	6.7	BD	BD	BD	BD
1100-1200	BD	BD	BD	11.2	≤4.0	BD	BD	BD
1200-1300	BD	BD	XX	13.6	≤6.3	BD	BD	BD
1300-1400	BD	BD	≤10.9	12.8	≤9.5	BD	3.3	BD
1400-1500	BD	BD	≤10.6	12.8	XX	≤4.9	7.8	BD
1500-1600	BD	XX	≤13.4	21.4	≤8.8	≤3.5	6.7	BD
1600-1700	BD	XX	≤11.8	19.2	≤6.7	BD	3.6	BD
1700-1800	BD	≤8.3	XX	8.7	XX	BD	BD	BD
1800-1900	BD	≤7.3	XX	BD	XX	BD	BD	BD
1900-2000	BD	BD	XX	BD	BD	BD	BD	BD
2000-2100	BD	BD	XX	BD	BD	BD	BD	BD
2100-2200	BD	BD	XX	BD	BD	BD	BD	BD

<sup>a</sup>At 23°C and 740 torr.

<sup>b</sup>Concentrations for periods earlier and later than the time periods shown are below detection limit (<4 ppb).

<sup>c</sup>BD: Below detection; XX indicates indeterminate concentration due to very high noise level in the spectra; ≤ symbol designates an upper limit estimate (dictated by the presence of significant noise in some of the spectra in the data set). Digits beyond 2 significant figures are retained only for the sake of format.

<sup>d</sup>Error: ±4 ppb.

Table V-5. Average HNO<sub>3</sub> Concentrations (ppb)<sup>a,b,c</sup> Measured by Long Pathlength FT-IR Spectroscopy for the Designated Sampling Periods During the Claremont Study in 1985

Sampling Period (PDT)	Sept 11	Sept 12	Sept 13	Sept 14	Sept 15	Sept 16	Sept 17	Sept 18	Sept 19
0000-0600		-	<4	-	<4	<4	<4	<4	<4
0800-1200	<4	<4	<4	4.5-6.5	<4	<4	<4	<4	
1200-1600	<4	<4	(10.1)	15.2	(8.4)	(2.1-4.1)	4.5-5.5	<4	
1600-2000	<4	XX	XX	7.0-9.0	XX	<4	<4	<4	
2000-2400	<4	<4	-	<4	<4	<4	<4	<4	

<sup>a</sup>Dash means incomplete or no data; XX designates an indeterminate value due to the presence of excessive noise levels in a significant number of spectra in the block.

<sup>b</sup>See text for the method used to estimate the concentration ranges for a particular block.

<sup>c</sup>An error of ±4 ppb applies to the values or range of values for September 14 and 17; an error of ±6.5 ppb has been estimated for the values in parentheses.

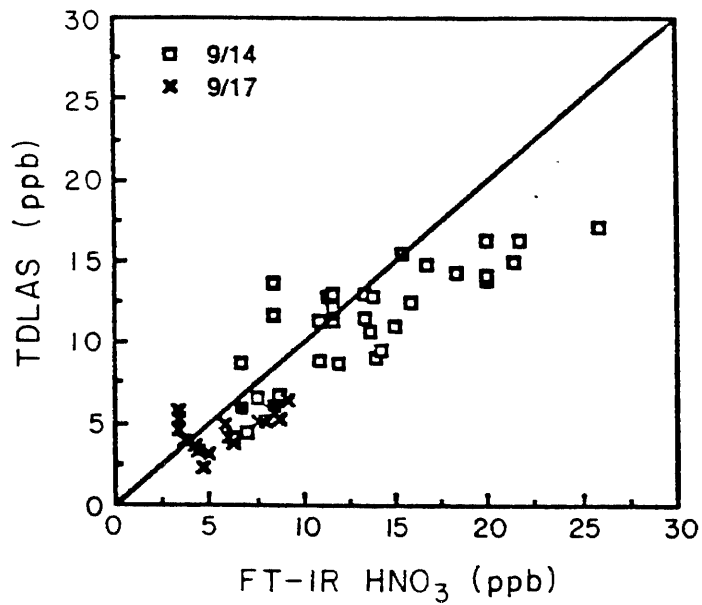
The XX entries in Table V-5 represent indeterminate values due to the periods of excessive noise which rendered the recorded spectra unusable. This problem was sufficiently severe (signal-to-noise ratios of 10:1 or less) during the evening hours on September 13 that the FT-IR system was shut down until the next morning. Values for the 1200-1600 hr sampling blocks on September 13, 15, and 16 are reported in parentheses, since cases which consisted of "normal" scans as well as moderately noisy spectra occurred during these time intervals. Errors for these values were estimated to be ±6.5 ppb.

Comparison of FT-IR HNO<sub>3</sub> Data with those from Other Methods. A comparison of the instantaneous data provided by the FT-IR and the tunable laser diode spectrometer (TDLS) systems is of particular interest to the

CARB, since good agreement between these two methods means that the TDLS, with its higher sensitivity ( $\sim 0.5$  ppb) and better portability, can be a convenient secondary standard for  $\text{HNO}_3$  measurement. The 52 FT-IR data points on September 14 and September 17, which are above the detection limit and which represent the FT-IR's best measurements, are compared with the coincident five-minute averages from the two TDLS instruments (operated by Unisearch Associates and Atmospheric Environment Service, Canada, respectively) in the scatter plot of Figure V-7. The ratio of the means (TDLS/FT-IR) is equal to 0.84. For the six highest reported  $\text{HNO}_3$  values, the TDLS measurements are significantly lower than those of the FT-IR, with the ratio of the means being 0.72.

The data obtained during the sampling period 1200-1600 PDT on September 14 permit a direct comparison between the FT-IR spectrometer and the non-continuous sampling methods employed in the Intercomparison Study. As noted earlier, during other periods the  $\text{HNO}_3$  levels were below the FT-IR detection limit, or else noise interferences affected the FT-IR spectrometer. The ratios of the mean of each method to the FT-IR period average of 15.2 ppb are as follows: TDLS, 0.84; ADM (annular denuder method), 0.95; DDM (denuder difference method), 1.03; FP (filter pack), 1.32. The closest agreement for this period is with the DDM value of 15.7 ppb, which is within 4% of the FT-IR value. The mean of the FP, DDM, ADM and TDLS results is also 15.7 ppb.

Sufficient data were obtained by FT-IR spectroscopy to give hourly average values for two or three of the four hours in the sampling periods 0800-1200 and 1600-2000 PDT on September 14 and for 1200-1600 PDT on September 17, 1986. A lower-limit and upper-limit concentration average can be calculated for each of these 4 hr periods by respectively assigning zero and the FT-IR detection limit of 4 ppb to the missing hourly averages. The upper limit average is expected to be closer to the true period average, especially for the two periods on September 14 when the general level of pollution was high. Indeed, when the missing FT-IR hourly data are estimated by dividing the corresponding TDLS data by the previously calculated (TDLS/FT-IR) factor of 0.84, the resulting period averages are close to the upper bound value. These FT-IR data are compared with those of the TDLS, FP, DDM and ADM for the above four-hour sampling periods in Figure V-8. Error bars on the FT-IR data are  $\pm 4$  ppb, although an additional error of  $\pm 1$  ppb may be assigned for periods with



Figures V-7. Comparison of 5-minute average concentrations from the TDLAS and FT-IR methods. The 1:1 line is shown (adapted from Hering et al. 1987).

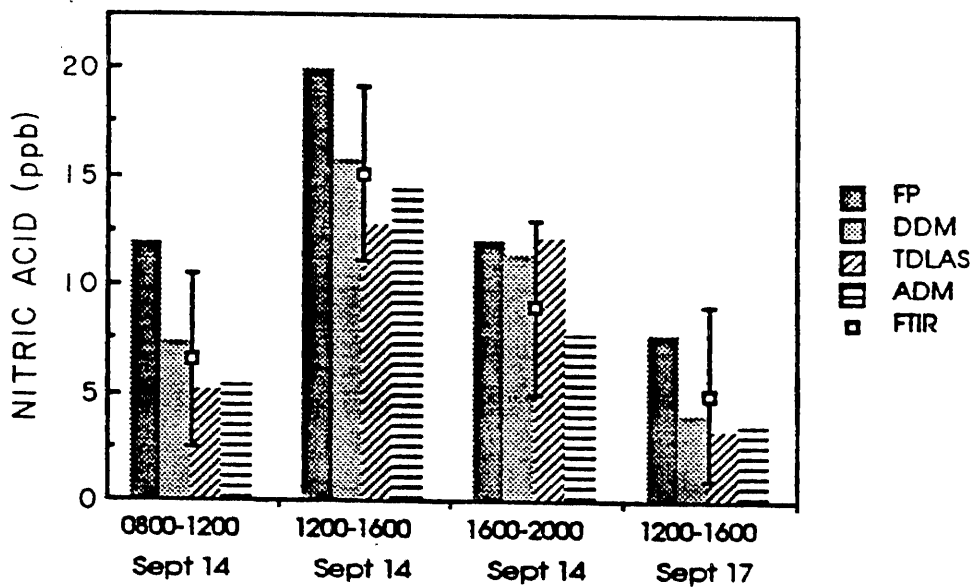


Figure V-8. Period averages measured by FT-IR compared to those of the other methods (adapted from Hering et al. 1987).

missing data. While the FT-IR data are closest to the DDM measurements, all of the methods agree to within their reported ranges of uncertainty.

A manuscript with the detailed data and a rigorous analysis of the results from the 1985 intercomparison study of nitric acid methods has been submitted for publication (Hering et al. 1987).

Ammonia. The measurement of  $\text{NH}_3$  is important because this compound reacts with gaseous  $\text{HNO}_3$  to form particulate  $\text{NH}_4\text{NO}_3$ . Indeed, the occurrence of  $\text{NH}_3$  at significant levels in the eastern part of the CSCAB is the reason for low observed  $\text{HNO}_3$  levels (even during moderate to severe smog episodes) together with corresponding high particulate nitrate levels (Doyle et al. 1979, Tuazon et al. 1980, Russell et al. 1983).

The hourly average ammonia data obtained during the eight-day period are given in Table V-6. They indicate that ~2-4 ppb was a typical background level of  $\text{NH}_3$  in Claremont during the field study period. Particularly high concentrations of  $\text{NH}_3$  were observed in the morning hours of September 13, 16, and 17. However, the highest hourly average concentrations occurred in the early afternoon of September 12, when 57 ppb of  $\text{NH}_3$  was measured. Sharp spikes in the concentrations of  $\text{NH}_3$  are evident in the plot of all of the  $\text{NH}_3$  data for September 12 to September 18 presented in Figure V-9. The periods with elevated  $\text{NH}_3$  concentrations all coincided with prevailing winds from the south or southeast, which clearly transported high levels of  $\text{NH}_3$  to Claremont from the predominantly agricultural areas of Chino and Ontario (~15 km away), which contain numerous poultry and dairy farms and feed lots.

Figure V-10 presents single-beam spectra recorded on the morning of September 16, during which the  $\text{NH}_3$  concentration increased rapidly from below the detection limit (<1.5 ppb) at 0819 hr to 18 ppb at 0831 hr, and to 84 ppb at 0856 hr, the latter instantaneous value being the highest  $\text{NH}_3$  concentration recorded by the longpath FT-IR technique during this study.

Comparison of FT-IR  $\text{NH}_3$  Data with those from Other Methods. Since the longpath FT-IR method has a higher degree of selectivity and sensitivity for the measurement of  $\text{NH}_3$  than for  $\text{HNO}_3$ , it was only logical that the FT-IR results should also be used as the standard for the comparison of  $\text{NH}_3$  methods. None of the other methods employed provided instantaneous measurements, but their results can be compared with the FT-IR average  $\text{NH}_3$  concentrations for the five designated sampling blocks presented in Table V-7.

Table V-6. Hourly Average NH<sub>3</sub> Concentrations (ppb)<sup>a,b,c</sup> Measured by Long Pathlength FT-IR Spectroscopy at Claremont, 1985

Hourly Period (PDT)	Sept 11	Sept 12	Sept 13	Sept 14	Sept 15	Sept 16	Sept 17	Sept 18	Sept 19
0000-0100		-	3.5	-	2.2	2.3	1.5	1.9	1.9
0100-0200		-	3.4	-	3.5	2.3	1.7	2.2	1.8
0200-0300		-	3.2	-	2.5	2.9	1.9	2.2	1.5
0300-0400		-	3.0	-	2.8	2.2	1.2	3.3	1.4
0400-0500		-	2.9	-	2.6	1.7	5.3	2.8	1.8
0500-0600		-	2.4	-	2.1	1.2	10.8	4.0	2.1
0800-0900	1.9	3.8	6.0	4.2	5.6	31.6	15.2	2.8	
0900-1000	2.8	5.4	6.6	4.4	5.7	23.4	17.3	2.0	
1000-1100	2.8	6.2	10.5	3.9	6.3	22.5	46.2	2.4	
1100-1200	2.2	4.9	33.6	3.6	6.9	33.3	39.7	2.0	
1200-1300	1.5	15.3	16.1 <sup>d</sup>	4.7	7.3	17.8	21.0	1.9	
1300-1400	1.7	42.4	7.6	4.0	6.5	6.0	6.0	1.0	
1400-1500	2.5	57.0	4.6	4.7	5.2 <sup>d</sup>	4.6	3.6	2.5	
1500-1600	2.4	14.5 <sup>d</sup>	4.6	3.8	4.3	3.2	2.9	3.0	
1600-1700	1.8	8.1 <sup>d</sup>	4.0	4.0	4.2	4.0	3.6	3.1	
1700-1800	2.3	4.9	4.3 <sup>d</sup>	4.9	3.4 <sup>d</sup>	3.0	2.7	4.1	
1800-1900	2.8	4.8	XX	4.6	3.5 <sup>d</sup>	3.4	2.1	4.3	
1900-2000	3.2	6.0	XX	5.6	4.1	3.1	2.3	2.9	
2000-2100	3.9	5.3	XX	4.3	4.8	3.3	3.4	3.5	
2100-2200	2.8	6.5	XX	4.8	2.3	3.0	3.3	2.5	
2200-2300	-	4.0	-	3.4	3.4	-	3.4	2.6	
2300-2400	-	3.6	-	3.0	3.1	-	2.6	2.6	

<sup>a</sup>At 23°C and 740 torr.

<sup>b</sup>Error: ±1.5 ppb; detection sensitivity = 1.5 ppb. Digits beyond 2 significant figures are retained only for the sake of format.

<sup>c</sup>Dash designates no data; XX indicates indeterminate concentrations due to very high noise levels in the spectra.

<sup>d</sup>A higher error limit of ±2.5 ppb has been estimated for these periods.

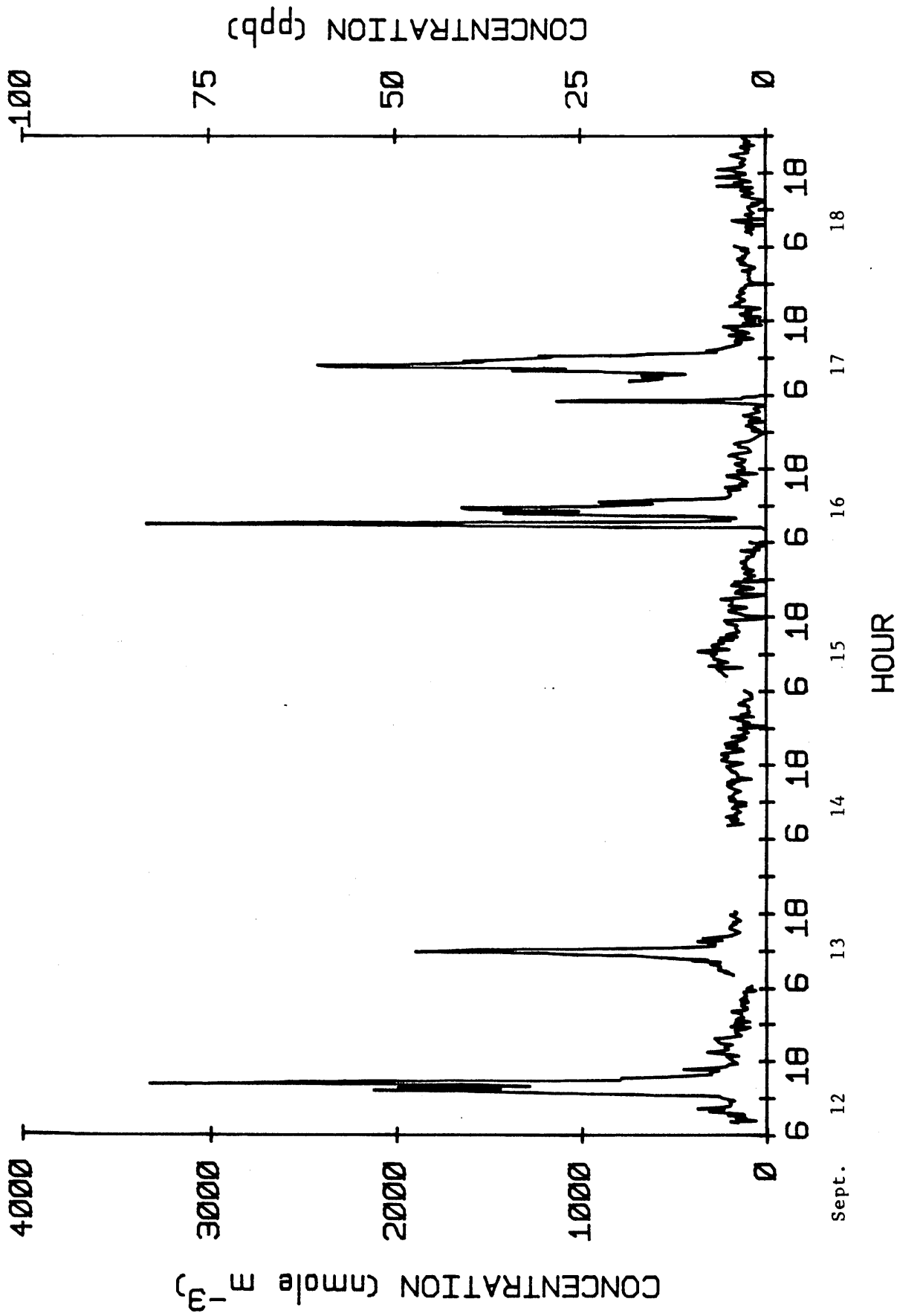


Figure V-9. Instantaneous  $\text{NH}_3$  concentrations in Claremont, CA, during the period September 12-18, 1985, as measured by FT-IR spectroscopy.

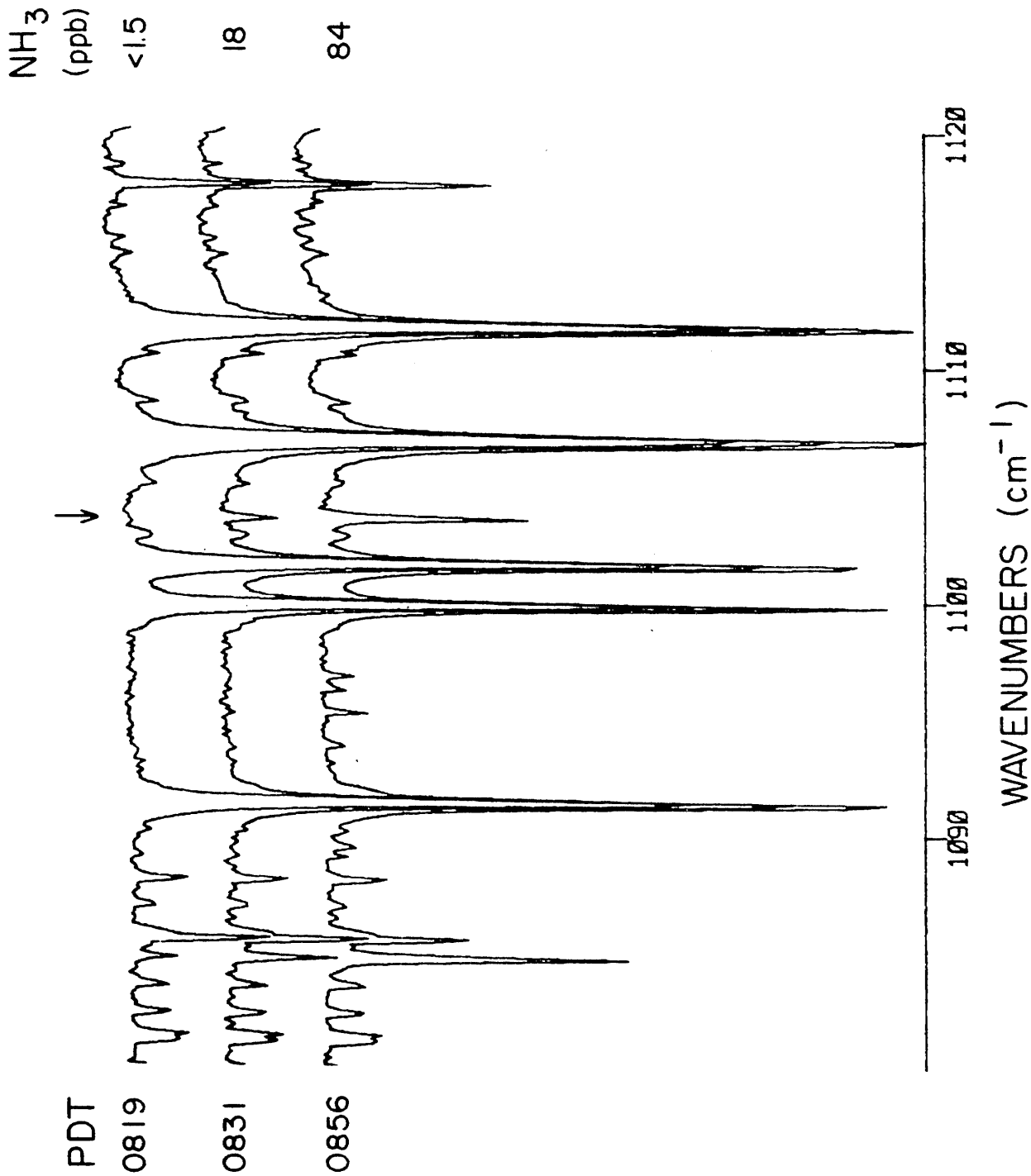


Figure V-10. FT-IR spectroscopic detection of NH<sub>3</sub> in Claremont, CA, on September 16, 1985. The arrow indicates the measurement peak of NH<sub>3</sub> at 1103.4 cm<sup>-1</sup>.

Table V-7. Average NH<sub>3</sub> Concentrations (ppb)<sup>a</sup> Measured by Long Pathlength FT-IR Spectroscopy for the Designated Sampling Periods

Sampling Period (PDT)	Sept 11	Sept 12	Sept 13	Sept 14	Sept 15	Sept 16	Sept 17	Sept 18	Sept 19
0000-0600		-	3.1	-	2.6	2.1	3.7	2.7	1.7
0800-1200	2.4	5.1	14.2	4.0	6.1	27.7	29.6	2.3	
1200-1600	2.0	32.3 <sup>b</sup>	8.2 <sup>b</sup>	4.3	5.8 <sup>b</sup>	7.9	8.4	2.1	
1600-2000	2.5	6.0 <sup>b</sup>	XX	4.8	3.8 <sup>b</sup>	3.4	2.7	3.6	
2000-2400	-	4.8	-	3.9	3.4	-	3.2	2.8	

<sup>a</sup>Dash means incomplete or no data; XX designates an indeterminate concentration due to the presence of excessive noise in a significant number of spectra in the block. Error = ±1.5 ppb unless noted otherwise.

<sup>b</sup>An uncertainty of ±2 ppb applies to these values.

The best agreement was with the filter pack method designated as CF1 (Hering et al. 1987), which employed a citric acid impregnated filter to collect NH<sub>3</sub> after Teflon (which removes particulates) and Nylon (which collects HNO<sub>3</sub>) filters. The linear regression of CF1 vs FT-IR data for the 33 sampling periods yields the relationship  $CF1 = -0.17 + 0.89(FT-IR)$  and correlation coefficient  $r = 0.987$ .

Another comparison was made with the technique designated QAI (Hering et al. 1987), which employed a train of annular denuders, one of which was coated with citric acid to collect NH<sub>3</sub>. The QAI vs FT-IR linear regression for 34 sampling periods yielded  $r = 0.939$ , but with a slope of only 0.56. Poor collection efficiency of the denuder segment at higher NH<sub>3</sub> levels is apparent from the comparison of individual data points. Similarly, the techniques which employed tungstic acid coated tubes gave erratic comparisons.

## 2. The 1985/1986 Winter Field Study at El Camino Community College (Torrance, CA)

The long pathlength FT-IR system obtained data during the period 1800 PST, February 23 to 0600 PST, February 27, 1986, which was the last of the three periods during which intensive ambient air sampling for PAH

and nitroarenes was carried out. A faulty cooling system for the infrared light source did not allow data to be obtained during the first (1700 PST, January 19 - 1700 PST, January 21) of those sampling periods. Just prior to the second sampling period (1700 PST, January 27 - 1700 PST, January 28) the FT-IR's computer malfunctioned due to heat build-up in the shed (which also housed all the support analytical instrumentation), resulting from a series of unexpectedly warm days and a temporary lack of an air conditioning unit. Due to a series of rainy periods and coastal storm conditions the third period of intensive sampling did not materialize until four weeks later.

The observed daytime concentrations of  $\text{HNO}_3$ , together with the simultaneously measured  $\text{NH}_3$  concentrations, for February 24, 25, and 26 are presented in Tables V-8, V-9, and V-10, respectively.  $\text{N}_2\text{O}_5$  was not detectable at any time during this study period, with a calculated upper limit concentration (see above) of 4 ppb.

The most probable background levels of  $\text{NH}_3$  at the study site did not become evident until the third day of this measurement period (February 26) when the measured concentrations were ~1-3 ppb throughout the day (Table V-9). For the two earlier days, the mid-morning to evening  $\text{NH}_3$  concentrations were less than 10 ppb (Tables V-8 and V-9). However, the significantly higher concentrations early in the mornings of these days (up to ~17 ppb) imply the presence of significant industrial sources in the area.

The photochemical activity during these three days in Torrance was characterized by  $\text{O}_3$  concentrations which attained peak values of ~60 ppb for the period 1200-1700 PST on February 24, ~150 ppb for 1300-1600 PST on February 25, and 40 to 60 ppb for the period 1200-1600 PST on February 26 (see Appendix C). While the  $\text{HNO}_3$  concentration profiles correlate with the  $\text{O}_3$  curve, the correlation is not as distinct as those shown in our previous measurements at Claremont (Tuazon et al. 1981) during severe air pollution episodes. However, the  $[\text{HNO}_3]/[\text{O}_3]$  ratio for the present Torrance data was generally significantly higher than the ratios observed in 1978 at Claremont (Tuazon et al. 1981).

Table V-8. HNO<sub>3</sub> and NH<sub>3</sub> Concentrations (ppb) vs. Time in Torrance, CA on February 24, 1986, Measured by Long Pathlength FT-IR Spectroscopy

PST	HNO <sub>3</sub>	NH <sub>3</sub>	PST	HNO <sub>3</sub>	NH <sub>3</sub>
0651	<3	13.9	1227	12.9	8.3
0704	<3	12.2	1242	13.3	6.6
0717	<3	10.1	1258	13.3	10.3
0730	<3	11.6	1318	13.5	9.5
0744	<3	11.3	1335	12.6	6.6
0757	<3	12.7	1354	12.3	7.8
0810	<3	13.4	1411	12.1	6.6
0823	<3	10.9	1424	12.1	5.6
0837	<3	11.2	1437	12.1	6.4
0850	<3	10.8	1453	10.0	7.2
0903	<3	10.3	1514	7.2	6.6
0916	<3	9.9	1531	6.9	6.4
0930	4.2	9.4	1547	7.1	5.2
0943	5.3	9.3	1603	6.8	6.6
0956	5.8	10.4	1618	6.2	6.0
1009	6.3	9.2	1635	6.7	5.2
1022	7.1	8.5	1650	6.5	5.3
1036	7.9	7.6	1707	5.0	6.0
1049	9.8	7.2	1723	3.3	4.5
1102	10.0	7.7	1739	<3	6.3
1115	9.1	7.8	1755	<3	5.4
1129	7.5	8.2	1812	<3	5.2
1142	9.1	8.0	1828	<3	7.2
1155	8.5	7.5	1845	<3	6.7
1210	9.6	7.4	1900	<3	6.4

Table V-9. HNO<sub>3</sub> and NH<sub>3</sub> Concentrations (ppb) vs. Time in Torrance, CA on February 25, 1986, Measured by Long Pathlength FT-IR Spectroscopy

PST	HNO <sub>3</sub>	NH <sub>3</sub>	PST	HNO <sub>3</sub>	NH <sub>3</sub>
0657	<3	7.7	1248	17.5	3.3
0710	<3	9.8	1304	20.1	2.9
0724	<3	9.0	1320	17.1	3.4
0737	<3	12.5	1336	21.1	3.8
0750	<3	16.5	1352	18.6	2.3
0803	<3	16.3	1409	21.6	2.5
0816	<3	16.7	1421	20.0	3.3
0829	<3	16.9	1435	21.7	3.0
0842	<3	15.0	1451	20.0	2.5
0856	<3	15.3	1506	16.5	3.1
0909	>3	14.8	1522	15.3	2.3
0922	>3	11.1	1540	15.6	2.5
0935	3.2	8.9	1556	15.6	2.6
0949	3.0	7.8	1611	13.3	2.1
1002	3.5	9.6	1627	12.9	2.0
1015	5.7	9.8	1644	12.5	1.9
1028	6.8	9.7	1700	10.5	2.7
1041	5.8	7.4	1716	11.9	3.4
1054	8.7	5.4	1732	9.9	3.6
1108	8.1	4.7	1750	8.2	3.6
1121	8.9	6.1	1805	7.3	5.1
1140	11.7	4.1	1822	<3	2.3
1156	10.5	4.5	1838	<3	6.1
1212	13.8	3.8	1854	<3	5.6
1229	14.9	4.3	1909	<3	2.2

Table V-10.  $\text{HNO}_3$  and  $\text{NH}_3$  Concentrations (ppb) vs. Time in Torrance, CA on February 26, 1986, Measured by Long Pathlength FT-IR Spectroscopy

PST	$\text{HNO}_3$	$\text{NH}_3$	PST	$\text{HNO}_3$	$\text{NH}_3$
0830	<3	2.2	1245	7.2	1.6
0843	<3	1.6	1301	7.5	2.8
0856	<3	1.7	1318	7.5	2.2
0910	<3	1.7	1334	7.9	2.0
0923	<3	1.7	1352	8.3	2.2
0936	3.3	2.0	1407	9.8	1.6
0949	6.2	2.8	1423	10.8	1.2
1002	5.4	2.6	1436	10.0	1.9
1015	5.8	2.4	1449	8.0	1.6
1029	5.5	2.2	1502	7.8	0.9
1042	6.3	0.7	1518	6.8	1.2
1055	8.3	3.1	1536	5.4	1.0
1108	7.6	2.6	1552	5.7	2.4
1121	8.1	1.9	1608	5.9	2.0
1135	9.0	2.8	1625	5.2	1.5
1148	8.5	2.9	1642	<3	1.8
1205	7.5	1.5	1657	<3	1.7
1223	8.0	1.5	1714	<3	<1

### 3. The 1986 Summer Field Study at Citrus College (Glendora, CA)

Our most intensive longpath FT-IR measurements during this program were conducted on the campus of Citrus College, which is situated on the boundary between the cities of Glendora and Azusa. As discussed in Section III, our measurements were conducted in conjunction with the CARB-sponsored carbonaceous species methods intercomparison study which occurred from 0800 PDT, August 12, to 0800 PDT, August 21, 1986. In contrast with the low level of air pollution during the 1985 Claremont summer field study, this August 1986 measurement period at Citrus College

was characterized by moderately high levels of photochemical activity. Except for the second day of measurements, the maximum hourly average  $O_3$  concentrations exceeded 200 ppb each day.

The FT-IR spectra obtained were analyzed for the simultaneous concentrations of  $HNO_3$ ,  $NH_3$  and  $HCHO$ . The detailed instantaneous data are presented in Appendix D of this report, and are plotted in Figure V-11. The hourly average concentrations are presented in Tables V-11 to V-13. Except for periods of power disruption on August 14 and the loss of most of the daytime data on August 17 due to a fault in archiving the data onto magnetic tapes, the FT-IR system provided continuous coverage of  $HCHO$  and  $NH_3$  concentrations since they were always above the respective detection limits of  $\sim 2-3$  ppb and  $\sim 1-1.5$  ppb.  $HNO_3$  was generally above the  $\sim 3-4$  ppb detection sensitivity between 0800 hr and 2000 hr each day throughout the study period. As for the 1985 Claremont and the 1986 Torrance studies,  $N_2O_5$  was not observed above the estimated detection limit of 4 ppb.

The FT-IR analysis of formaldehyde was easily carried out with the use of single-beam spectra, since the  $HCHO$  infrared spectrum has a Q-branch at  $2781.0\text{ cm}^{-1}$  well isolated from other atmospheric absorptions.  $HCHO$  was included as one of the species to be measured by FT-IR (except during the first day) because of the need for a standard against which other  $HCHO$  methods employed at this study could be compared. Our contribution to this aspect of the carbonaceous species study was to provide  $HCHO$  measurements by both DOAS and FT-IR spectroscopy, either method of which can serve as a benchmark standard. A comparison of the two sets of spectroscopic data for  $HCHO$  has been discussed in Section IV, and comparison with the results of the other  $HCHO$  methods is currently being carried out by Dr. Douglas Lawson of the CARB.

The  $NH_3$  concentrations observed in Glendora (Table V-12) during the first six days of the field study (September 12-17) were generally in the range of 2-4 ppb. These levels are similar to those measured during the 1985 Claremont study (Table V-6) for the periods when there was no localized transport of  $NH_3$  to the latter site from nearby agricultural sources.  $NH_3$  levels during the remaining days (August 18-21) were more variable and generally about twice the above range of values (Figure V-11). The erratic pattern found in the  $NH_3$  concentrations during these three days, which is also noticeable in the more well-defined  $HCHO$  and

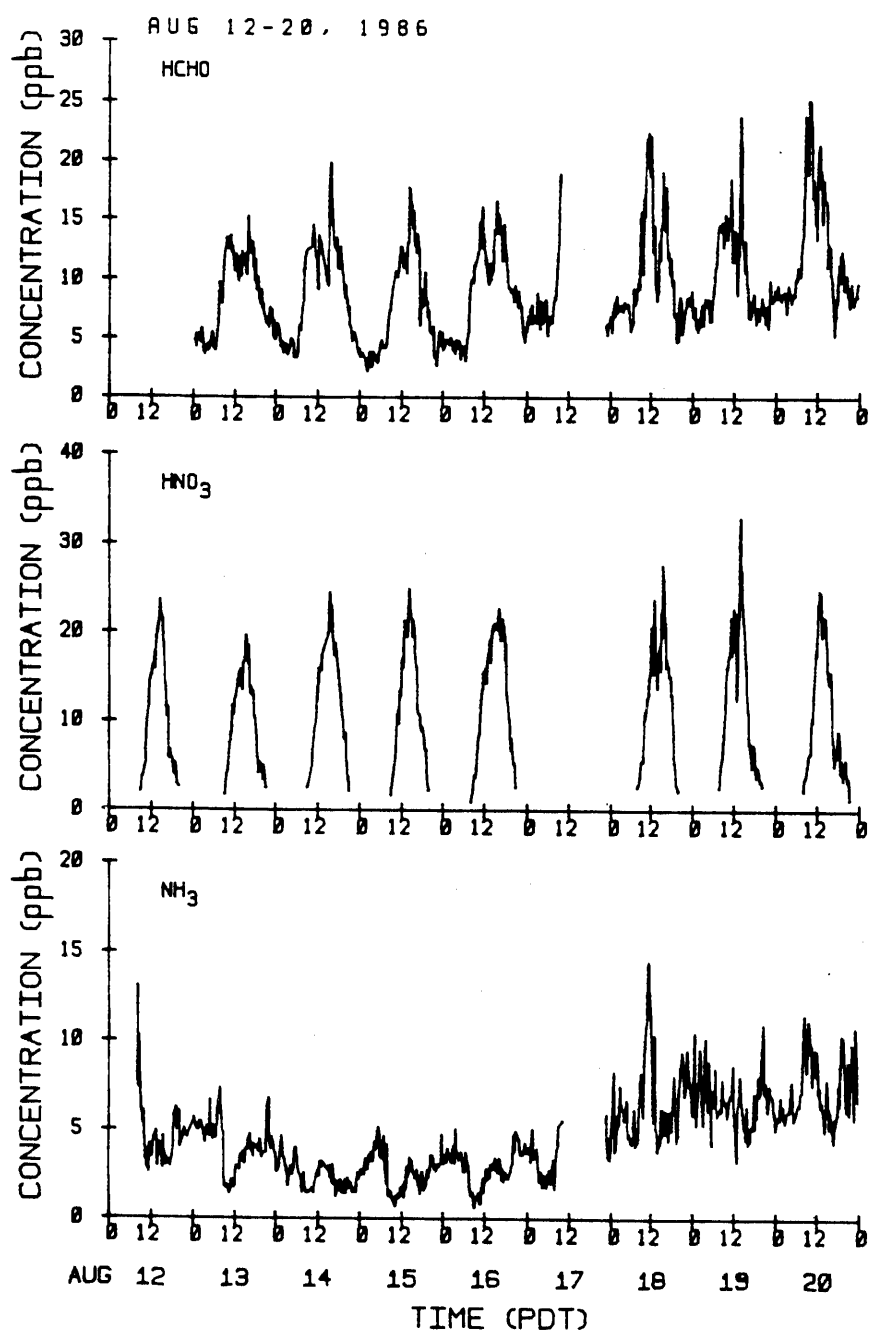


Figure V-11. Time-concentration profiles for formaldehyde, nitric acid and ammonia measured by long pathlength FT-IR spectroscopy during the 1986 Citrus College study.

Table V-11. Hourly Average HNO<sub>3</sub> Concentrations (ppb) at Glendora, CA, August 12-20, 1986, Measured by Long Pathlength FT-IR Spectroscopy

PDT	Aug 12	Aug 13	Aug 14	Aug 15	Aug 16	Aug 17	Aug 18	Aug 19	Aug 20
0700-0800	<3	<3	<3	<3	<3	<3	<3	<3	<3
0800-0900	<3	<3	<3	<3	2.8	<3	3.3	5.5	3.6
0900-1000	3.4	3.0	x	3.7	4.4	<3	5.9	10.8	5.9
1000-1100	7.1	6.7	x	8.3	9.0	x	11.0	17.0	10.2
1100-1200	13.1	10.5	x	12.3	14.2	x	14.0	20.1	16.5
1200-1300	15.9	13.3	14.8	17.1	15.8	x	19.6	18.7	22.5
1300-1400	18.2	15.0	x	20.7	18.0	x	17.1	22.6	21.2
1400-1500	22.0	15.6	x	22.7	20.3	x	17.2	23.9	19.0
1500-1600	19.6	18.1	22.3	20.3	20.9	x	23.9	15.6	14.9
1600-1700	11.9	14.9	19.3	14.3	20.4	x	19.2	7.8	8.9
1700-1800	6.1	12.4	17.4	9.9	19.5	x	14.9	6.5	6.2
1800-1900	4.9	8.0	13.3	7.9	12.6	x	8.9	4.8	7.2
1900-2000	3.3	4.9	9.5	4.0	7.8	x	3.4	3.7	4.7
2000-2100	<3	4.2	5.3	<3	4.5	x	<3	<3	4.6
2100-2200	<3	<3	<3	<3	<3	x	<3	<3	<3

x - Designates no data due to power interruptions on August 14 and fault in archiving on August 17.

Table V-12. Hourly Average NH<sub>3</sub> Concentrations (ppb) at Glendora, CA, August 12-21, 1986, Measured by Long Pathlength FT-IR Spectroscopy<sup>a</sup>

PDT	Aug 12	Aug 13	Aug 14	Aug 15	Aug 16	Aug 17	Aug 18	Aug 19	Aug 20	Aug 21
0000-0100		5.4	2.9	2.6	3.3	3.9	5.9	7.5	5.5	6.0
0100-0200		5.1	3.6	2.9	3.6	3.9	4.6	6.5	6.1	6.5
0200-0300		5.3	3.6	3.2	3.4	3.7	6.1	8.2	5.8	7.5
0300-0400		4.6	2.4	3.4	4.1	2.6	6.3	7.4	6.0	7.1
0400-0500		5.1	2.7	4.0	3.5	2.3	6.0	7.6	6.8	7.1
0500-0600		5.0	3.5	4.7	3.4	2.2	4.7	6.7	5.8	6.5
0600-0700		4.9	3.1	3.8	3.2	2.3	4.5	7.0	6.3	6.4
0700-0800		6.4	2.1	3.1	2.1	2.4	4.9	6.2	7.2	
0800-0900	8.8	5.1	1.9	1.8	1.3	3.8	5.7	6.6	9.9	
0900-1000	6.2	1.9	x	1.1	1.1	5.4	7.1	6.7	10.0	
1000-1100	3.9	1.6	x	1.1	1.2	x	9.9	6.3	9.0	
1100-1200	3.4	1.9	x	1.4	1.9	x	13.2	7.3	8.9	
1200-1300	3.9	2.6	2.7	1.6	2.4	x	8.2	5.0	7.9	
1300-1400	4.4	3.1	x	2.3	2.6	x	6.4	6.2	6.3	
1400-1500	3.9	3.5	x	3.1	3.0	x	4.4	6.4	6.0	
1500-1600	3.7	3.8	2.6	2.6	2.9	x	5.8	5.2	6.2	
1600-1700	3.2	4.3	2.3	2.3	2.9	x	5.5	4.6	5.0	
1700-1800	3.1	3.8	1.7	2.1	2.4	x	5.4	5.4	5.5	
1800-1900	5.1	4.1	1.9	2.0	2.3	x	6.5	6.2	7.5	
1900-2000	5.9	4.0	1.8	2.3	2.9	x	5.6	7.4	9.7	
2000-2100	4.4	3.6	1.9	3.3	4.5	x	7.1	9.0	7.4	
2100-2200	4.8	5.3	2.0	3.1	4.1	x	8.5	6.9	7.1	
2200-2300	4.8	4.9	1.6	3.0	3.7	x	8.1	7.0	8.0	
2300-2400	5.2	4.1	2.2	3.7	3.9	3.9	7.5	6.3	8.4	

<sup>a</sup>Blank means outside the schedule.

x - Designates no data due to power interruptions on August 14 and fault in archiving on August 17.

Table V-13. Hourly Average HCHO Concentrations (ppb) at Glendora, CA, August 13-21, 1986, Measured by Long Pathlength FT-IR Spectroscopy<sup>a</sup>

PDT	Aug 13	Aug 14	Aug 15	Aug 16	Aug 17	Aug 18	Aug 19	Aug 20	Aug 21
0000-0100	4.8	5.6	3.7	4.5	6.3	6.5	7.7	8.9	10.4
0100-0200	5.1	4.9	3.3	4.8	7.1	7.7	6.4	8.5	10.2
0200-0300	5.2	4.2	2.8	4.7	6.7	7.6	6.9	8.6	9.1
0300-0400	4.0	4.0	3.1	4.3	7.4	7.6	7.4	8.7	9.2
0400-0500	4.2	4.7	3.6	4.6	7.4	7.8	8.1	8.5	8.4
0500-0600	5.0	3.9	3.4	4.0	7.5	7.4	7.0	9.2	9.8
0600-0700	4.3	4.1	4.5	3.8	6.3	6.2	9.6	10.5	10.1
0700-0800	7.5	6.3	4.3	5.9	7.1	8.5	13.0	11.7	
0800-0900	9.2	10.1	6.5	9.7	9.4	9.7	14.5	19.5	
0900-1000	12.4	x	9.0	11.2	15.4	13.8	14.2	22.5	
1000-1100	13.1	x	10.4	13.1	x	17.4	14.4	20.8	
1100-1200	11.9	x	11.7	14.5	x	21.1	14.4	15.9	
1200-1300	11.3	12.0	11.8	11.7	x	16.8	12.3	19.2	
1300-1400	10.6	x	11.7	10.1	x	10.5	14.5	17.1	
1400-1500	11.4	x	16.1	11.4	x	11.1	14.9	15.9	
1500-1600	11.9	15.9	15.1	14.8	x	15.7	10.6	12.2	
1600-1700	13.3	14.6	13.2	14.2	x	15.2	7.5	8.0	
1700-1800	12.1	12.7	9.0	13.2	x	11.6	8.1	7.6	
1800-1900	10.0	11.4	8.8	11.0	x	9.2	7.0	11.1	
1900-2000	8.4	9.9	8.0	9.1	x	6.4	7.3	10.5	
2000-2100	7.3	8.2	6.1	8.4	x	7.0	7.7	9.2	
2100-2200	6.4	6.3	4.8	8.5	x	6.2	6.9	8.6	
2200-2300	6.9	5.2	3.7	7.5	x	7.9	8.6	8.2	
2300-2400	6.0	4.2	5.1	5.4	6.1	8.2	8.6	9.0	

<sup>a</sup>Blank means outside the schedule.

x - Designates no data due to power interruptions on August 14 and fault in archiving on August 17.

HNO<sub>3</sub> concentration profiles (Figure V-11), could well be due to the prevailing wind conditions.

The maximum instantaneous concentrations of HNO<sub>3</sub> attained 20 ppb or higher during the eight days that the FT-IR measurements provided detailed HNO<sub>3</sub> profiles (Figure V-11), with the highest concentration of 33 ppb being observed on August 19. Comparison of our Dasibi ozone data with the FT-IR measurements of HNO<sub>3</sub> showed a strong correspondence between the HNO<sub>3</sub> and O<sub>3</sub> maxima. This is illustrated in Figure V-12 for the pollution episodes of August 15-16, where the hourly average HNO<sub>3</sub> concentrations (by FT-IR) are compared with the half-hourly average O<sub>3</sub> concentrations. The correspondence of the HNO<sub>3</sub> concentration profile with that of the O<sub>3</sub> curve is even more pronounced in the similar plot in Figure V-13 for the August 18-19 episodes. Figures V-12 and V-13 also include the hourly average NO<sub>2</sub> concentrations (DOAS data, Section IV), which clearly show the expected minimum at the times of the maximum O<sub>3</sub> and HNO<sub>3</sub> concentrations. However, the maximum levels of HNO<sub>3</sub> could not be correlated with the maximum levels of NO<sub>2</sub> that prevailed during the morning hours.

As noted above, detailed comparisons of the FT-IR spectroscopic data obtained during the intercomparison studies at Claremont and Glendora are being prepared by the CARB staff, and will be presented in the peer-reviewed literature. Further discussion of the spectroscopic data obtained in this program is given in Section XI.B.

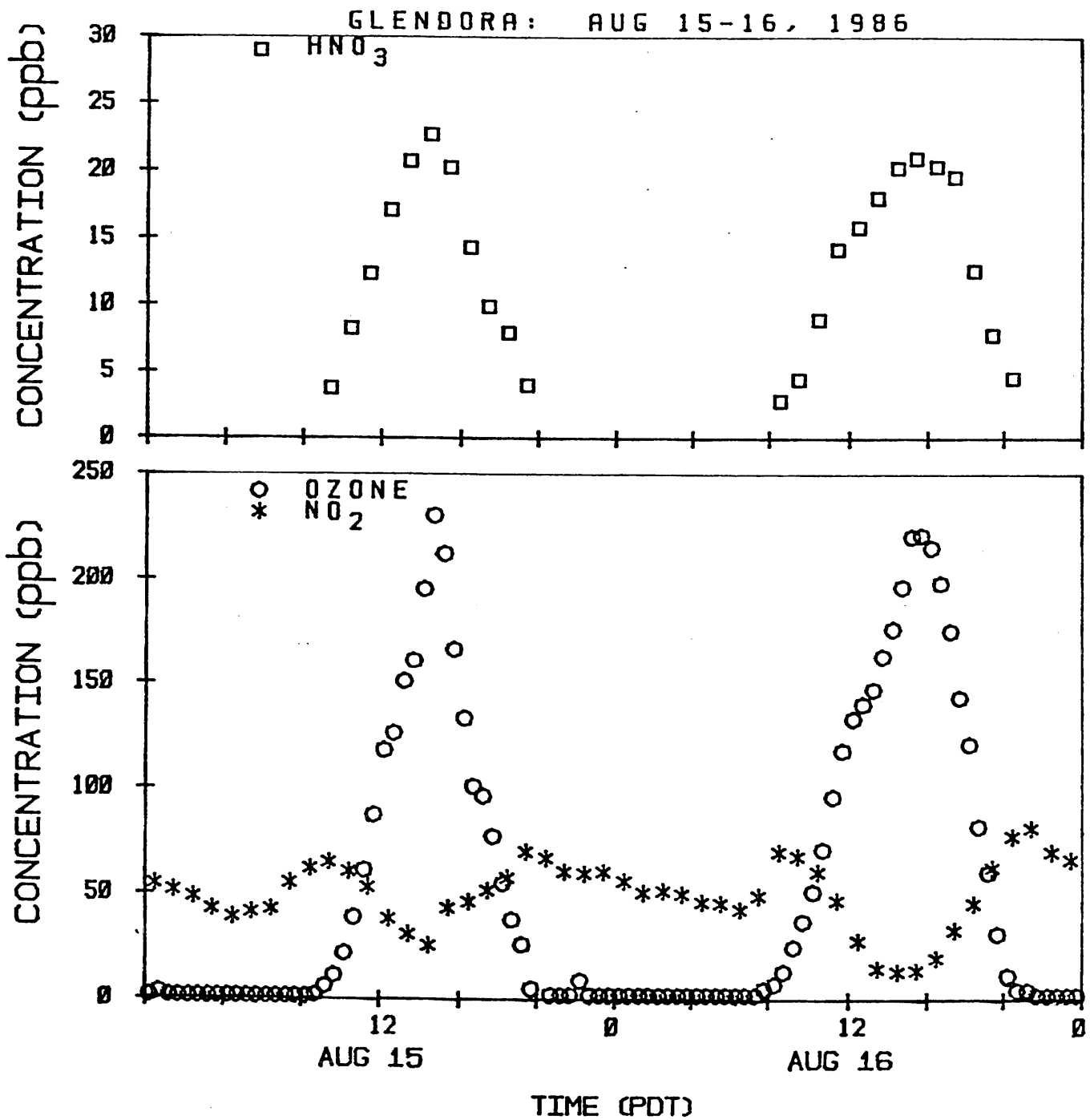


Figure V-12. Time-concentration plots of average  $\text{HNO}_3$  (FT-IR),  $\text{NO}_2$  (DOAS), and  $\text{O}_3$  (Dasibi monitor) at Citrus College for August 15-16, 1986.

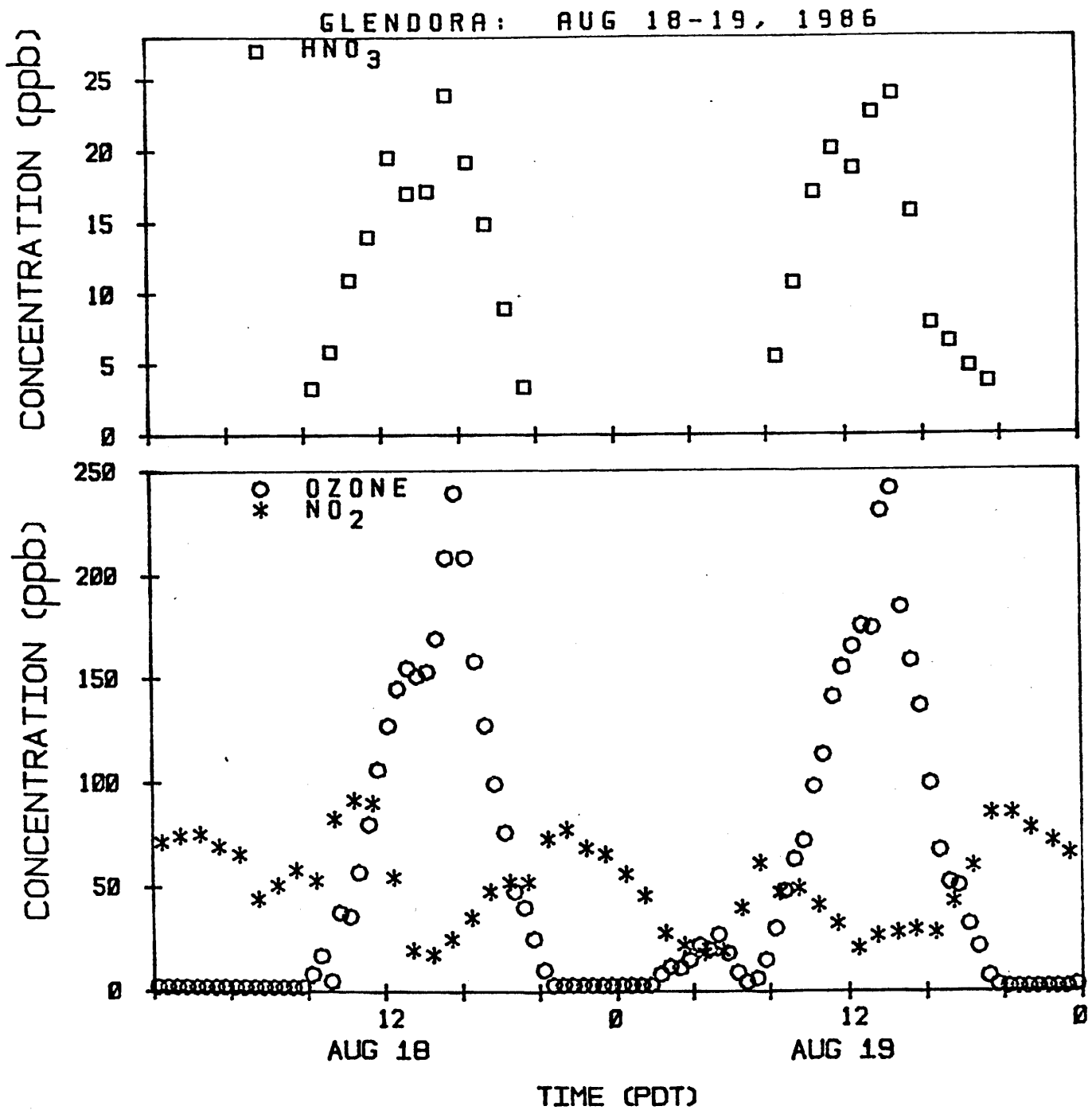


Figure V-13. Time-concentration plots of average  $\text{HNO}_3$  (FT-IR),  $\text{NO}_2$  (DOAS), and  $\text{O}_3$  (Dasibi monitor) at Citrus College for August 18-19, 1986.



## VI. AMBIENT MEASUREMENTS OF GASEOUS AND PARTICLE-ASSOCIATED POLYCYCLIC AROMATIC HYDROCARBONS AND MUTAGENIC NITROARENES

### A. Introduction

In this Section, the results of our measurements of ambient atmospheric concentrations of a series of selected PAH and nitroarenes are reported. Our study of the role of nitrogenous pollutants in the formation of atmospheric mutagens concentrated on the nitroarenes since these species are both highly mutagenic and known to be present in ambient POM. It was important, therefore, that we measured the nitroarenes present in ambient POM concurrent with our field study measurements of the nitrogenous gas-phase species. Thus, collections of ambient air particulate samples were made on September 13-14, 1985, during a photochemical air pollution episode in Claremont, CA, and in January and February 1986 during a wintertime, high-NO<sub>x</sub>, episode in Torrance, CA. The specific site locations and the meteorological conditions during these two studies are described in Section III above.

During our summertime field study in Claremont, the SAPRC "mega-sampler" (Fitz et al. 1983) was used to collect the ambient particulate samples, and thus the PAH and nitroarenes which were measured were only those associated with particulate matter. In contrast, we used a combination of sampling methods during our wintertime field study in Torrance. Specifically, in addition to several standard Hi-vol filter particle collections, ambient air samples were also collected on Hi-vol filters backed with polyurethane foam (PUF) plugs and on Tenax-GC solid adsorbent in order to measure the concentration of selected PAH and nitroarenes present either in the gas phase or "blown off" the filters during Hi-vol collection. The January Torrance samples were analyzed for particle-associated nitroarenes, while the February Torrance samples were analyzed for the full spectrum of gaseous and particle-associated PAH and nitroarenes.

### B. Experimental

#### 1. Pomona College (Claremont) Summer Field Study: Sample Collection and Extraction

Samples were collected from 1200 hr to 2400 hr on Friday, September 13 and from 0600 hr on Saturday, September 14, through 0600 hr

on Sunday, September 15, 1985. Collections of particulate matter were made at 6-hr intervals with the SAPRC-designed and constructed ultra-high volume "mega-sampler" (Fitz et al. 1983). This sampler has an inlet with a 50% cutoff point of 20  $\mu\text{m}$ , and has a total flow rate of approximately 640 SCFM through four 16-in. x 20-in. filters. This sampling rate results in a face velocity at the filters very similar to those occurring during standard Hi-vol sampling.

The TIGF filters (Pallflex T60A20) used for particle collection were prewashed by sequential Soxhlet extraction with dichloromethane ( $\text{CH}_2\text{Cl}_2$ ) and methanol ( $\text{CH}_3\text{OH}$ ). The particle loadings after sampling were determined by differential weighing of the filters. After particulate collection, two 16-in. x 20-in. filters from each time period were Soxhlet extracted for 18 hr with  $\text{CH}_2\text{Cl}_2$ . Pyrene- $\text{d}_{10}$  at  $\sim 3 \mu\text{g}$ , perylene- $\text{d}_{12}$  at  $\sim 1 \mu\text{g}$ , and 2-nitrofluoranthene- $\text{d}_9$ , 1-nitropyrene- $\text{d}_9$ , 1,3-, 1,6- and 1,8-dinitropyrene- $\text{d}_8$  at  $\sim 0.3 \mu\text{g}$  each were added as internal standards to these  $\text{CH}_2\text{Cl}_2$  extracts. The extracts were precleaned by open-column silica (deactivated by the addition of 5%  $\text{H}_2\text{O}$  by weight) chromatography to remove aliphatic hydrocarbons (eluted with hexane) and polar material (left on the column). The fractions of interest (those eluted with  $\text{CH}_2\text{Cl}_2$ ) were further fractionated by high performance liquid chromatography (HPLC) using an Altex semi-preparative scale Ultrasphere Silica column (1 cm x 25 cm). The HPLC system consisted of a Spectra-Physics Model 8100 chromatograph, Model 4100 computing integrator, Model 8400 uv/vis detector and ISCO fraction collector. The mobile phase program employed was: n-hexane/ $\text{CH}_2\text{Cl}_2$  at 95%/5% for 10 min, then a linear gradient to 100%  $\text{CH}_2\text{Cl}_2$  over 15 min, held at 100%  $\text{CH}_2\text{Cl}_2$  for 10 min, followed by a linear gradient to 100% acetonitrile ( $\text{CH}_3\text{CN}$ ) over 10 min.

The PAH-containing fraction was collected from 4 min to 13 min and a fraction containing the nitrofluoranthene and nitropyrene isomers was collected between 22-25 min. When analyzed by gas chromatography/mass spectrometry (GC/MS) the nitroarene-containing fraction caused rapid degradation of the GC column, resulting in poor isomer resolution. Therefore, the nitrofluoranthene and nitropyrene containing fraction was further cleaned prior to the GC/MS analyses (detailed below) by additional chromatography on an Altex semi-preparative Ultrasphere-ODS column (1 cm x 25 cm), using a Beckman Model 334 HPLC equipped with a Beckman Model 164

uv/vis detector. Isocratic elution by CH<sub>3</sub>OH/H<sub>2</sub>O at 80%/20% resulted in the nitrofluoranthene and nitropyrene isomers (and the deuterated nitrofluoranthene and nitropyrene internal standards used) eluting between 22 and 32 min.

2. El Camino Community College (Torrance) Winter Field Study: Sample Collection, Extraction and Fractionation

At the Torrance field study site, ambient air samples were collected during three high-NO<sub>x</sub> pollution episodes in the months of January and February, 1986, using 12-hr (day and night) sampling periods. The complete range of samples (i.e., Tenax cartridges, PUF plugs and Hi-vol filters) from the February 24-25 sampling period were analyzed for PAH and nitroarenes. In addition, POM collected on TIGF filters during the January 19-20 and 27-28 sampling periods was analyzed for nitroarenes.

Tenax-GC cartridge. Gas-phase PAH were sampled using 10 cm x 4 mm i.d. Pyrex tubes packed with 0.1 g of Tenax-GC solid adsorbent and doped with 610 ng of naphthalene-d<sub>8</sub>. The flow rate was 1.15 liter min<sup>-1</sup>, yielding an ~0.8 m<sup>3</sup> volume of air sampled for each 12-hr sampling period. A second Tenax cartridge was placed in series downstream to check for breakthrough from the first cartridge.

The cartridges were eluted with 3 ml of diethyl ether, and 60 and 67 ng of the internal standards phenanthrene-d<sub>10</sub> and anthracene-d<sub>10</sub>, respectively, were added to the eluate, which was then concentrated with a micro-Snyder apparatus. The concentrated extracts were analyzed for PAH by GC/MS with multiple ion detection (MID), as described below.

Hi-vol filter followed by three PUF plugs. A single high-volume sampler system consisting of a TIGF filter followed by three PUF plugs (each ~9 cm diameter x 5 cm thickness) [Figure VI-1] was run at 30 SCFM for 12-hr intervals, yielding ambient samples collected from 610 m<sup>3</sup> of air. The TIGF filters and PUF plugs were precleaned by Soxhlet extraction with CH<sub>2</sub>Cl<sub>2</sub> and CH<sub>3</sub>OH. After sample collection, the filter and each PUF plug were separately Soxhlet extracted in CH<sub>2</sub>Cl<sub>2</sub> and analyzed. Deuterated internal standards were added to the filter, PUF plug #1, PUF plug #2, and PUF plug #3, respectively, as follows (in µg): naphthalene-d<sub>8</sub> (1.1, 5.3, 5.3, 5.3); phenanthrene-d<sub>10</sub> (2.0, 10.0, 10.0, 10.0); anthracene-d<sub>10</sub> (2.2, 11.2, 11.2, 11.2); fluoranthene-d<sub>10</sub> (1.2, 11.2, 1.2, 0.0); pyrene-d<sub>10</sub> (1.2, 11.0, 1.2, 0.0); benzo(a)pyrene-d<sub>12</sub> (1.1, 0.0, 0.0, 0.0);

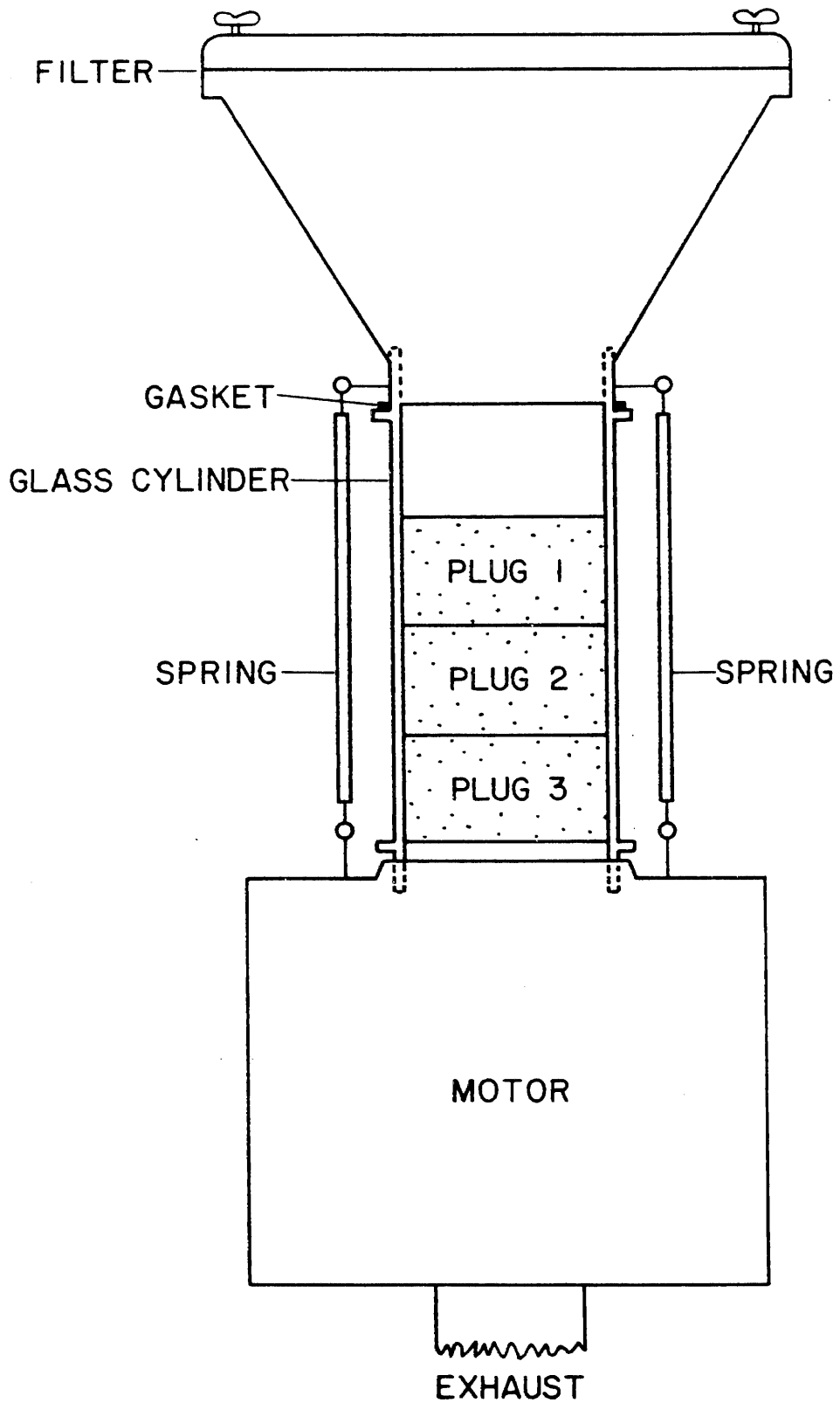


Figure VI-1. Schematic of modified Hi-vol sampler with PUF plugs underneath the filter to collect gas phase species and compounds "blown-off" the filter.

perylene-d<sub>12</sub> (1.0, 0.0, 0.0, 0.0); and 1-nitronaphthalene-d<sub>7</sub> (0.6, 1.2, 1.2, 1.2). The amounts added to the filter and PUF plug extracts were similar to the non-deuterated PAH and nitroarene concentrations observed.

The PUF plug extracts were concentrated by rotary evaporation and fractionated by HPLC using an Altex semi-preparative scale Ultrasphere Silica column (1 cm x 25 cm), with the mobile phase program as described above for the Claremont filters, i.e.,: n-hexane/CH<sub>2</sub>Cl<sub>2</sub> at 95%/5% for 10 min, then a linear gradient to 100% CH<sub>2</sub>Cl<sub>2</sub> over 15 min, held at 100% CH<sub>2</sub>Cl<sub>2</sub> for 10 min, followed by a linear gradient to 100% CH<sub>3</sub>CN over 10 min. The PAH-containing fraction was collected from 4 min to 13 min and a nitroarene-containing fraction from 13 min to 25 min. The latter fraction contained the lower molecular weight nitroarenes as well as the nitrofluoranthenes and nitropyrenes. The fractions were concentrated by rotary evaporation, then taken just to dryness under a stream of nitrogen. After dissolving in CH<sub>2</sub>Cl<sub>2</sub>, the PAH and nitroarene fractions were analyzed by GC/MS - MID as described below. The filter extracts were fractionated as described below.

Hi-vols with TIGF filters. In order to collect sufficient particulate organic matter for analyses of the nitrofluoranthene and nitropyrene isomers, TIGF filters from simultaneous Hi-vol collections of POM were combined. The twelve-hr "day" and "night" collections for the two January POM sampling periods were made from 0500-1700 hr and 1700-0500 hr, respectively. The January 19-20 day and night samples each consisted of nine composited filters. The January 27-28 day and night samples were each composites of eight filters. The deuterated internal standards added to each composited day or night sample were (in µg): pyrene-d<sub>10</sub> (12.2), perylene-d<sub>12</sub> (2.6), 1-nitropyrene-d<sub>9</sub> (1.2), 2-nitrofluoranthene-d<sub>9</sub> (1.3), 1,2-dinitrofluoranthene-d<sub>8</sub> (1.1), dinitropyrene-d<sub>8</sub> mixture (1.7).

For the February 24-25 sampling period, when additional experiments were being conducted (see Section IX), the Hi-vols were run at either 30 or 40 SCFM and the total volumes of air sampled were: 1800-0600 hr, 1960 m<sup>3</sup> (3 filters composited); 0600-1800 hr, 3190 m<sup>3</sup> (4 filters). The filters comprising the "day" and "night" samples were Soxhlet extracted in pairs in CH<sub>2</sub>Cl<sub>2</sub> and each doped proportionately so that the total amount of internal standard added for each composite day and night sample was (in µg): 2-nitrofluoranthene-d<sub>9</sub> (0.6), 1-nitropyrene-d<sub>9</sub> (0.5), pyrene-d<sub>10</sub>

(6.1), perylene-d<sub>12</sub> (4.3), 1,2-dinitrofluoranthene-d<sub>8</sub> (0.6), dinitropyrenes-d<sub>8</sub> (0.9).

The CH<sub>2</sub>Cl<sub>2</sub> filter extracts were precleaned by open-column silica chromatography to segregate the aliphatic hydrocarbons and polar material (eluted with methanol). As described above, the fractions of interest (eluted from the silica with CH<sub>2</sub>Cl<sub>2</sub>) were further fractionated by HPLC on an Ultrasphere Silica column and the nitrofluoranthene and nitropyrene-containing fraction (eluting between 22-25 min) was further cleaned prior to GC/MS-MID analysis by additional chromatography on an Altex semi-preparative Ultrasphere-ODS column.

### 3. Analysis

Compound identifications and quantifications were made using a Finnigan 3200 quadrupole GC/MS operating in the electron impact mode (70 eV) and interfaced to a Teknivent data system. The GC was equipped with a cool on-column injection system and a 30 m or 60 m DB-5 fused silica capillary column (both from J & W Scientific, Inc.) eluting directly into the MS ion source.

For the Claremont samples the PAH were quantified by ratioing the area of the GC/MS-MID molecular ion peak to that of the deuterated internal standard (i.e., either pyrene-d<sub>10</sub> or perylene-d<sub>12</sub>) closest in molecular weight to the compounds quantified. 2-Nitrofluoranthene and 1-nitropyrene were quantified by area comparison with the deuterated internal standards. 2-Nitropyrene was quantified using the 1-nitropyrene-d<sub>9</sub> internal standard with a response factor correction of 2 (that is, the m/z 247 ion response of 2-nitropyrene was measured to be twice that of 1-nitropyrene).

For the Torrance samples the quantifications of naphthalene, phenanthrene, anthracene, fluoranthene, pyrene, benzo(a)pyrene and perylene were made by ratioing the area of the GC/MS-MID molecular ion peak to that of the corresponding deuterated internal standard. For the methyl-naphthalene isomers and biphenyl, an external calibration of the molecular ion peak to that of naphthalene-d<sub>8</sub> or phenanthrene-d<sub>10</sub> was made, and for benzo(e)-pyrene the deuterated benzo(a)pyrene internal standard ion was used.

Identifications of the nitroarenes (apart from the methyl-nitro-naphthalenes for which 14 isomers are possible) by GC/MS-MID were made on the basis of the presence, in correct abundance, of all of the major

fragment ions (as given in Table VI-1), as well as retention time matching. Authentic samples of all eight of the nitrofluoranthene and nitropyrene isomers and all three of the nitrobiphenyl isomers were available for retention time and fragment ion abundance comparisons. Quantifications for 1-nitronaphthalene, 2-nitrofluoranthene and 1-nitropyrene were made by comparison with the deuterated internal standards. 2-Nitronaphthalene, 3-nitrobiphenyl and 9-nitroanthracene were quantified by external calibration of the molecular ion peak to that of the 1-nitronaphthalene-d<sub>7</sub> internal standard. 2-Nitropyrene was quantified using the 1-nitropyrene-d<sub>9</sub> internal standard as described above.

Chemicals. The following chemicals were obtained from commercial sources: phenanthrene-d<sub>10</sub>, anthracene-d<sub>10</sub>, pyrene-d<sub>10</sub>, benzo(a)pyrene-d<sub>12</sub> and perylene-d<sub>12</sub> (Cambridge Isotope Laboratories); fluoranthene-d<sub>10</sub> (MSD Isotopes Inc.); naphthalene-d<sub>8</sub>, 1-nitronaphthalene-d<sub>7</sub>, biphenyl, 1- and 2-nitronaphthalene, 2-, 3- and 4- nitrobiphenyl and 9-nitroanthracene (Aldrich Chemical Co.); 1- and 2-methylnaphthalene (Chem Service); Standard Reference Material 1647, certified PAH, (National Bureau of Standards). Commercially available 1-nitropyrene (Pfaltz and Bauer, Inc.) was purified according to the method described by Paputa-Peck et al. (1983).

2-Nitrofluoranthene-d<sub>9</sub> and 1-nitropyrene-d<sub>9</sub> were synthesized as described by Zielinska et al. (1986a) and Pitts et al. (1985c). 2-Nitropyrene was provided by Dr. D. Schuetzle (Ford Motor Co.; Dearborn, MI) and 4-nitropyrene by Dr. A. Berg (University of Aarhus, Denmark). The 1-, 2-, 3-, 7- and 8-nitrofluoranthenes were synthesized as described previously (Ramdahl et al. 1985a, Zielinska et al. 1986a).

## C. Results and Discussion

### 1. Claremont Summertime Samples

Table VI-2 gives the concentrations of selected PAH in the POM samples collected at Claremont, September 14-15, 1985, during four consecutive 6-hr time periods. In addition, the average temperature and other relevant particulate data for these time periods are also given.

The concentrations of 2-nitrofluoranthene (2-NF), 1-nitropyrene (1-NP) and 2-nitropyrene (2-NP) in these four 6-hr time periods and in two additional time periods, namely 1200-1800 hr and 1800-2400 hr on September 13, are given in Table VI-3. It should be noted from this table that the POM sample collected on September 13 during the 1800-2400 hr time period

Table VI-1. Molecular Ions, Characteristic Fragment Ions and Relative Abundances Used for Identification of Nitroarenes by GC/MS-MID

	m/z and Relative Abundance for Authentic Compound <sup>a</sup>						
	[M] <sup>+</sup>	[M-CO] <sup>+</sup>	[M-NO] <sup>+</sup>	[M-NO <sub>2</sub> ] <sup>+</sup>	[M-HNO <sub>2</sub> ] <sup>+</sup>	[M-H <sub>2</sub> NO <sub>2</sub> ] <sup>+</sup>	[M-CNO <sub>2</sub> ] <sup>+</sup>
1-Nitronaphthalene	173 (0.4)	145 (0.1)	143 (0.1)	127 (1.0)	126 (0.4)		115 (0.9)
2-Nitronaphthalene	173 (0.5)		143 (0.04)	127 (1.0)	126 (0.3)		115 (0.4)
Methylnitronaphthalenes <sup>b</sup>	187		157	141	140		129
3-Nitrobiphenyl	199 (0.7)		169 (0.03)	153 (0.7)	152 (1.0)	151 (0.3)	141 (0.1)
9-Nitroanthracene	223 (0.7)		193 (0.6)	177 (0.7)	176 (1.0)		165 (0.8)
2-Nitrofluoranthene	247 (0.7)		217 (0.04)	201 (1.0)	200 (0.7)		189 (0.3)
1-Nitropyrene	247 (0.5)		217 (0.4)	201 (1.0)	200 (0.7)		189 (0.5)
2-Nitropyrene	247 (0.5)		217 (0.04)	201 (1.0)	200 (0.5)		189 (0.2)

<sup>a</sup>Relative abundances are given in parentheses.

<sup>b</sup>14 isomers are possible, individual relative abundances not given.

Table VI-2. Particle Concentrations, Percent Extractable, Average Temperature and Concentrations of Selected PAH in Ambient POM Samples Collected on September 14-15, 1985, at Claremont, CA

	Time Periods (hr)			
	0600- 1200	1200- 1800	1800- 2400	0000 -0600
Temperature, °C	21	32	23	17
Particle Conc. ( $\mu\text{g m}^{-3}$ )	89	71	52	47
% Extractable	21	17	22	24
-----				
Compound	$\text{pg m}^{-3}$			
Phenanthrene	60	40	50	20
Anthracene	5	2	5	2
Fluoranthene	110	70	130	50
Pyrene	140	80	140	60
Benzo[ghi]- fluoranthene	90	50	100	40
Benz[a]anthracene	60	30	60	20
Chrysene/ Triphenylene	170	130	190	80
Benzo[b,j&k]- fluoranthenes	580	260	680	250
Benzo[e]pyrene	280	130	360	130
Benzo[a]pyrene	90	40	140	30
Perylene	20	6	30	6
Indeno[1,2,3-cd]- pyrene	370	140	450	170
Benzo[ghi]- perylene	1,100	360	1,600	500
-----				
Total PAH	3,100(35) <sup>a</sup>	1,300(18) <sup>a</sup>	3,900(77) <sup>a</sup>	1,300(29) <sup>a</sup>

<sup>a</sup>  $\mu\text{g g}^{-1}$  particulate.

Table VI-3. The Concentrations of 2-Nitrofluoranthene (2-NF), 1-Nitropyrene (1-NP) and 2-Nitropyrene (2-NP) in Ambient POM Samples Collected on TIGF Filters in September 1985 at Claremont, CA

Date	Time Period (hr)	Volume Air Sampled (m <sup>3</sup> )	Weight of Particles (g)	% Extractable <sup>b</sup>	Concentration, pg m <sup>-3</sup> (μg g <sup>-1</sup> ) <sup>a</sup>		
					2-NF	1-NP	2-NP
9/13	1200-1800	3262	0.2642	16	40 (0.5)	2 (0.03)	0.9 (0.01)
9/13	1800-2400	4893	0.3726	20	1,700 (22)	11 (0.14)	8 (0.11)
9/14	0600-1200	3262	0.2903	21	80 (0.9)	30 (0.4)	3 (0.025) <sup>c</sup>
9/14	1200-1800	3262	0.2316	17	30 (0.4)	10 (0.2)	1 (0.01) <sup>c</sup>
9/14	1800-2400	3262	0.1696	22	500 (10)	30 (0.6)	5 (0.1) <sup>c</sup>
9/15	0000-0600	3262	0.1533	24	100 (2.1)	10 (0.3)	2 (0.03) <sup>c</sup>

<sup>a</sup> μg g<sup>-1</sup> particulate.

<sup>b</sup> % Extractable = (weight of CH<sub>2</sub>Cl<sub>2</sub> extract/weight of particles) x 100.

<sup>c</sup> These values have been corrected from those previously published (Ramdahl et al. 1986) which assumed a response factor for the 2-nitropyrene to the deuterated internal standard of 1-nitropyrene-d<sub>9</sub> of unity. The value of this response factor has since been measured and determined to be ~2.

contained the highest concentration of 2-nitrofluoranthene we have measured to date.

## 2. Torrance Wintertime Samples

Gas- and Particulate-Phase PAH and Nitroarenes. The measured concentrations of PAH and their nitro-derivatives are given in Tables VI-4 and VI-5 for the nighttime (1800-0600 hr, February 24-25) and daytime (0600-1800 hr, February 25) samples, respectively. The most abundant gas-phase PAH observed on the Tenax cartridges were naphthalene, the 1- and 2-methylnaphthalenes and biphenyl, with lesser amounts of C<sub>2</sub>-naphthalenes, fluorene and phenanthrene also being observed. Breakthrough of naphthalene-d<sub>8</sub> on the Tenax collection system was <3%, showing that these PAH were quantitatively collected under the sampling conditions employed.

On the first of the PUF plugs (sampling gas-phase PAH and those "blown-off" the particles collected by the filter), phenanthrene was the most abundant PAH. Clearly, as seen from the data given in Tables VI-4 and VI-5 for PUF plugs #2 and #3 and the Tenax cartridges, the PAH more volatile than phenanthrene were not quantitatively collected on the PUF plugs. Thus, for example, in the night sample <3% of the naphthalene, and in the day sample <0.5% of this PAH, was retained on the three PUF plugs. For phenanthrene, there was reasonable agreement between the concentrations quantified on the Tenax cartridges and the sum of the phenanthrene concentrations observed on the filter plus the three PUF plugs. Clearly, at higher temperatures, Tenax sampling is necessary for quantitative collection of phenanthrene and other PAH and nitroarenes of similar or greater volatility.

As expected, quantifications of ambient concentrations of fluoranthene and pyrene based solely on extracts from the filter-collected POM were significantly low, but a single PUF plug was adequate to retain these PAH at the sampling temperatures encountered during this study (for temperature and selected co-pollutant data see Appendix C). Benz(a)-anthracene and chrysene were not quantified in this study, but only traces of these PAH (of m.w. 228) were observed on the first PUF plug. Consistent with this observation, none of the isomeric m.w. 252 compounds were observed on the PUF plugs.

It is interesting to note that the ratios of the reactive PAH benzo(a)pyrene and perylene to the reportedly nonreactive benzo(e)pyrene

Table VI-4. Ambient Concentrations ( $\text{ng m}^{-3}$ ) of PAH and Nitroarenes. Nighttime Sample Collected at El Camino Community College, Torrance, CA, February 24 - 25, 1986, 1800 - 0600 hr

Compound	M.W.	$\text{ng m}^{-3}$					Filter	$\Sigma(\text{Filter} + \text{PUF's})$	Tenax
		PUF#1	PUF#2	PUF#3	Filter	$\Sigma(\text{Filter} + \text{PUF's})$			
<u>PAH</u>									
Naphthalene	128	29	24	22	0.27	75	2,800		
2-Methylnaphthalene	142	a	a	a			1,100		
1-Methylnaphthalene	142	a	a	a			1,200		
Biphenyl	154	a	a	a			62		
Phenanthrene	178	70	9.4	1.0	0.28	81	90		
Anthracene	178	9.5	1.5	0.28	0.03	11	7.2		
Fluoranthene	202	9.1	0.06	n.d. <sup>b</sup>	0.53	9.7			
Pyrene	202	8.8	2.7 <sup>c</sup>	n.d.	0.67	12			
Benzo(e)pyrene	252	n.d.			2.1	2.1			
Benzo(a)pyrene	252	n.d.			1.6	1.6			
Perylene	252	n.d.			0.47	0.5			
<u>Nitroarenes</u>									
1-Nitronaphthalene	173	1.6	0.53	0.12	0.01	2.3			
2-Nitronaphthalene	173	0.90	0.19	0.03	0.002	1.1			
3-Nitrobiphenyl	199	0.38	0.15	0.04	0.01	0.6			
9-Nitroanthracene	223	n.d.			0.11	0.1			
2-Nitrofluoranthene	247	0.04			0.32	0.4			
1-Nitropyrene	247	n.d.			0.03	0.03			
2-Nitropyrene	247	n.d.			0.03 <sup>d</sup>	0.03			

<sup>a</sup>As was the case with naphthalene, each PUF retained a similar small amount of this compound and was therefore not useful for quantification purposes.

<sup>b</sup>n.d. = None detected.

<sup>c</sup>Value suspect; see, for example, fluoranthene in this table, and fluoranthene and pyrene in Table VI-5.

<sup>d</sup>Quantification by reverse phase HPLC.

Table VI-5. Ambient Concentrations ( $\text{ng m}^{-3}$ ) of PAH and Nitroarenes. Daytime Sample Collected at El Camino Community College, Torrance, CA February 25, 1986, 0600 - 1800 hr

Compound	M.W.	$\text{ng m}^{-3}$					Filter	$\Sigma(\text{Filter} + \text{PUF's})$	Tenax
		PUF#1	PUF#2	PUF#3	Filter	$\Sigma(\text{Filter} + \text{PUF's})$			
<u>PAH</u>									
Naphthalene	128	4.7	4.5	4.9	0.45	15	3,300		
2-Methylnaphthalene	142	a	a	a			900		
1-Methylnaphthalene	142	a	a	a			1,100		
Biphenyl	154	a	a	a			60		
Phenanthrene	178	33	32	13	0.33	78	78		
Anthracene	178	2.3	2.7	1.1	0.03	6.1	6.1		
Fluoranthene	202	7.1	0.44	n.d. <sup>b</sup>	0.47	8.0	8.0		
Pyrene	202	7.0	0.36	n.d.	0.60	8.0	8.0		
Benzo(e)pyrene	252	n.d.			2.1	2.1	2.1		
Benzo(a)pyrene	252	n.d.			0.59	0.6	0.6		
Perylene	252	n.d.			0.18	0.2	0.2		
<u>Nitroarenes</u>									
1-Nitronaphthalene	173	1.3	1.0	0.67	0.05	3.0 <sup>c</sup>			
2-Nitronaphthalene	173	1.4	1.1	0.38	0.006	2.9			
3-Nitrobiphenyl	199	5.7	0.29	0.01	0.03	6.0			
9-Nitroanthracene	223	n.d.			0.05	0.05			
2-Nitrofluoranthene	247	0.009			0.28	0.3			
1-Nitropyrene	247	n.d.			0.04	0.04			
2-Nitropyrene	247	n.d.			0.04	0.04			

<sup>a</sup>As was the case with naphthalene, each PUF retained a similar small amount of this compound and was therefore not useful for quantification purposes.

<sup>b</sup>n.d. = None detected.

<sup>c</sup>Lower limit, due to the observed breakthrough through the three PUF's used.

(Nielsen 1984) were lower in the POM collected during the day than during the night, suggesting the occurrence of daytime chemical loss processes for benzo(a)pyrene and perylene and/or of differing PAH emission sources during these sampling intervals.

Particulate Nitrofluoranthenes and Nitropyrenes. In addition to the quantification of the full spectrum of PAH and nitroarenes in the ambient air samples collected on February 24-25 (see Tables VI-4 and VI-5), the POM samples collected on January 19-20 and January 27-28 were quantitatively analyzed for 1- and 2-nitropyrene and 2-nitrofluoranthene. Table VI-6 lists the concentrations of these nitroarenes for these sampling periods as well as for those in February (for which the data are also given in Tables VI-4 and VI-5). It can be seen from Tables VI-3 through VI-6 that, in agreement with our previous data (Pitts et al. 1985d, Ramdahl et al. 1986), 2-nitrofluoranthene was the most abundant nitroarene observed in the ambient POM extracts at both Claremont and Torrance.

It is clear, however, from Tables VI-4 and VI-5 that in the ambient air sample collected on February 24-25, and perhaps in general, the most abundant nitroarenes are the more volatile species. Figure VI-2 shows the GC/MS-MID traces for extracts of the first PUF plug from the nighttime (Figure VI-2A) and daytime (Figure VI-2B) samples for the molecular ions of the 1-nitronaphthalene- $d_7$  internal standard, the 1- and 2-nitronaphthalenes, the methylnitronaphthalenes, and the nitrobiphenyls.

The 1- and 2-nitronaphthalenes and 3-nitrobiphenyl were identified on the basis of their retention times and fragment ion abundances matching those of authentic standards. The presence of 5-nitroacenaphthene, an isomer of the nitrobiphenyls, in ambient POM has previously been reported by Tokiwa et al. (1981). However, the recently reported GC retention index of 5-nitroacenaphthene (Robbat et al. 1986a) clearly shows that this nitroarene would be well resolved from any of the nitrobiphenyl isomers. Since it was determined using authentic standards that 2- and 4-nitrobiphenyl, as well as 3-nitrobiphenyl, eluted in the HPLC nitroarene-containing fraction, it is clear from Figure VI-2 that 2- and 4-nitrobiphenyl were not detected in these ambient air samples.

The presence of several methylnitronaphthalene isomers is evident from the  $m/z$  187 ion traces shown in Figure VI-2 (similar peaks were observed for all the methylnitronaphthalene fragment ions listed in Table

Table VI-6. The Concentrations of 2-Nitrofluoranthene (2-NF), 1-Nitropyrene (1-NP) and 2-Nitropyrene (2-NP) in Ambient POM Samples Collected on TIGF Filters During January and February 1986 at Torrance, CA

Date	Time Period (hr)	Volume Air Sampled (m <sup>3</sup> )	Weight of Particles (g)	% Extractable <sup>b</sup>	Concentration, pg m <sup>-3</sup> (μg g <sup>-1</sup> ) <sup>a</sup>		
					2-NF	1-NP	2-NP
1/19-20	1700-0500	7339	0.4283	15 <sup>c</sup>	40 (0.7)	3 (0.05)	1 (0.025)
1/20	0500-1700	7339	0.5142	13 <sup>c</sup>	60 (0.82)	10 (0.14)	1 (0.02)
1/27-28	1700-0500	6524	0.8852	17 <sup>c</sup>	690 (5.1)	90 (0.7)	50 (0.35)
					750 <sup>d</sup>	50 <sup>d</sup>	60 <sup>d</sup>
1/28	0500-1700	6524	0.7837	15 <sup>c</sup>	410 (3.4)	60 (0.5)	50 (0.4)
2/24-25	1800-0600	1960	0.1554	15	320 <sup>e</sup> (4.1)	30 (0.37)	30 (0.37)
2/25	0600-1800	3190	0.5207	17	280 (1.7)	40 (0.24)	40 (0.24)

<sup>a</sup> μg g<sup>-1</sup> of particulate.

<sup>b</sup> % Extractable = (weight of CH<sub>2</sub>Cl<sub>2</sub> extract/weight of particles) x 100.

<sup>c</sup> Estimated % extractable based on the weight of the hexane, CH<sub>2</sub>Cl<sub>2</sub> and methanol eluates from the open-column silica chromatography of the CH<sub>2</sub>Cl<sub>2</sub> Soxhlet extract.

<sup>d</sup> Independent replicate quantification made using a 60 m column for the GC/MS-MID analyses. See text for detailed discussion.

<sup>e</sup> A small amount (40 pg m<sup>-3</sup>) of 2-nitrofluoranthene was detected on PUF plug #1 of the filter plus PUF plug sampler used.

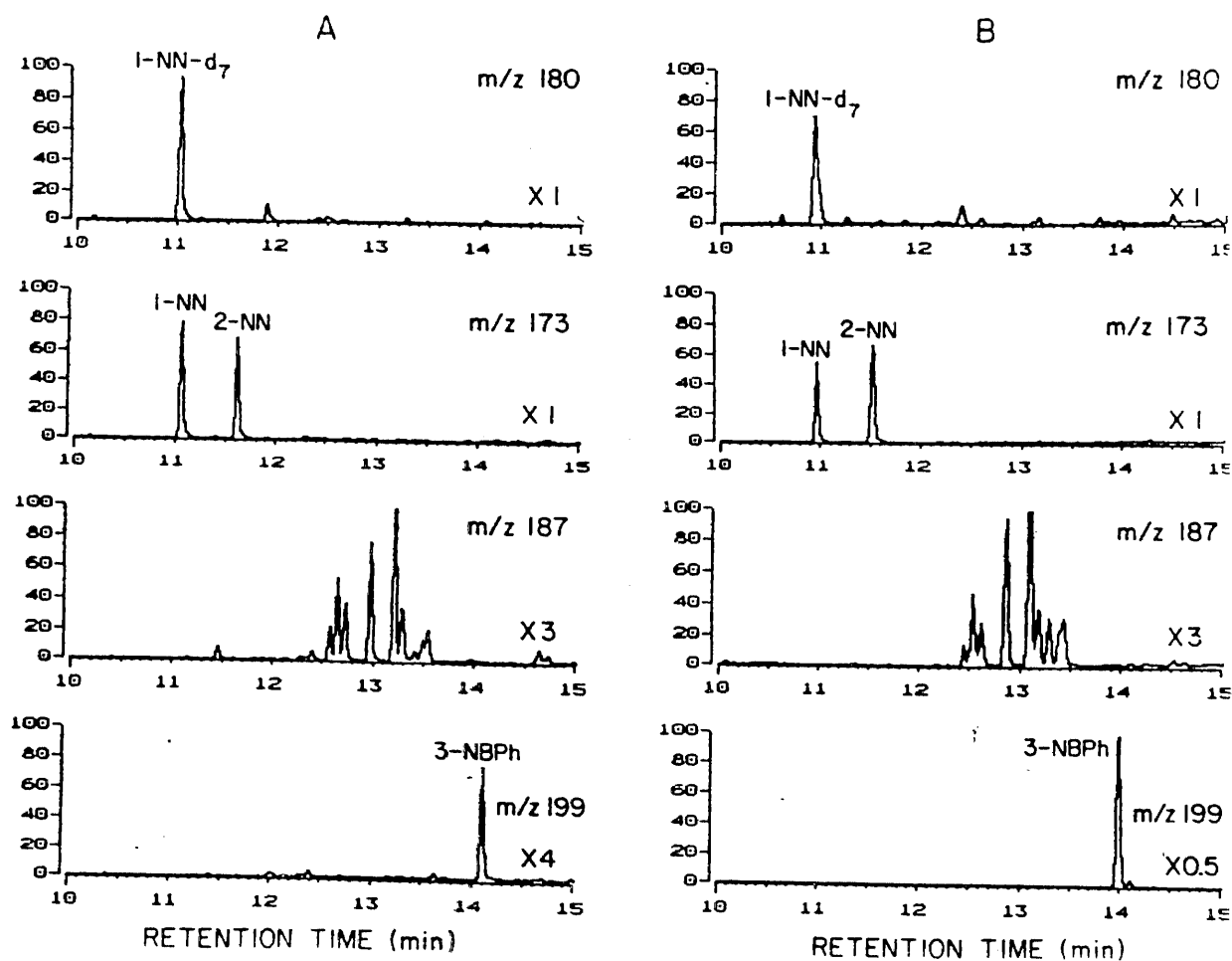


Figure VI-2. GC/MS-MID traces showing nitroarene molecular ion peaks for: A: Nitroarene-containing HPLC fraction of extract from first PUF plug, nighttime sample (1800-0600 hr). B: Nitroarene-containing HPLC fraction of extract from first PUF plug, daytime sample (0600-1800 hr).  $m/z = 180$ , Molecular ion of deuterated 1-nitronaphthalene (1-NN-d<sub>7</sub>) added to both extracts in equal amounts as an internal standard;  $m/z = 173$ , molecular ion of nitronaphthalenes (NN);  $m/z = 187$ , molecular ion of methylnitronaphthalenes;  $m/z = 199$ , molecular ion of nitrobiphenyls (NBPh). GC separation on a 30 m DB-5 fused silica capillary column. Injection at 50°C, then programmed at 8°C min<sup>-1</sup> to 250°C. (Additional retention times: 2-nitrobiphenyl, 12.2-12.3 min; 4-nitrobiphenyl 14.4-14.5 min.) [From Arey et al. 1987].

VI-1). However, the lack of authentic standards for the 14 isomeric methylnitronaphthalenes made specific isomer identification impossible. It can be seen from Figure VI-2 that 3-nitrobiphenyl was more abundant during the daytime (Figure VI-2B) than during the nighttime (Figure VI-2A) sampling period. Although not obvious from Figure VI-2, which only shows the extracts from the first PUF plugs, the 1- and 2- nitronaphthalenes were also more abundant in the daytime sample [see the  $\Sigma$ (Filter + PUFs) column, Tables VI-4 and VI-5]. This diurnal variation was not observed for the less volatile nitroarenes such as 9-nitroanthracene and 2-nitrofluoranthene, which were present mainly in the POM.

### 3. Claremont Summertime and Torrance Wintertime Samples

Less Abundant Nitroarenes of Molecular Weight 247. In addition to 2-nitrofluoranthene and 1- and 2-nitropyrene, which are among the most abundant nitroarenes in ambient POM, we have observed other, less abundant, nitroarenes of molecular weight 247. For example, Figure VI-3 shows the GC/MS-MID traces of the m/z 247 ion of the ambient POM extract collected at Torrance on January 28 between 0500-1700 hr (Arey et al. 1986). This nitroarene analysis was made using a 30 m fused silica capillary column. In addition to 1- and 2-nitropyrene and 2-nitrofluoranthene, several other peaks were observed, and 7- and 8-nitrofluoranthene were tentatively identified. The incomplete resolution of 8-nitrofluoranthene and 1-nitropyrene, however, prohibited quantification of the 8-nitrofluoranthene present. In order to quantify 8-nitrofluoranthene, as well as to conclusively identify the remaining less abundant m/z 247 isomers, we have more recently employed a 60 m DB-5 capillary column for GC/MS-MID analysis.

As can be seen from Figure VI-4A, by using a 60 m narrow bore capillary column we were able to resolve all eight of the nitrofluoranthene and nitropyrene isomers. The isomer resolution shown in this figure was quite reproducible, but the absolute retention times observed varied by several seconds between GC runs. However, by use of the deuterated 2-nitrofluoranthene-d<sub>9</sub> and 1-nitropyrene-d<sub>9</sub> internal standards as precise retention time markers we were able to conclusively identify the isomers present in the ambient POM extracts. Thus, the relative retention times of the m/z 247 ion traces shown in Figure VI-4 have been adjusted by aligning the m/z 256 ion traces of the deuterated internal standards

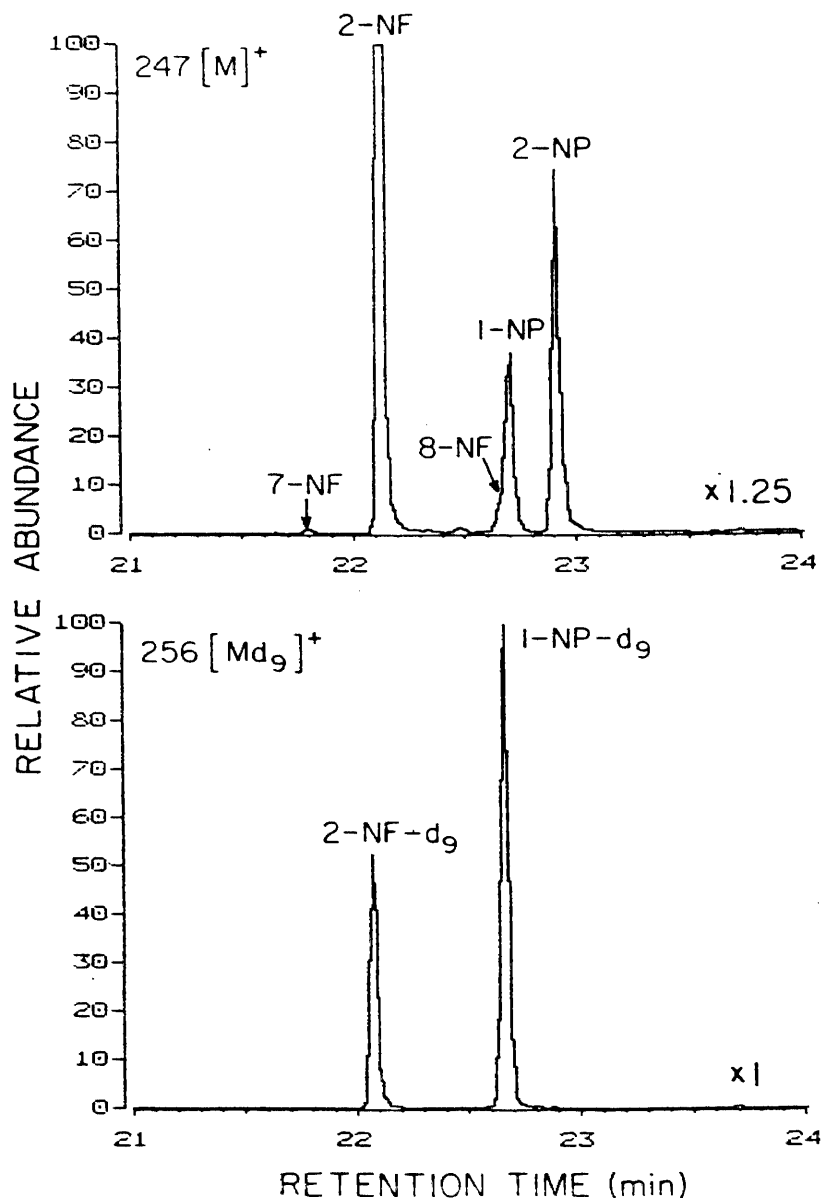


Figure VI-3. GC/MS-MID traces from the analysis of an HPLC fraction of an extract of an ambient POM sample collected at Torrance, CA from 0500-1700 hr on January 28, 1986. Shown are the m/z 247 molecular ion of the nitrofluoranthene (NF) and nitropyrene (NP) isomers and the m/z 256 molecular ion of the deuterated internal standards, 2-nitrofluoranthene-d<sub>9</sub> (2-NF-d<sub>9</sub>) and 1-nitropyrene-d<sub>9</sub> (1-NP-d<sub>9</sub>). Chromatography was done on a 30 m DB-5 fused silica capillary column with injection at 50°C, then programming at 8°C min<sup>-1</sup> (from Arey et al. 1986).

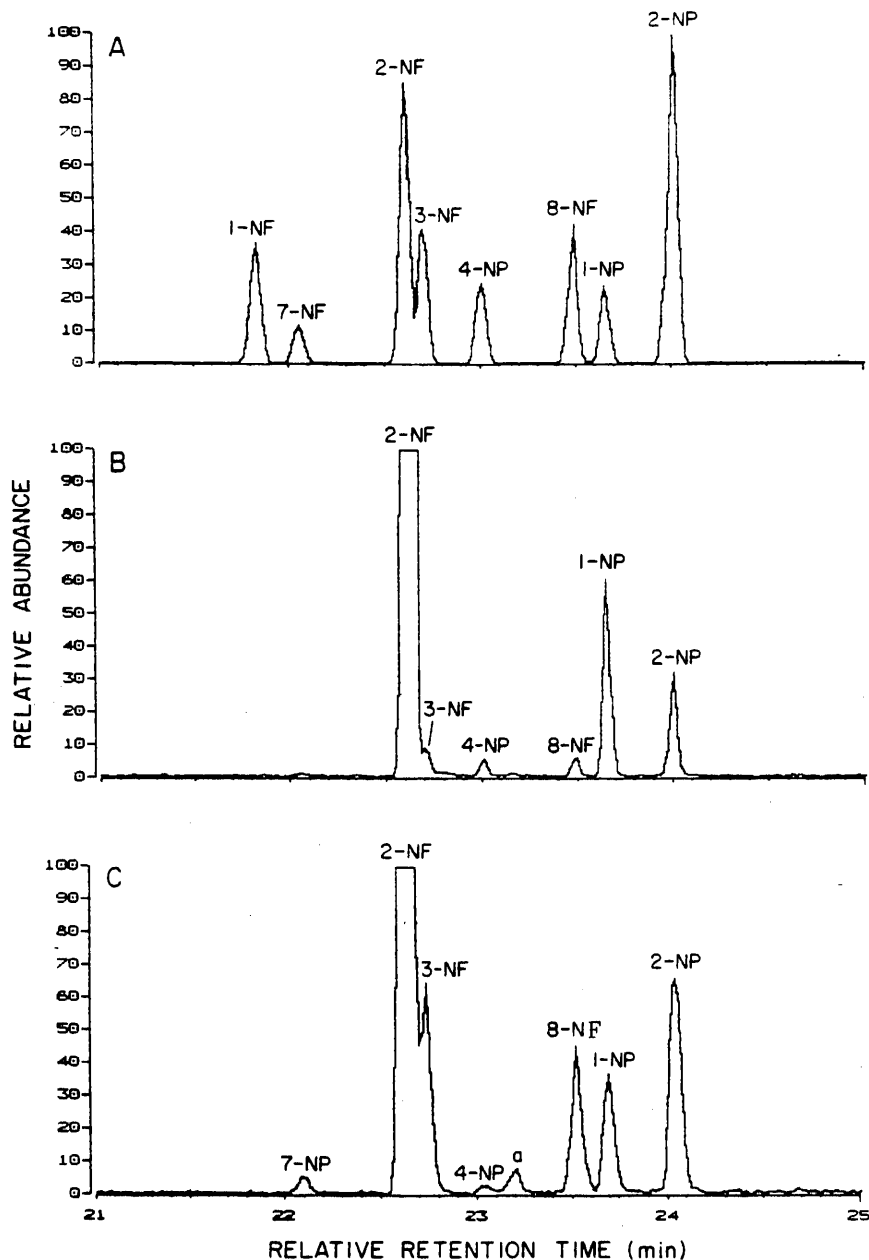


Figure VI-4. GC/MS-MID traces of the  $m/z$  247 molecular ion of the nitrofluoranthenes (NF) and nitropyrenes (NP) using a 60-m DB-5 narrow bore fused-silica capillary column directly interfaced to the MS. A: Analysis of a standard mixture of all eight NF and NP isomers. B: Analysis of Claremont 1800-2400 hr 9/14/85 ambient POM sample. C: Analysis of Torrance 1700-0500 hr 1/27-28/86 ambient POM sample. The peak labeled "a" is a nitroacephenanthrylene isomer (see Section XI.C for detailed discussion). See text for details of POM extraction and HPLC fractionations. Column conditions: injection at  $50^{\circ}\text{C}$ , programmed at  $20^{\circ}\text{C min}^{-1}$  to  $200^{\circ}\text{C}$ , then at  $4^{\circ}\text{C min}^{-1}$  to  $\sim 340^{\circ}\text{C}$ . Complete ion traces showing fragment ion and deuterated internal standards are given in Appendix E.

(Appendix E shows the ambient POM analyses which were repeated using this 60 m column and includes both the m/z 247 and m/z 256 ion traces as well as characteristic fragment ions). As labeled in Figures VI-4B and C, the 3-, 7- and 8-nitrofluoranthene and 4-nitropyrene isomers have been identified in the ambient POM extracts. Thus, peaks corresponding to 4-nitropyrene and 3- and 8-nitrofluoranthene are present in the MID traces of samples from both Claremont and Torrance. In the Torrance sample two additional peaks of m/z 247 are present, one corresponding to 7-nitrofluoranthene and the other identified as a nitroacephenanthrylene isomer (see Section XI.C for a more complete discussion of the sources of the observed nitroarenes).

The nighttime Torrance sample of January 27-28 (Figure VI-4C) was unusual in that the 8-nitrofluoranthene and 3-nitrofluoranthene peaks were comparable in abundance to the 1- and 2-nitropyrene peaks. It was recognized that in this particular sample these nitrofluoranthene isomers could make a significant contribution to the mutagenicity of the extract since both 8- and 3-nitrofluoranthene are highly mutagenic (see Section VII for the contributions of the observed nitroarenes to the measured ambient mutagenicity). For this reason purified samples of 3- and 8-nitrofluoranthene [purified by chromatography and crystallization from a mixture of these isomers obtained by the reaction of fluoranthene with  $N_2O_4$  (Pitts et al. 1985c, Zielinska et al. 1986a)] were used to determine a response factor for the m/z 247 ion abundance of these compounds in relation to the m/z 256 molecular ion of 1-nitropyrene- $d_9$ . The sample was then reanalyzed and these isomers were quantified in addition to 2-nitrofluoranthene and 1- and 2-nitropyrene.

The results obtained for 2-, 3- and 8-nitrofluoranthene were, respectively: 750, 70 and 50  $pg\ m^{-3}$ , and for 1- and 2-nitropyrene 50 and 60  $pg\ m^{-3}$ , respectively. Comparing these values with those for 2-nitrofluoranthene and 1- and 2-nitropyrene previously obtained (Table VI-6), there is good agreement for 2-nitrofluoranthene and 2-nitropyrene, but the previously reported value for 1-nitropyrene was somewhat high, presumably due to incomplete resolution of 8-nitrofluoranthene and 1-nitropyrene (see, for example, Figure VI-3) on the 30 m column used. This interference is expected to be minor in the other samples analyzed.

Direct emission from combustion sources is still viewed as the primary source of nitroarenes in ambient air, as evidenced by the recent review of Tokiwa and Ohnishi (1986). However, the present work and recent ambient air measurements and laboratory studies (Nielsen et al. 1984, Pitts et al. 1985d, Arey et al. 1986, Nielsen and Ramdahl 1986, Ramdahl et al. 1986, Sweetman et al. 1986, Zielinska et al. 1986b) show that this conclusion must be significantly modified.

A detailed discussion of our current knowledge concerning the sources of the nitroarenes we have observed in ambient air is given in Section XI.C, together with the major conclusions reached on the basis of the data presented in this Section.

